



University  
of Glasgow

Dodds, Colin J. (1972) *The response of vehicle components to random road surface undulations*. PhD thesis.

<http://theses.gla.ac.uk/4784/>

Copyright and moral rights for this thesis are retained by the author

A copy can be downloaded for personal non-commercial research or study, without prior permission or charge

This thesis cannot be reproduced or quoted extensively from without first obtaining permission in writing from the Author

The content must not be changed in any way or sold commercially in any format or medium without the formal permission of the Author

When referring to this work, full bibliographic details including the author, title, awarding institution and date of the thesis must be given

THE RESPONSE OF VEHICLE COMPONENTS TO  
RANDOM ROAD SURFACE UNDULATIONS

Colin J. Dodds, B.Sc.

DEPARTMENT OF MECHANICAL ENGINEERING  
UNIVERSITY OF GLASGOW

Thesis submitted for the Degree

of

Doctor of Philosophy

August 1972

**BEST COPY**

**AVAILABLE**

Variable print quality

ABSTRACT

DEPARTMENT OF MECHANICAL ENGINEERING  
UNIVERSITY OF GLASGOW

Doctor of Philosophy

THE RESPONSE OF VEHICLE COMPONENTS TO  
RANDOM ROAD SURFACE UNDULATIONS

by

Colin J. Dodds

Standard techniques of random vibration analysis have been applied to the problem of determining the response of vehicle components to random road surface undulations. A simple road classification method, which will typify the general terrain inputs to vehicles is proposed and is based on the knowledge of the spectral density of any longitudinal track. Finally, this work introduces a novel technique for simulating in the laboratory the response of a vehicle to road profile excitation.

Three analytical models of increasing complexity are used to describe the road surface roughness. The first considers the road as consisting of a cylindrical surface which can be defined by means of a single longitudinal track,  $y_r(x)$ , treated as a member function of a Gaussian random process  $\{y_r(x)\}$ . In this case the spectral density,  $S_r(n)$ , of the track,  $y_r(x)$ , completely defines the process.

To introduce lateral irregularities into the road surface description, a second model is discussed in which the surface is considered to consist of random fluctuations in the longitudinal direction with a constant lateral slope which varies randomly for each longitudinal increment. Complete description of this surface is provided by the spectral density,  $S_D(n)$ , of any longitudinal track and the coherency function,  $q(n)$ , which describes the related properties of any two parallel tracks; in this case it is implicitly assumed that the coherency function is invariant with track width.

Finally an examination of the surface as forming part of a completely homogeneous two dimensional random process is shown to have definite promise and to provide perhaps the most accurate and yet analytically simple method of road description; it is demonstrated that the spectral density,  $J_D(n)$ , of any longitudinal track provides the exhaustive probability characteristic necessary to describe the surface.

General response relationships are derived for the various mathematical models used to describe the vehicle. Models with one, two and four inputs are considered. In the case of one particular vehicle, the predicted responses of selected components are compared with those actually measured on the vehicle. The degree of agreement obtained is encouraging; exceedingly simple road-vehicle models being necessary to achieve this.

Finally a simulation technique which will enable vehicle response to be reproduced in the laboratory is proposed. The test, which is currently under development, is described; synthesised displacements, based on a knowledge of road profile spectra, are applied to the vehicle. It is shown that there are considerable difficulties in basing such a test on previously recorded stress histories, and that this new technique, coupled with the response analysis derived for the various vehicle models, seems likely to provide a very good simulation of vehicle response to road surface undulations.

### ACKNOWLEDGEMENTS

The author gratefully acknowledges the help received from the Motor Industry Research Association (MIRA), Nuneaton, England in establishing parameters for the test vehicles and for providing experimental facilities and response spectra. Particular thanks are due to Dr. M.A. Macaulay, Mr. S. Andrew and Dr. R.P. LaBarre of MIRA for their continued interest and helpful discussions. Thanks are also due to Mr. N.F. Barter of MIRA for providing the wide range of road spectra necessary for the road classification discussed in Chapter 4, Section 4.2 and to members of B.S. panel MEE/158/3/1 for their comments and discussion on this proposed method.

The work presented in Chapter 5 was carried out with the support of the Department of Trade and Industry (National Engineering Laboratory) under a research contract and the author acknowledges the helpful discussions with particular staff of NEL and the computational facilities provided.

The author also wishes to express his gratitude to Professor J.D. Robson for his guidance, encouragement and valuable comments during this investigation.

## CONTENTS

	<u>PAGE</u>
LIST OF SYMBOLS	
CHAPTER 1 :	1
INTRODUCTION	
CHAPTER 2 :	10
ANALYSIS OF THE MOTION OF A VEHICLE MOVING WITH CONSTANT VELOCITY ALONG A RANDOM TRACK	
2.1 Response of a system to multiple random excitation.	10
2.2 Single input case; point follower on a random track.	12
2.3 Double input case; two point followers separated by a simple lag.	15
2.4 The double input transfer function.	17
2.5 Four input road-vehicle model.	20
2.6 The coherency function, $\gamma(n)$ .	26
2.7 The road as a completely homogeneous surface.	31
2.8 Stationarity, ergodicity and linearity.	36
CHAPTER 3 :	39
THE RESPONSE CHARACTERISTICS OF VEHICLE MODELS TO HARMONIC AND RANDOM EXCITATION	
3.1 Response relationship: single degree of freedom, single input model.	39
3.2 Single degree of freedom, double input case.	44
3.3 Two degree of freedom - single input model.	47
3.4 Double-input models.	52
3.5 Models with four inputs.	56
CHAPTER 4 :	62
THE RESPONSE OF VEHICLE COMPONENTS TO RANDOM ROAD SURFACE IRREGULARITIES	
4.1 Road surface descriptions.	62
4.2 The surface as a single realisation of a random process $\{\gamma_j(x)\}$ .	67
4.3 The probability characteristics of three test routes	73

	<u>PAGE</u>
4.4 Consideration of the properties of two parallel tracks along the direction of travel.	78
4.5 The road surface as a completely homogeneous random surface.	81
4.6 An examination of vehicle response spectra, vehicle model parameters and testing technique.	83
4.7 Comparison between experimental and predicted vehicle response.	86
CHAPTER 5 : THE LABORATORY SIMULATION OF VEHICLE SERVICE STRESSES	92
5.1 The nature of the problem.	93
5.2 Prototype based testing.	94
5.3 Test based on road profile spectra.	98
5.4 Some practical considerations in the simulation of road surface undulations.	101
CHAPTER 6 : CONCLUSIONS	106
REFERENCES	110
APPENDIX 1: A range of road sections measured by MIRA	116
APPENDIX 2: The measurement and analysis of road surface roughness	119
A2.1 Measurement of road surface undulations	119
A2.2 Analysis of road surface roughness	120
References for Appendix 2	126
APPENDIX 3: Test vehicle parameters	123
FIGURES 1-69	

## LIST OF SYMBOLS

This list applies to the complete work, with the exception of Chapter 2, Section 2.1 in which a slightly different notation is used, which conforms to reference [1].

a	wheelbase
b	one half vehicle track width
c	linear damping coefficient in Ns/m
f	frequency in Hz
$f_n$	natural frequency in Hz
$f_1$	upper frequency limit
$f_2$	lower frequency limit
i	$\sqrt{-1}$
k	linear spring stiffness coefficient in N/m
$l_1, l_2$	lengths, such that $l_1 + l_2 = a$
m	mass in kg.
n	spatial frequency in c/m
$n_0$	$1/2\pi$ c/m
p	$k + i\omega c$
r	integer variable
s	integer variable
t	time variable
v	vehicle velocity
w	integer exponent
$w_1$	integer exponent
$w_2$	integer exponent
x	longitudinal distance variable
y	lateral distance variable

$\alpha_{rs}$	receptance
$\beta_{rs}$	receptance
$\delta$	distance lag
$\zeta$	damping ratio
$\eta$	distance lag
$\theta$	phase angle
$\lambda$	number of standard deviations (Gaussian distribution)
$v$	random variable
$\xi$	distance lag
$\rho$	distance lag
$\sigma$	root mean square value
$\tilde{\sigma}$	band limited ( $f_1, f_2$ ) root mean square value
$\tau$	time lag
$\phi$	$2\pi na$
$\chi_{rs}$	receptance
$\omega$	frequency in $\text{sec.}^{-1}$
$\omega_n$	natural frequency in $\text{sec.}^{-1}$
$\Delta x$	data spacing
$q(n)$	coherency function in space domain
$g_v(f)$	coherency function in time/frequency domain
$h(\delta)$	Fourier transform of $q(n)$
$\chi(x)$	single track road profile as a function of longitudinal distance, $x$ .
$q(x, y)$	road surface undulations as a function of longitudinal distance, $x$ , and lateral distance $y$ .
$z_r(t)$	function of time denoting displacement of point $r$
$\chi'(x)$	road slope as a function of distance
$p(q)$	probability distribution of heights, $q$ .

$\alpha_r(if)$	receptance due to input at point r; used sometimes omitting the (if)
$\alpha_r^*(if)$	complex conjugate of $\alpha_r(if)$
$\gamma(f)$	coherency function
$\psi(x)$	angle of inclination of transverse cross-section of road surface as a function of distance
$B_e$	equivalent frequency bandwidth
F	force in N
$I_p$	pitch moment of inertia
[M]	mass matrix
[C]	damping matrix
[K]	stiffness matrix
[I]	input matrix
A(f)	composite functions of the receptances $\alpha_r(if), \alpha_s(if)$
B(f)	
C(f)	
D(f)	
E(f)	
F(f)	
P( $\delta$ )	lag window
Q(n)	spectral window as function of frequency, n.
$R_r(\tau)$	autocorrelation function of the random signal, $z_r(t)$
$R_{rs}(\tau)$	cross-correlation function of the random signals, $z_r(t), z_s(t)$
$R_r(\delta)$	autocorrelation function of the random track, $\mathcal{Y}_r(x)$ .
$R_{rs}(\delta)$	cross-correlation function of the random tracks, $\mathcal{Y}_r(x), \mathcal{Y}_s(x)$ .

$R(\xi, \eta)$	two dimension correlation function of the road surface
$S_r(f)$	spectral density function of the random signal, $z_r(t)$ .
$S_{rs}(f)$	cross spectral density function of the random signals, $z_r(t)$ , $z_s(t)$ .
$J(n_0)$	roughness coefficient; the value of the road spectrum at frequency $n_0$
$J_r(n)$	spectral density function of the random track, $\xi_r(x)$
$J_D(n)$	spectral density of any longitudinal track along road
$J_{rs}(n)$	cross spectral density function of the random tracks, $\xi_r(x)$ , $\xi_s(x)$
$J_{rs}^*(n)$	complex conjugate of $J_{rs}(n)$
$J_x(n)$	real valued cross spectral density of the random tracks, $\xi_r(x)$ , $\xi_s(x)$
$J_1$	a constant
X	single degree of freedom model receptance
$ T(f) ^2$	double input transfer function
$[T_D(f)]^2$	direct transfer function, four input model
$[T_X(f)]^2$	cross transfer function, four input model
$[\Lambda(f)]^2$	simulation error function
$\{x(t)\}$	random process containing $x(t)$
$\langle x(t) \rangle$	mean value of $x(t)$ ; angular brackets denote averaging over all time or distance

## CHAPTER 1

### INTRODUCTION

When a vehicle travels along a road the undulations of the road surface impose continuously varying displacements at the points of contact of the tyres and the road, and so give rise to responses in the form of stresses or accelerations in the various components of the vehicle. Since, on normal roads, the surface irregularities are in general random in nature, it is difficult in vibrating systems as complex as motor vehicles to analyse and understand the response by purely experimental means, and resort to mathematical analysis is essential.

Road surfaces appear amenable to representation as random processes, provided that the effects of such occasional large irregularities as potholes are removed from the analysis and treated separately: these must not of course be ignored. If this is the case, description of the road surface as a stationary random process will permit analysis based on stochastic process theory which has been developed into the theory of random vibration, treated from various aspects by ROBSON [1], CRANDALL [2,3], BLACKMAN and TUKEY [4], BENDAT and PIERSOL [5], CRANDALL and MARK [6] and LIN [7].

In the particular case of stationary random excitations with a Gaussian distribution and zero mean value, it is necessary to consider the time histories of the excitations and compute their second order moments/...

moments, or in effect, their spectral densities, to provide a sufficient statistical description of the process. This description of the road, coupled with a harmonic analysis of the vehicle will provide a response analysis which will describe, precise enough to be useful, the response of the system expressed in terms of displacement, acceleration or stress.

A four wheeled vehicle running along a road is subjected to four imposed displacement-excitations, one at each wheel. Complete description of the road surface would therefore need to provide enough information to describe adequately the displacement imposed at each wheel (at least in statistical terms) and any correlation between the four displacements.

There is clearly no major difficulty in providing a digital survey of the two road tracks along which the vehicle will traverse. This sampled data can then be used to compute the statistical parameters necessary to provide the required description. The computational problems in handling large volumes of data have now largely been overcome with the advancement of computer hardware and the techniques of random data analysis have greatly improved since the days of BLACKMAN and TUKEY [4] with the introduction of the Fast Fourier Transform algorithm (COOLEY and TUKEY [8]).

Using conventional survey techniques to establish the statistical description of road surface profiles, although accurate, is very slow and time consuming. However, other methods of measurement have been developed which permit a fast traverse of the road. MACAULAY [9] gave an account of the state of the art as it was/...

it was in 1963 and MIRA (The Motor Industry Research Association) reported on their first profilometer in 1964 [10]. Subsequent development produced their existing profilometer [11, 12] which was used to establish the spectral densities of a wide range of British and Continental roads (1970) [12]. A similar programme of road measurement was carried out in Germany under MITSCHKE at the Institut für Fahrzeugtechnik der Technischen Universität Braunschweig, and reported by BRAUN [13] in 1966. Braun developed a profilometer, contained in a single-wheel trolley, which was pulled behind a vehicle and measured the response of a known system from which he derived the spectral description of the surface undulations.

However, this previous work has been based on establishing the statistical properties of a single track and no account has been taken of correlation between two adjacent tracks. Work by PARKHILOVSKI [14] in 1968 has suggested that the cross-correlation properties are not as complex as they may appear at first sight and descriptions of the cross properties of two parallel tracks have been presented independently by KANESHIGE [15] and DODDS and ROBSON [16].

However a theory which will define in statistical terms a sufficient description of the road surface in both longitudinal and lateral directions has not previously been available and it is shown in Chapter 2 that consideration of the road surface as part of a two-dimensional random process with homogeneous properties will provide a complete description of the vehicle excitation environment.

To determine the response characteristics of the vehicle to road surface undulation requires not only a statistical description of the excitation but also a knowledge of the harmonic response of the vehicle. Virtually complete dynamical description of a vehicle is possible if sufficient degrees of freedom are involved. Such complete description of the problem is not always necessary, however, and for practical purposes and in an effort to understand the vehicle-road interaction simplified models are to be preferred.

However, to satisfy this form of analytical treatment two important restrictions are placed on the vehicle models. Firstly, to maintain stationarity in the response requires the vehicle to traverse the road surface at constant speed. This is not as severe a restriction as may seem at first sight, as it has been shown by VIRCHIS and ROBSON [17], who considered the response of a single degree of freedom vehicle model to random profile excitation, that for speeds and accelerations likely to be of practical importance in road vehicles it would be, at least to a first approximation, reasonable to neglect such non-stationary effects due to vehicle acceleration. Secondly, to ensure the applicability of the spectral density approach in which the response spectrum of the system is given by the equation [see eg. 1]

$$S^0(f) = |\alpha(if)|^2 S^1(f) \quad 1$$

where  $S^1(f)$  is the excitation spectral density and  $\alpha(if)$  the frequency response function of a constant parameter system, requires not only stationarity in the excitation, but also for a rigorous use/...

use of equation (1) requires  $\alpha(\omega)$  to be linear. This important assumption is discussed in Section 2.8.

There have been many notable contributions to the study of vehicle dynamics by such authors as ELLIS [18, 19] BARSON [20] and HALES [21], but these have generally been concerned with particular problems associated with deterministic inputs and not directly relevant to the problem under consideration. Contributions to the problem of profile excited vehicle response prior to 1967 suffered from a relative lack of road surface descriptions, although KOZIN and BOGDANOFF [22] (1962) advanced a response theory in which the description of the excitation was based on the models favoured by oceanographers studying the surface of the sea [23].

The application of the simple relation (1) between the spectral densities of the response and excitation for the vehicle problem was demonstrated by BIENIEK [24] in 1960 and later by RAPIN [25, 26] in 1962 and 1965, who developed the spectral response for a single and double input vehicle model, but was prevented from applying the relationships to a successful prediction of vehicle response by the lack of road surface information. More recent work by VAN DEUSEN [27] (1967) and ROSSINI [28] (1969) consolidated particular aspects of the vehicle response problem, and it was shown by DODDS and ROBSON [29] (1970) that successful analytical prediction of vehicle component response could be carried out using simple analytical models and a statistical description of the road surface/...

surface. In this latter paper the authors considered single, double and four input vehicle models and developed the ideas of PARKHOLLOVSKI [14] to provide a simple yet complete description of the cross and direct properties of two random tracks.

It is the object of this present work to show that the response of vehicle components to road surface undulations can be described in statistical terms from a knowledge of the road and vehicle characteristics. Various mathematical models describing the road surface undulations will be presented and their relative success in predicting the actual properties discussed.

The behaviour of a number of simplified analytical vehicle models will be examined. In the first instance we shall assume a model system in which only one imposed displacement affects the response. This is not an inconceivable situation: there are many components in whose response a single imposed displacement has a predominating effect. We shall take a greatly simplified dynamical model, which also simplifies the analysis. Following this, systems having two inputs and four inputs will be considered - these necessitating correspondingly more complex dynamical models.

The predicted analytical response of various vehicle components will be compared with experimental response measurements taken from a test vehicle.

Finally the ultimate aim of the work is to show how the testing of vehicles and their components in the laboratory as an/...

as an alternative to, or in order to supplement, road testing is possible with recourse to the analysis (coupled with the experimental verification) presented for road and response description.

Since attention will be confined to the case where a vehicle runs at constant velocity and is subjected only to vertical random displacement excitations the techniques presented in this work are to be regarded as an essential step towards the solution of the complete road-vehicle problem rather than offering the complete solution. Many other environmental and driver controlled inputs will affect the response, and although ignored here, must be included in any vehicle design or vehicle test specification.

In Chapter 2, the theory of profile excited vehicle response is presented drawn from the basic theory of random vibration [1] to [7]. The response relationships for single and double (inputs fore and aft) input vehicle models are presented and following from the hypothesis suggested by PARKHILOVSKI [14] a greatly simplified response relationship is derived for a four input (real vehicle) road-vehicle model. The conception of a coherency function,  $g(n)$ , is introduced and its usefulness in the road descriptive process explained. Finally it is shown how a complete road surface description can be achieved by consideration of the homogeneous properties of a two dimensional random process.

It is assumed throughout this work, and discussed at the end of Chapter 2, that, for stretches long enough for statistical descriptions to be meaningful, representation of the road surface as a realisation of a stationary Gaussian process is permissible.

In Chapter 3, the response relationships derived in Chapter 2 are applied to a series of vehicle models of increasing complexity. Their response characteristics to random profile and harmonic excitation are examined. This approach makes it possible to assess the value of increased complexity not only in the vehicle model, but also in the method of road-surface description.

The probability characteristics of road surface roughness are described in Chapter 4. Three road-surface models, based on the analysis presented in Chapter 2, are proposed, and in each case, their applicability to the description of actual road surfaces discussed. Experimental response spectra, computed from measurements taken on test vehicles are examined to validate the response analysis. Finally, the response spectra of selected components on the test vehicle are compared with predicted response spectra from the analysis derived in Chapter 2 and using as input data one of the measured test surfaces.

Finally, in Chapter 5 it is shown that with a successful response analysis available, together with a sufficient knowledge of road surface properties, the whole concept/...

concept of vehicle testing may be changed by bringing complete vehicles or their components into the laboratory for simulated response testing. The drawbacks of simulation testing based on pre-recorded data are demonstrated and a new technique proposed which is founded simply on a knowledge of the road surface properties, and built on the analytical techniques developed for response prediction.

## CHAPTER 2

### ANALYSIS OF THE MOTION OF A VEHICLE MOVING WITH CONSTANT VELOCITY ALONG A RANDOM TRACK

The object of this chapter is to present the theory applicable to the determination of the response of a vehicle moving along a random track with constant velocity. A brief exposition of the theory of random vibration will be given, from material drawn from references [1,2,3,6,7], and this will form a basis for the subsequent analytical treatment. It is also considered appropriate at this stage to discuss the assumptions of stationarity, ergodicity and linearity and their applicability to the present problem.

#### 2.1 Response of a system to multiple random excitation

Consider the system shown in figure 1, excited by a random point displacement  $x_1(t)$  having a response at point  $x_0(t)$ . The impulse function of the linear system is  $W(\tau)$  and its frequency response function,  $\alpha(if)$  is given by the Fourier Transform of  $W(\tau)$  -

$$\alpha(if) = \int_{-\infty}^{\infty} W(\tau) e^{-i2\pi f\tau} d\tau \quad 2.1.1$$

The response  $x_0(t)$  to the random excitation  $x_1(t)$  is given by

$$x_0(t) = \int_0^{\infty} x_1(t-\tau_1) W(\tau_1) d\tau_1 \quad 2.1.2$$

The autocorrelation,  $R_0(\tau)$  of the response is defined as

$$R_0(\tau) = \langle x_0(t) \cdot x_0(t+\tau) \rangle \quad 2.1.3$$

where the angular brackets denote averaging over all time and

Wiener and Khinchin showed independently that the spectral density  $S(f)$  could be defined by taking the Fourier transform

of  $R(\tau)$  -

$$S(f) = \int_{-\infty}^{\infty} 2 R(\tau) e^{-i2\pi f\tau} d\tau \quad 2.1.4$$

Since the inverse relationship is also true

$$R(\tau) = \int_{-\infty}^{\infty} 1/2 S(f) e^{i2\pi f\tau} df \quad 2.1.5$$

the useful relationship between the mean square value of the signal and its spectral density can be simply derived.

$$\begin{aligned} \langle x^2(t) \rangle &= R(0) = \int_{-\infty}^{\infty} 1/2 S(f) df \\ &= \int_0^{\infty} S(f) df \end{aligned} \quad 2.1.6$$

These quantities have been defined in terms of a single realisation, of infinite duration, of a random process  $\{x_0(t)\}$ ; but, if the process is stationary and ergodic they are characteristic of the process as a whole. Moreover, if the process is Gaussian, the three related quantities,  $\langle x^2(t) \rangle$ ,  $R(\tau)$  and  $S(f)$  completely define the process.

The spectral density of the response  $x_0(t)$  in terms of the spectral density of the excitation  $x_1(t)$  can then be shown

[1,5,6,7] to be

$$S_0(f) = \alpha(if) \alpha^*(if) S_1(f) \quad 2.1.7$$

where/...

where the asterisk indicates complex conjugate. The cross-correlation function  $R_{10}(\tau)$  between the excitation and response is defined as

$$R_{10}(\tau) = \langle x_1(t) \cdot x_0(t + \tau) \rangle \quad 2.1.8$$

and the Cross-Spectral density is related to the input spectrum by

$$S_{10}(f) = \alpha_{01}(if)S_1(f) \quad 2.1.9$$

Consider now the model shown in figure 2 where the linear system is excited by the imposed displacement inputs  $x_1(t), x_2(t) \dots x_n(t)$ , which have spectral densities  $S_1(f), S_2(f) \dots S_n(f)$  and cross spectral densities  $S_{12}(f), S_{13}(f) \dots S_{23}(f) \dots$ . The response spectrum will contain contributions from all the direct spectral densities as in equation 2.1.7 and from all the cross-spectral densities and is given by

$$S_0(f) = \sum_{r=1}^n \sum_{s=1}^n \alpha_r^*(if) \cdot \alpha_s(if) S_{rs}(f) \quad 2.1.10$$

Noting that we write  $S_1(f)$  for  $S_{11}(f)$  etc., and that the frequency response function  $\alpha_r(if)$  is the response of the system to the  $r^{\text{th}}$  input, all other inputs being quiescent.

## 2.2 Single input case; point follower on a random track

Suppose a road (figure 3) to have a profile  $z(x)$  which can be considered to be a member function of an ergodic random process  $\{z(x)\}$ . Suppose that a vehicle moves along it with constant velocity  $v$ .

In considering the response of a vehicle we shall be interested in the displacement imposed on the vehicle at the point of contact as a function of time, and this we will denote by  $z(t)$ . It is obvious that the displacement  $z(x)$  and  $z(t)$  coincide for corresponding values of  $x$  and  $t$ , and since

$$x = vt \quad 2.2.1$$

then

$$z(vt) = z(t) \quad 2.2.2$$

When we consider the response we will use the spectral density  $S(f)$  of the process  $\{z(t)\}$ . However, as this will be velocity dependent we will need to define a spectral density of the process  $\{z(x)\}$ . Let this be denoted by  $f(n)$  where  $n$  represents the spatial frequency.

The relationship between these two spectral densities can be derived as follows.

Define the autocorrelation function of the process  $\{z(x)\}$ :

$$R(\delta) = \langle z(x) \cdot z(x + \delta) \rangle \quad 2.2.3$$

Now if  $R(\tau)$  is the autocorrelation function of the process  $\{z(t)\}$  then

$$\begin{aligned} R(\tau) &= \langle z(t) \cdot z(t + \tau) \rangle \\ &= \langle z(vt) \cdot z(vt + v\tau) \rangle \\ &= \langle z(x) \cdot z(x + \delta) \rangle \quad \delta = v\tau \\ &= R(\delta) \end{aligned} \quad 2.2.4$$

The spectral density  $S^i(f)$  is given by

$$\begin{aligned}
 S^i(f) &= \int_{-\infty}^{\infty} 2R(\tau) e^{-i2\pi f\tau} d\tau \\
 &= \int_{-\infty}^{\infty} 2R(\delta) e^{-i2\pi v n \frac{\delta}{v}} d\left(\frac{\delta}{v}\right) \\
 (f = vn \quad \text{and} \quad \delta = v\tau) \\
 &= \frac{1}{v} \int_{-\infty}^{\infty} 2R(\delta) e^{-i2\pi n\delta} d\delta \\
 &= \frac{1}{v} \mathcal{J}(n)
 \end{aligned}
 \tag{2.2.5}$$

Thus if the profile spectrum  $\mathcal{J}(n)$  is known the response of the vehicle at any speed can be determined by

$$S^o(f) = |\alpha(if)|^2 \frac{1}{v} \mathcal{J}(n) \tag{2.2.6}$$

if we can evaluate the linear transfer function,  $\alpha(if)$ . This equation is analagous to equation 2.1.7.

Equation 2.2.6 gives the response relationship for a particularly simple case of profile-imposed excitation, but already some characteristic features can be identified. Consider the effect of varying the traversal velocity  $v$  at any given frequency. Firstly, by virtue of the factor  $1/v$  an increase in velocity tends to reduce response, and secondly response is also affected by the presence of  $v$  in the argument of  $\mathcal{J}(f/v)$ . If for example

$$\mathcal{J}(n) \propto 1/n^2 \tag{2.2.7}$$

then  $\mathcal{J}(f/v)$  would be considerably increased by any change of  $v$ , and as a result of the two factors together, the response would increase proportionally with  $v$ .

In certain cases the form of  $f(n)$  [30, 31] may be such that a change of  $v$  may bring into prominence - or suppress - a particular peak of the receptance curve, and so may have a considerable influence on response.

The factor  $|a(if)|^2$  is a property of the vehicle system only and is of course independent of  $v$ .

### 2.3 Double input case; two point followers separated by a simple lag

Consider now the case, shown in figure 4, where the vehicle is excited by the given profile  $z(x)$  at two points 1 and 2 separated by the distance,  $a$ . This corresponds to one pair of front and rear wheels. We assume that the rear follower will always follow the same profile  $z(x)$  as the front, but separated by a constant lag, i.e.

$$\begin{aligned} z_1(x) &= z(x) \\ z_2(x) &= z(x - a) \end{aligned} \quad 2.3.1$$

Again for constant velocity

$$\begin{aligned} z_1(t) &= z_1(vt) = z_1(x) = z(x) \\ z_2(t) &= z_2(vt) = z_2(x) = z(x - a) \end{aligned} \quad 2.3.2$$

To establish the response relationship we note from equation 2.1.10 that we must first establish the cross-spectra,  $S_{12}^i(f)$ , and  $S_{21}^i(f)$  in terms of the road profile spectrum  $f(n)$ .

The cross-correlation function is given by

$$\begin{aligned}
 R_{12}(\tau) &= \langle z_1(t) \cdot z_2(t + \tau) \rangle \\
 &= \langle \mathcal{Y}_1(vt) \cdot \mathcal{Y}_2(vt + v\tau) \rangle \\
 &= \langle \mathcal{Y}_1(x) \cdot \mathcal{Y}_2(x + \delta) \rangle \\
 &= \langle \mathcal{Y}(x) \cdot \mathcal{Y}(x + \delta - a) \rangle \\
 &= \mathcal{R}(\delta - a)
 \end{aligned}
 \tag{2.3.3}$$

and hence the cross-spectrum

$$\begin{aligned}
 S_{12}^i(f) &= \int_{-\infty}^{\infty} 2R_{12}(\tau) e^{-i2\pi f\tau} d\tau \\
 &= \int_{-\infty}^{\infty} 2\mathcal{R}(\delta - a) e^{-i2\pi n v \frac{\delta}{v}} \frac{\delta}{v} d\left(\frac{\delta}{v}\right) \\
 &= \frac{1}{v} \int_{-\infty}^{\infty} 2\mathcal{R}(\delta - a) e^{-i2\pi n\delta} d\delta \\
 &= \frac{1}{v} \int_{-\infty}^{\infty} 2\mathcal{R}(\delta - a) e^{-i2\pi n(\delta-a)} d(\delta-a) e^{-i2\pi na} \\
 &= \frac{1}{v} e^{-i2\pi na} \mathcal{J}(n)
 \end{aligned}
 \tag{2.3.4}$$

Similarly

$$S_{21}^i(f) = \frac{1}{v} e^{i2\pi na} \mathcal{J}(n)
 \tag{2.3.5}$$

The response relationship can now be derived.

$$\begin{aligned}
 S^o(f) &= \alpha_1^*(if) \alpha_1(if) S_1^i(f) + \alpha_1^*(if) \alpha_2(if) S_{12}^i(f) \\
 &+ \alpha_2^*(if) \alpha_1(if) S_{21}^i(f) + \alpha_2^*(if) \alpha_2(if) S_2^i(f)
 \end{aligned}
 \tag{2.3.6}$$

$$= \frac{1}{v} \left[ \alpha_1^* \alpha_1 + \alpha_2^* \alpha_2 + \alpha_1^* \alpha_2 e^{-i2\pi na} + \alpha_2^* \alpha_1 e^{i2\pi na} \right] \mathcal{J}(n)$$

2.3.7

(omitting, for simplicity, the (if) )

The  $\alpha$ 's are receptances connecting the response with the imposed displacement  $z(t)$  at the excitation point concerned; in order that superposition should be permissible it is essential that each receptance should be established with the other excitation point assumed fixed.

This may be conveniently written as

$$S^o(f) = \frac{1}{v} [A(f) + B(f) \cos 2\pi na + C(f) \sin 2\pi na] \cdot J(n) \quad 2.3.8$$

where

$$\left. \begin{aligned} A(f) &= \alpha_1^* \alpha_1 + \alpha_2^* \alpha_2 \\ B(f) &= 2 \operatorname{Re}[\alpha_1^* \alpha_2] \\ C(f) &= 2 \operatorname{Im}[\alpha_1^* \alpha_2] \end{aligned} \right\}$$

Equation 2.3.8 establishes the response spectrum for a single track vehicle, provided we can evaluate the receptances  $\alpha_1$  (if) and  $\alpha_2$  (if), which again will be only vehicle dependent. However it may be noted that at all frequencies the traversal velocity  $v$  now appears in the exponential factors (because  $n = f/v$ ) as well as in the factor  $1/v$  and in the profile spectral density. It will be worthwhile to obtain a meaningful physical picture of this response relationship and to predict how changes in velocity might affect the response of such systems in general.

#### 2.4 The double input transfer function

Examination of equation 2.3.8 shows the response spectrum is related to the road spectrum  $J(n)$  by the function

$$\begin{aligned} |T(f)|^2 &= A(f) + B(f) \cos 2\pi na + C(f) \sin 2\pi na \\ &= \alpha_1^* \alpha_1 + \alpha_2^* \alpha_2 + \alpha_1^* \alpha_2 e^{-i2\pi na} + \alpha_2^* \alpha_1 e^{i2\pi na} \quad 2.4.1 \end{aligned}$$

i.e. 
$$S^o(f) = \frac{1}{v} |T(f)|^2 f(n) \quad 2.4.2$$

This is similar to equation 2.2.6 for the response of a single input system. It is therefore worthwhile to consider some of the properties and special cases of this function,  $|T(f)|^2$ . Whereas the single input receptance, or transfer function, is dependent only on the dynamic properties of the vehicle system this new function is also dependent on the vehicle speed since

$$n = f/v \quad 2.4.3$$

From 2.4.1 we have

$$\begin{aligned} |T(f)|^2 &= \alpha_1^* \alpha_1 + \alpha_2^* \alpha_2 + (\alpha_1^* \alpha_2 + \alpha_2^* \alpha_1) \cos 2\pi n a + i(\alpha_2^* \alpha_1 - \alpha_1^* \alpha_2) \sin 2\pi n a \\ &= \alpha_1^* \alpha_1 + \alpha_2^* \alpha_2 + 2 \sqrt{\alpha_1^* \alpha_1 \alpha_2^* \alpha_2} \cos (2\pi n a - \theta) \end{aligned} \quad 2.4.4$$

$$\text{where } \tan \theta = \frac{i(\alpha_2^* \alpha_1 - \alpha_1^* \alpha_2)}{\alpha_1^* \alpha_2 + \alpha_2^* \alpha_1} = \frac{\frac{Im(\alpha_2)}{Re(\alpha_2)} - \frac{Im(\alpha_1)}{Re(\alpha_1)}}{1 + \frac{Im(\alpha_2)}{Re(\alpha_2)} \cdot \frac{Im(\alpha_1)}{Re(\alpha_1)}} \quad 2.4.5$$

The phase angle  $\theta$  is in fact simply the phase difference between the two receptances, and the form of 2.4.4 emphasises the significance of  $|T(f)|$  which is the magnitude of the vector sum of the two receptances with relative phase modified by the quantity  $an$ .

As  $n$  changes equation 2.4.4 will oscillate between the two values:

$$\left[ (\alpha_1^* \alpha_1)^{\frac{1}{2}} \pm (\alpha_2^* \alpha_2)^{\frac{1}{2}} \right]^2$$

and/...

and its general form is given in figure 5, for one particular frequency  $f$  with the velocity  $v$  varying. It can be seen that the response is a minimum at certain speeds. A similar graph is obtained when plotting  $|T(f)|^2$  against  $a$ , the wheelbase of the vehicle.

These results may be interpreted as meaning that there are certain values for any given vehicle, of wheelbase or velocity which can produce a maximum or minimum response.

Some appreciation of the quantity  $|T(f)|^2$  in the two point problem can be obtained by considering one particular case of equation 2.4.4, when the vehicle is symmetrical fore and aft, i.e.

$$\alpha_1 = \alpha_2 \quad 2.4.6$$

Equation 2.4.4 reduces in this instance to

$$|T(f)|^2 = 2\alpha_1^* \alpha_1 \left(1 + \cos 2\pi \frac{fa}{v}\right) \quad 2.4.7$$

This will have maximum values when

$$v = fa, \frac{fa}{2}, \dots \quad 2.4.8$$

and minimum values when (figure 6)

$$v = 2fa, \frac{2}{3}fa, \dots \quad 2.4.9$$

In general, the  $\alpha$ 's will not be equal, but this special case should be close to the general case and shows that at a correct choice of speed,  $v$ , or wheelbase,  $a$ , any particular resonance peak can be eliminated.

## 2.5 Four input road-vehicle model

To take account of all four inputs of a four wheeled vehicle will require analysis in which, even if the rear wheels can be assumed to follow in the track of the front wheels, the spectra - and cross spectra - of the two separate tracks must be considered. The need to consider cross-spectra introduces considerable complexity, but it will be shown that this can be mitigated somewhat.

If we assume that the rear wheels follow the same profile as the front, so that  $\mathcal{J}_R(n)$ ,  $\mathcal{J}_{RL}(n)$ ,  $\mathcal{J}_{LR}(n)$  and  $\mathcal{J}_L(n)$  represent the direct and cross spectral densities of the two tracks  $\mathcal{Z}_R(x)$  and  $\mathcal{Z}_L(x)$  (figure 7) we can derive the response spectrum,  $S^0(f)$  starting from the general response relationship given in equation

2.1.10

$$\text{i.e. } S^0(f) = \sum_{r=1}^n \sum_{s=1}^n \alpha_r^* \alpha_s S_{rs}^i(f) \quad 2.5.1$$

Simplification of the above equation is achieved by noting

that

$$S_{11}^i(f) = S_{22}^i(f) = \frac{1}{v} \mathcal{J}_R(n) \quad 2.5.2$$

$$S_{33}^i(f) = S_{44}^i(f) = \frac{1}{v} \mathcal{J}_L(n) \quad 2.5.3$$

from Section 2.2, and that

$$S_{12}^i(f) = \frac{1}{v} e^{-i2\pi na} \mathcal{J}_R(n) \quad 2.5.4$$

$$S_{34}^i(f) = \frac{1}{v} e^{-i2\pi na} \mathcal{J}_L(n) \quad 2.5.5$$

$$S_{21}^i(f) = \frac{1}{v} e^{i2\pi na} \mathcal{J}_R(n) \quad 2.5.6$$

$$S_{43}^i(f) = \frac{1}{v} e^{i2\pi na} \mathcal{J}_L(n) \quad 2.5.7$$

from Section 2.3.

Consider now the cross-correlation function between the excitations at the offside and nearside front wheels.

$$\begin{aligned}
 R_{13}(\tau) &= \langle z_1(t) \cdot z_3(t + \tau) \rangle \\
 &= \langle \zeta_R(vt) \cdot \zeta_L(vt + v\tau) \rangle \\
 &= \langle \zeta_R(x) \zeta_L(x + \delta) \rangle \\
 &= \mathcal{R}_{RL}(\delta)
 \end{aligned}
 \tag{2.5.8}$$

Similarly,

$$\left. \begin{aligned}
 R_{31}(\tau) &= \mathcal{R}_{LR}(\delta) \\
 R_{24}(\tau) &= \mathcal{R}_{RL}(\delta) \\
 R_{42}(\tau) &= \mathcal{R}_{LR}(\delta)
 \end{aligned} \right\}
 \tag{2.5.9}$$

Using the transform relationship we obtain the corresponding input spectra e.g.

$$S_{13}^i(f) = \frac{1}{v} \mathcal{J}_{RL}(n) = \frac{1}{v} \mathcal{J}_{LR}^*(n)
 \tag{2.5.10}$$

By similar argument it can be proved that the relationships between the four remaining pairs of cross-spectra,  $S_{14}^i(f)$ ,  $S_{32}^i(f)$ ,  $S_{23}^i(f)$ ,  $S_{41}^i(f)$  are

$$\left. \begin{aligned}
 S_{14}^i(f) &= \frac{1}{v} e^{-i2\pi na} \mathcal{J}_{RL}(n) \\
 &= \frac{1}{v} e^{-i2\pi na} \mathcal{J}_{LR}^*(n)
 \end{aligned} \right\}
 \tag{2.5.11}$$

$$S_{32}^i(f) = \frac{1}{v} e^{-i2\pi na} \int_{LR}(n) \quad 2.5.12$$

$$S_{41}^i(f) = \frac{1}{v} e^{i2\pi na} \int_{LR}(n) \quad 2.5.13$$

$$S_{23}^i(f) = \frac{1}{v} e^{i2\pi na} \int_{LR}^*(n) \quad 2.5.14$$

Substituting the relevant relationships established above into equation 2.5.1 we reduce the response relationship to the apparently longer, but in fact simpler, form:

$$\begin{aligned} vS^0(f) = & \left[ \alpha_1^* \alpha_1 + \alpha_2^* \alpha_2 + \alpha_1^* \alpha_2 e^{-i\phi} + \alpha_2^* \alpha_1 e^{i\phi} \right] \int_R(n) \\ & + \left[ \alpha_3^* \alpha_3 + \alpha_4^* \alpha_4 + \alpha_3^* \alpha_4 e^{-i\phi} + \alpha_4^* \alpha_3 e^{i\phi} \right] \int_L(n) \\ & + \left[ \alpha_1^* \alpha_3 + \alpha_2^* \alpha_4 + \alpha_1^* \alpha_4 e^{-i\phi} + \alpha_2^* \alpha_3 e^{i\phi} \right] \int_{LR}^*(n) \\ & + \left[ \alpha_3^* \alpha_1 + \alpha_4^* \alpha_2 + \alpha_3^* \alpha_2 e^{-i\phi} + \alpha_4^* \alpha_1 e^{i\phi} \right] \int_{LR}(n) \end{aligned} \quad 2.5.15$$

where  $\phi = 2\pi \frac{f}{v} a$ , and asterisks indicate complex conjugate as before.

Equation 2.5.15 gives the response spectrum in terms of the two direct spectral densities and the complex-valued cross spectral densities of the route. Determination of the response of any component in the vehicle is thus seen to necessitate prior determination of the cross spectral densities of the road in addition to the two direct spectral densities and the various linear receptances,  $\alpha$ . If the surface profile forms part of a stationary, Gaussian random process with a mean value of zero then equation 2.5.15 completely defines the probability and frequency characteristic of the response, as the Gaussian distribution will remain Gaussian through the linear transformation [32].

Simplification of equation 2.5.15 can be achieved and prior determination of the cross spectra can be avoided if we develop certain assumptions suggested by PARKHILOVSKI [14] in 1968.

Parkhilovski suggested that the road surface be characterised by two random functions, (figure 8a)  $z(x)$ , the ordinate of the centre track and  $\psi(x)$  the angle of inclination of a transverse cross-section. Then if  $z_R(x)$  and  $z_L(x)$  are the track profiles as shown in figure 8a,

$$\left. \begin{aligned} z(x) &= \frac{z_R(x) + z_L(x)}{2} \\ \psi(x) &= \frac{z_R(x) - z_L(x)}{2b} \end{aligned} \right\} \quad 2.5.16$$

Parkhilovski assumed that the mean height  $z(x)$  and the transverse slope  $\psi(x)$  of the two random signals  $z_R(x)$  and  $z_L(x)$  were uncorrelated, so that the cross spectral density,  $S_{z\psi}(n)$  of  $z(x)$ ,  $\psi(x)$  satisfied

$$S_{z\psi}(n) = 0 \quad 2.5.17$$

Now, since this implies that the cross correlation function,  $R_{z\psi}(\delta)$  is also zero we have

$$\begin{aligned} R_{z\psi}(\delta) &= \langle z(x) \cdot \psi(x + \delta) \rangle \\ &= \left\langle \frac{z_R(x) + z_L(x)}{2} \cdot \frac{z_R(x + \delta) - z_L(x + \delta)}{2b} \right\rangle \\ &= \frac{1}{4b} \{ R_R(\delta) - R_L(\delta) + R_{LR}(\delta) - R_{RL}(\delta) \} \\ &= 0 \end{aligned}$$

which/...

which if  $R_R(\delta) = R_L(\delta)$  2.5.18

then  $R_{LR}(\delta) = R_{RL}(\delta) = R_{LR}(-\delta)$  2.5.19

Thus if we assume that the direct spectra of the tracks  $\mathcal{Z}_R(x)$  and  $\mathcal{Z}_L(x)$  are identical then it follows from Parkhilovski's hypothesis that,  $\mathcal{J}_{LR}(n)$ , the cross spectral density of the two profiles, is a real valued quantity.

The response equation 2.5.15 can be reduced now, using the above simplifications to the form

$$S^o(f) = \frac{1}{v} \left\{ [A(f) + B(f) \cos \phi + C(f) \sin \phi] \mathcal{J}_D(n) + [D(f) + E(f) \cos \phi + F(f) \sin \phi] \mathcal{J}_X(n) \right\}$$

2.5.20

where  $\mathcal{J}_D(n) = \mathcal{J}_L(n) = \mathcal{J}_R(n)$

$\mathcal{J}_X(n) = \mathcal{J}_{LR}^*(n) = \mathcal{J}_{LR}(n)$

$A(f) = \alpha_1^* \alpha_1 + \alpha_2^* \alpha_2 + \alpha_3^* \alpha_3 + \alpha_4^* \alpha_4$

$B(f) = 2 \operatorname{Re}[\alpha_1^* \alpha_2 + \alpha_3^* \alpha_4]$

$C(f) = 2 \operatorname{Im}[\alpha_1^* \alpha_2 + \alpha_3^* \alpha_4]$

$D(f) = 2 \operatorname{Re}[\alpha_1^* \alpha_3 + \alpha_2^* \alpha_4]$

$E(f) = 2 \operatorname{Re}[\alpha_1^* \alpha_4 + \alpha_3^* \alpha_2]$

$F(f) = 2 \operatorname{Im}[\alpha_1^* \alpha_4 + \alpha_3^* \alpha_2]$

$\phi = 2\pi \frac{f}{v} a$

which/...

which can be written as

$$S^0(f) = \frac{1}{v} [\Gamma_D(f)]^2 \mathcal{J}_D(n) + \frac{1}{v} [\Gamma_X(f)]^2 \mathcal{J}_X(n) \quad 2.5.21$$

where

$$\left. \begin{aligned} [\Gamma_D(f)]^2 &= A(f) + B(f) \cos \phi + C(f) \sin \phi \\ [\Gamma_X(f)]^2 &= D(f) + E(f) \cos \phi + F(f) \sin \phi \end{aligned} \right\} \quad 2.5.22$$

If we define a coherency function  $g(n)$  by

$$g^2(n) = \frac{|\mathcal{J}_{IR}(n)|^2}{\mathcal{J}_L(n) \cdot \mathcal{J}_R(n)} \quad 2.5.23$$

(here the quantity  $g^2(n)$  is analogous to the quantity  $\gamma^2(f)$  as used elsewhere in the literature [5] ) then for the case under consideration this reduces to

$$g(n) = \mathcal{J}_X(n) / \mathcal{J}_D(n) \quad 2.5.24$$

We can then define a corresponding  $g_v(f)$  such that

$$g_v(f) = g_v(nv) = g(n) \quad 2.5.25$$

and it should be noted that for any given  $n$ ,  $g_v(f)$  must be a function of velocity.

From equations 2.5.21 and 2.5.25 we obtain

$$S^0(f) = \frac{1}{v} \left\{ [\Gamma_D(f)]^2 + g_v(f) [\Gamma_X(f)]^2 \right\} \mathcal{J}_D(n) \quad 2.5.26$$

This equation describes the response of a four wheeled vehicle to random road surface inputs. It implies that the response depends on

i) the quantities  $\Gamma_D(f)$  and  $\Gamma_X(f)$ .

These quantities in turn define the dynamic properties of the vehicle and are functions of frequency and velocity due to the phased input at the rear.

ii) the coherency function  $g_v(f)$  which is derived from  $g(n)$  and thus is dependent on the road surface properties and the velocity  $v$ , because of the relationship between  $n$  and  $f$ . Moreover, it is implicitly assumed in the definition of the coherency function  $g(n)$  that it must also be dependent on the track width  $2b$ , i.e. the distance between the measured tracks  $z'_R(x)$  and  $z'_L(x)$ . The exact relationship is not at all clear at this stage but will be explained later.

iii) the direct spectrum  $J_D(n)$  of either track in the direction of traverse of the vehicle.

## 2.6 The coherency function, $g(n)$

To elucidate some of the implications of the response equation 2.5.26, let us first consider two special cases, that when

$$\left. \begin{array}{l} \text{i) } g(n) = 1 \\ \text{ii) } g(n) = 0 \end{array} \right\} \quad 0 \leq n \leq \infty \quad 2.6.1$$

Coherency function  $g(n) = 1$

This implies an equality between the direct and cross-spectra, and produces a road surface of a cylindrical nature, with random undulations only in the direction of traverse. Consideration of the dynamic properties of the vehicle will permit the assumption that

$$\left. \begin{aligned} \alpha_1 &= \alpha_3 \\ \alpha_2 &= \alpha_4 \end{aligned} \right\} \quad 2.6.2$$

provided we measure the response at a point along the centre line between the two tracks. This then reduces the response equation to

$$S^o(f) = \frac{1}{v} \left\{ [T_D(f)]^2 + [T_X(f)]^2 \right\} S_D(n) \quad 2.6.3$$

and expanding inside the bracket and substituting the relationship of equation 2.6.2 we obtain

$$S^o(f) = \frac{4}{v} \left\{ \alpha_1^* \alpha_1 + \alpha_2^* \alpha_2 + \alpha_1^* \alpha_2 e^{-i\phi} + \alpha_2^* \alpha_1 e^{i\phi} \right\} S_D(n) \quad 2.6.4$$

which is of the form of the response relationship obtained in the two input case when the excitation was considered to be due to a single track (equation 2.3.7), noting that in this case, because of the model considered the  $\alpha$ 's will each be one half of the  $\alpha$ 's in the double input problem.

From 2.5.16 we can derive the spectra of the mean track and slope between the two tracks in terms of the spectra and cross-spectra/...

spectra of the two measured tracks.

$$\begin{aligned} S^{\mathcal{Z}}(n) &= \frac{1}{4} \left[ S_R(n) + S_L(n) + S_{RL}(n) + S_{LR}(n) \right] \\ &= \frac{1}{2} \left[ S_D(n) + S_X(n) \right] \end{aligned} \quad 2.6.5$$

and

$$\begin{aligned} S^{\mathcal{Y}}(n) &= \frac{1}{4b^2} \left[ S_R(n) + S_L(n) - S_{RL}(n) - S_{LR}(n) \right] \\ &= \frac{1}{2b^2} \left[ S_D(n) - S_X(n) \right] \end{aligned} \quad 2.6.6$$

If we now insert the relationship for the coherency function from (2.5.24) we obtain

$$S^{\mathcal{Z}}(n) = \frac{1+g(n)}{2} S_D(n) \quad 2.6.7$$

$$S^{\mathcal{Y}}(n) = \frac{1-g(n)}{2b^2} S_D(n) \quad 2.6.8$$

For the case under consideration when  $g(n) = 1$  this implies that

$$\left. \begin{aligned} S^{\mathcal{Z}}(n) &= S_D(n) \\ S^{\mathcal{Y}}(n) &= 0 \end{aligned} \right\} \quad 2.6.9$$

which satisfies our physical picture of the problem.

Coherency function  $g(n) = 0$

From equation 2.5.24 this implies that the cross-spectrum between the two tracks  $\mathcal{Z}_R(x)$  and  $\mathcal{Z}_L(x)$  is zero, i.e.

$$S_X(n) = 0 \quad 2.6.10$$

The response equation under the same assumptions stated in the previous section reduces to

$$S^0(f) = \frac{2}{v} \left\{ \alpha_1^* \alpha_1 + \alpha_2^* \alpha_2 + \alpha_1^* \alpha_2 e^{-i\phi} + \alpha_2^* \alpha_1 e^{i\phi} \right\} J_D(n) \quad 2.6.11$$

which at each frequency  $f$  is one half the value of the completely coherent case, implying a 3 dB reduction in the response,  $z_0(t)$ , of the system.

From equations 2.6.7 and 2.6.8 putting  $g(n) = 0$  yields

$$\left. \begin{aligned} S^3(n) &= J_D(n)/2 \\ S^4(n) &= J_D(n)/2b^2 \end{aligned} \right\} \quad 2.6.12$$

which gives the relationship between the mean and slope spectra for two incoherent tracks to be

$$S^3(n) = b^2 S^4(n) \quad 2.6.13$$

remembering also that  $\frac{\partial S^4(n)}{\partial \phi} = 0$ .

General case, coherency function  $0 < g(n) < 1$

For roads in general neither of the above cases will be true, but it will be possible to define certain limits on the value of this function. Just as the more common coherency function  $\gamma^2(f)$  satisfies for all  $f$  [5]

$$0 \leq \gamma^2(f) \leq 1 \quad 2.6.14$$

so/...

so by similar argument used to derive 2.6.14 [5] the function  $g(n)$  must satisfy the same conditions for all  $n$ .

Moreover, from practical considerations it is possible to say that  $g(n)$  must approach unity for small wavenumbers, i.e. long wavelength, and zero for large wave numbers, i.e. short wavelength.

Consider the definition of coherency expressed in equation 2.5.24:

$$g(n) = \frac{J_X(n)}{J_D(n)} \quad 2.6.15$$

Transposing this equation gives

$$J_X(n) = g(n) J_D(n) \quad 2.6.16$$

and thus this function,  $g(n)$  which must be real since it was shown (equation 2.5.19) that  $J_X(n)$  was real, can be considered as the amplification factor by which the direct spectrum must be multiplied to obtain the cross spectrum. Clearly then this coherency function is simply analogous to the amplitude gain of a linear system expressed in terms of the cross-spectrum between the response and the excitation spectrum which can be derived from equation 2.1.9:

$$|\alpha_{01}(f)|^2 = \frac{|s_{10}(f)|^2}{[s_1(f)]^2} \quad 2.6.17$$

Taking/...

Taking the Fourier transforms of equation 2.6.16 yields

$$R_X(\delta) = \int_0^{\infty} h(\delta - \delta') R_D(\delta') d\delta' \quad 2.6.18$$

where  $h(\delta)$  is the Fourier transform of  $g(n)$ . This equation gives the relationship between the cross-correlation function of the two tracks, which is even, and the autocorrelation of either one of them.

## 2.7 The road as a completely homogeneous surface

In our treatment of the problem of road surface description we have only considered the statistical properties along the direction of traverse. This has enabled us to define a coherency function  $g(n)$  which although simply defined by equation 2.5.24 left in doubt its exact relationship with the surface properties in a direction perpendicular to the traversal direction. Thus although for any given vehicle track width  $2b$ , equation 2.5.26 completely defines the response, if we change the vehicle track to  $2b'$  whereas the direct spectrum of the road surface irregularities will not change the coherency function may. To obtain a response relationship will require a new measurement of the new tracks  $Z_R(x)$  and  $Z_L(x)$  to obtain the new cross spectrum  $S_X(n)$ , (there is no reason to assume that the assumptions of equal direct spectra and a real valued cross-spectrum will not be valid) and hence a new coherency function

$$g'(n) = S_X(n) / S_D(n) \quad 2.7.1$$

In order to examine the possibility of deriving  $q'(n)$  for a track width  $2b'$  from any given  $q(n)$  for a track width  $2b$  let us now consider an analysis of the surface irregularities, treating them as part of a two dimensional stationary Gaussian random process  $\{z(x,y)\}$ .

The two dimensional correlation function can be defined as

$$R(\xi, \eta) = \lim_{\substack{x \rightarrow \infty \\ y \rightarrow \infty}} \frac{1}{xy} \int_{-x}^x \int_{-y}^y z(x,y) \cdot z(x+\xi, y+\eta) dx dy \quad 2.7.2$$

which with our usual notation of angular brackets to denote averaging can be written as

$$R(\xi, \eta) = \langle z(x,y) \cdot z(x+\xi, y+\eta) \rangle \quad 2.7.3$$

Putting respectively  $\eta = 0$ , and  $\xi = 0$  in equation 2.7.3 gives the autocorrelation functions in the x and y directions.

$$R_x(\xi) = R(\xi, 0) \quad 2.7.4$$

$$R_y(\eta) = R(0, \eta) \quad 2.7.5$$

and hence we can assume that  $R(\xi, \eta)$  will be even in  $\xi$  for  $\eta = 0$  and even in  $\eta$  for  $\xi = 0$ .

Consider the two tracks  $z_R(x)$  and  $z_L(x)$  (figure 8b) along the road surface which are defined for  $y_R = -b$  and  $y_L = +b$ . The mean heights  $\bar{z}(x)$  and slope  $\psi(x)$  between these tracks can be written as

$$\left. \begin{aligned} \bar{z}(x) &= \frac{z(x, -b) + z(x, +b)}{2} \\ \psi(x) &= \frac{z(x, -b) - z(x, +b)}{2b} \end{aligned} \right\} \quad 2.7.6$$

Examination of the cross-correlation between these two parameters yields

$$\begin{aligned}
 R_{\delta y}(\xi) &= \frac{1}{4b} \langle [z(x, b) + z(x, -b)] [z(x + \xi, b) - z(x + \xi, -b)] \rangle \\
 &= \frac{1}{4b} \langle z(x, b) \cdot z(x + \xi, b) \rangle \\
 &\quad - \langle z(x, -b) \cdot z(x + \xi, -b) \rangle - \langle z(x, b) \cdot z(x + \xi, -b) \rangle \\
 &\quad + \langle z(x, -b) \cdot z(x + \xi, b) \rangle \\
 &= \frac{1}{4b} [R(\xi, 0) - R(\xi, 0) - R(\xi, -2b) + R(\xi, 2b)] \\
 &= \frac{1}{4b} [R(\xi, 2b) - R(\xi, -2b)] \qquad 2.7.7 \\
 &= 0
 \end{aligned}$$

only if  $R(\xi, \eta)$  is even in  $\xi, \eta$ , or if  $\xi = 0$ .

The cross correlation between the two original tracks

$$\left. \begin{aligned}
 z_R(x) &= z(x, -b) \\
 z_L(x) &= z(x, b)
 \end{aligned} \right\} \qquad 2.7.8$$

has been defined by

$$\begin{aligned}
 R_{RL}(\xi) &= \langle z_R(x) \cdot z_L(x + \xi) \rangle \\
 &= \langle z(x, -b) \cdot z(x + \xi, b) \rangle \\
 &= R(\xi, 2b) \qquad 2.7.9
 \end{aligned}$$

and thus  $R(\xi, \eta)$  can be obtained by measuring  $R_{RL}(\xi)$  for a range of values of  $2b$ .

However/...

However, since

$$R_{LR}(\xi) = R(\xi, -2b) \quad 2.7.10$$

and since the previous analysis has exhibited that (equations 2.5.17, 2.5.18, 2.5.19)

$$R_{RL}(\xi) = R_{LR}(\xi) \quad 2.7.11$$

then it is reasonable to suggest that  $R(\xi, \eta)$  will be even in both  $\xi$  and  $\eta$ , and that the surface will be completely homogeneous.

If homogeneity is complete then not only must

$$R(\xi, 0) = R(0, \eta) \quad 2.7.12$$

but also the autocorrelation function of the profile along any straight line must be identical in form to that taken along any other straight line. This requires

$$R(\rho \cos \theta, \rho \sin \theta) = R(\rho), \quad 2.7.13$$

the latter being defined in the usual way along a line making an angle  $\theta$  with the x axis (figure 8b).

Equations 2.7.10 and 2.7.13 together imply that

$$R_{LR}(\xi) = R(\rho) = R(\sqrt{\xi^2 + 4b^2}) \quad 2.7.14$$

and if use is made of the ergodic hypothesis this may seem to be obvious, the definitions of both sides being identical and equal to  $\langle z(x_1, y_1) \cdot z(x_2, y_2) \rangle$  and averaging across the ensemble causes no difficulty.

The direct and cross spectral densities of the two tracks  $Z_R(x)$  and  $Z_L(x)$  separated by a distance  $2b$  follow by Fourier transformation.

$$S_R(n) = S_L(n) = S_D(n) = \int_{-\infty}^{\infty} 2R(\xi) e^{-i2\pi n\xi} d\xi \quad 2.7.15$$

$$\begin{aligned} S_{LR}(n) = S_{RL}(n) = S_X(n) &= \int_{-\infty}^{\infty} 2R_{LR}(\xi) e^{-i2\pi n\xi} d\xi \\ &= \int_{-\infty}^{\infty} 2R(\rho) e^{-i2\pi n\xi} d\xi \end{aligned} \quad 2.7.16$$

$$\text{where } \rho = \sqrt{\xi^2 + 4b^2} \quad 2.7.17$$

Thus from a knowledge of the autocorrelation function  $R(\xi)$  of any single track along the road the cross-correlation  $R_{LR}(\xi)$  can be derived from equation 2.7.14 by first evaluating the autocorrelation function

$$R(\rho) = R(\sqrt{\xi^2 + 4b^2}) \quad 2.7.18$$

and then equating

$$R_{LR}(\xi) = R(\rho) \quad 2.7.19$$

The coherency function  $g(n)$  defined by equation 2.5.24 can then be obtained for any value of track width  $2b$  since

$$\begin{aligned} g(n) &= \frac{S_X(n)}{S_D(n)} = \frac{S_{LR}(n)}{S_D(n)} = \frac{2 \int_{-\infty}^{\infty} R_{LR}(\xi) e^{-i2\pi n\xi} d\xi}{2 \int_{-\infty}^{\infty} R(\xi) e^{-i2\pi n\xi} d\xi} \\ &= \frac{\int_{-\infty}^{\infty} R(\sqrt{\xi^2 + 4b^2}) e^{-i2\pi n\xi} d\xi}{\int_{-\infty}^{\infty} R(\xi) e^{-i2\pi n\xi} d\xi} \end{aligned} \quad 2.7.20$$

## 2.8 Stationarity, ergodicity and linearity

Throughout this work it has been assumed that for stretches long enough for statistical descriptions to be meaningful, representation of the road surface as a realisation of a stationary Gaussian process is permissible. DOOB [33] showed that a Gaussian random process whose power spectral density functions are absolutely continuous will be ergodic and hence the random process  $\{z(x)\}$  which represents the road surface will be an ergodic stationary process. It has been shown by DAVENPORT and ROOT [32] that if a Gaussian process undergoes a linear transformation, then the output will still be a Gaussian process, and hence the vehicle response will conform to the same form of description as the input if the vehicle model is assumed linear throughout.

Road surface spectra [12, 13] are continuous, i.e. no delta functions corresponding to infinite mean square densities at discrete frequencies, and thus we need only satisfy ourselves on the conditions of stationarity and that the surface is characterised by a Gaussian distribution.

One basic requirement for a Gaussian profile to be (nearly) stationary is that it has zero mean, or constant mean. Although this may not be true of "raw" road data, as most roads exhibit trends in slope, clearly as these slopes will not affect the dynamic response of the vehicle (slopes containing wavelengths greater than 50 m would require a vehicle to travel at a speed of  $50 \times f$  m/s to excite any frequency  $f$ ) they must therefore be filtered from the data, and the subsequent analysis carried out using the new filtered/...

filtered data as the random process characterising the road. This filtered data will contain a zero mean value and hence indicate that the assumption of stationarity is acceptable provided we can satisfy one further condition: the autocorrelation function  $R(\delta)$  will yield the same results for all values of  $x$ , i.e. it is independent of the length of road taken for measurement. As the spectral densities of similar road surfaces (e.g. motorways) are similar [12,13] and as it is shown in this work that the same spectral density is obtained for any longitudinal track along the road, then it seems reasonable to accept that the random process  $\{z_0(x)\}$  characterising the road surface is (weakly) stationary.

To justify the assumption that the road irregularities follow a Gaussian distribution is much more difficult as, in the first instance, only a finite data length is available for analysis. ROBSON [1] showed that the expectation of a peak greater than  $\lambda\sigma_x$  per unit time of a Gaussian process was given by

$$\frac{1}{2\pi} \frac{\sigma_{\dot{x}}}{\sigma_x} e^{-\lambda^2/2} \quad 2.8.1$$

where  $\sigma_{\dot{x}}^2 = \langle \dot{x}^2(t) \rangle \quad 2.8.2$

For the problem under consideration converting equation 2.8.1 to the spatial domain we observe that the expectation of a peak greater than  $\lambda\sigma_y$  per unit distance is given by

$$\frac{1}{2\pi} \frac{\sigma_{z'}}{\sigma_y} e^{-\lambda^2/2} \quad 2.8.3$$

$$= \left[ \frac{\int_0^\infty n^2 J(n) dn}{\int_0^\infty J(n) dn} \right] \frac{1}{2} e^{-\lambda^2/2} \quad 2.8.4$$

which for a typical road spectrum  $S(n)$  in which low frequency will predominate will be small especially when considering peaks greater than  $3\sigma$  (i.e.  $\lambda = 3$ ). Hence it is difficult for a finite data length ever to completely satisfy the Gaussian distribution for a signal whose spectrum is proportional to  $1/n^2$  as is the present case.

However, in the present study, it is shown that a Gaussian distribution can be fitted to the experimental data, bearing in mind that the fit is obtained over the mean position, but there is little published evidence to support this claim, although many authors in this field widely accept this assumption.

To justify a rigorous analytical treatment of the response problem by the methods outlined in this Chapter requires the model characterising the vehicle to be a linear constant parameter system. It has often been remarked in engineering circles that "the world is non-linear" and this phrase is quite applicable to the dynamic vehicle model. Suspension springs and shock absorbers are generally non-linear units and there is an appreciable amount of friction in the suspension system as a whole. However, a linear model is necessary to analyse the vehicle motions and while it places some restrictions on the model analysis it does allow for a convenient solution that will yield a good deal of insight into the vehicle behaviour.

In the last resort justification of the validity of all these assumptions can be confirmed from the comparison between analysis and experiment which is presented in Chapter 4.

## CHAPTER 3

### THE RESPONSE CHARACTERISTICS OF VEHICLE MODELS TO HARMONIC AND RANDOM EXCITATION

Having developed the basic theory of random vibration as it can be applied to the problem of profile excitation we may proceed with the study of the response of some simple models to profile excited vibration. This simplification is necessary since before we can apply this theory to predict the response of a real vehicle, we must first understand the response behaviour. Initially therefore the system to be considered will be a single-degree of freedom system with one input. The excitation will be assumed to be a stationary random Gaussian process  $\{z(x)\}$  with zero mean value and a spectral density given by

$$S_D(n) = \frac{S_1}{4\pi^2 n^2}$$

(which implies an excitation spectrum which is white in terms of slope). We will then proceed to examine a model with two inputs and so cover the simple cases as fully as possible. Models of increasing complexity will be presented and their significant trends in behaviour examined.

#### 3.1 Response relationship: single degree of freedom, single input model

The response relationship for a single input system is given by

$$S^o(f) = |\alpha(if)|^2 S^i(f) \quad 3.1.1$$

where/...

where

$$S^i(f) = \frac{1}{v} \mathcal{J}(n) \quad 3.1.2$$

and

$$f = vn$$

It is possible to interpret this relationship in a variety of ways. While the input variable is best kept displacement, the output could reasonably be displacement, velocity, or acceleration, or even relative displacement. The receptance, or transfer function, must of course be defined to conform with the chosen input and output.

It will therefore be convenient to use a more specific notation; we shall use e.g.  $S^0(\ddot{z}, f)$  for acceleration output spectrum

$$\alpha(\ddot{z}, z, f) \text{ for displacement-acceleration receptance.}$$

For a single degree of freedom system (figure 9) the receptances will be as follows

$$\alpha(z, z_1, f) = X$$

$$\alpha(\dot{z}, z_1, f) = i2\pi fX \quad 3.1.3$$

$$\alpha(\ddot{z}, z_1, f) = -4\pi^2 f^2 X$$

where

$$X = \frac{f_n^2 + i2\zeta f f_n}{f_n^2 - f^2 + i2\zeta f f_n} \quad 3.1.4$$

and

$$\alpha(z - z_1, z_1, f) = \frac{f^2}{f_n^2 - f^2 + i2\zeta f f_n} \quad 3.1.5$$

In order to explore the response of this system to a stationary Gaussian random process with zero mean, it is important that we choose a typical profile spectrum. This need not reproduce closely any actual profile spectrum but should possess the essential features of actual spectra and, consistent with this, should be as simple as possible.

The forms of observed spectra [12,13] suggest that a white slope spectrum would form a suitable basis to establish the fundamental response characteristics, i.e.

$$J(\zeta', n) = J_1 \quad 3.1.6$$

whence the profile spectrum is given by

$$J(n) = \frac{J_1}{4\pi^2 n^2} \quad 3.1.7$$

These imply an infinite mean square,  $\langle \zeta'(x) \rangle$  and also that  $J(n)$  has an infinite density at  $n = 0$ . However, as it is neither practical nor possible to evaluate response at these extremes we will take our limits of integration to be finite and non-zero.

It follows from 3.1.7 that the input spectrum to the vehicle is given by

$$\begin{aligned} S^i(f) &= \frac{1}{v} \cdot \frac{J_1}{4\pi^2 f^2 / v^2} \\ &= \frac{J_1 v}{4\pi^2 f^2} \end{aligned} \quad 3.1.8$$

and it/...

and it can be seen that increasing the velocity,  $v$ , simply has the effect of increasing  $S^i(f)$  at all frequencies.

After an initial transient lasting several correlation intervals the response,  $z(t)$ , becomes a stationary Gaussian process with zero mean. The response spectral density can be obtained by combining equations 3.1.1, 3.1.8 and the suitable receptance.

$$S^o(z, f) = |X|^2 \frac{v}{4\pi^2 f^2} S_1 \quad 3.1.9$$

$$\begin{aligned} S^o(\ddot{z}, f) &= 16\pi^4 f^4 |X|^2 \frac{v}{4\pi^2 f^2} S_1 \\ &= 4\pi^2 f^2 |X|^2 v S_1 \end{aligned} \quad 3.1.10$$

Again, increasing  $v$  has the effect of increasing the response at all frequencies.

The mean square response can be evaluated by integration of the response spectrum. However, to avoid difficulties arising from this integration we shall define a band-limited mean square,  $\tilde{\sigma}^2$ , to be

$$\tilde{\sigma}^2 = \int_{f_2}^{f_1} S(f) df \quad 3.1.11$$

In the examination of the response characteristics of this simple road-vehicle model (figure 9) we will be interested in two response parameters:

- i) displacement of the mass  $m$ ,  $z(t)$
- ii) acceleration of the mass  $m$ ,  $\ddot{z}(t)$ .

Their response spectra are given by equations 3.1.9 and 3.1.10 respectively. The displacement response spectrum is shown in figure 11 for parameters given in Table 1 which are typical of a real vehicle-road system. It is obvious from equation

TABLE 1

$f_n$	$\zeta$	$f_1$	$f_2$
1.5 Hz	0.1	0.1 Hz	25 Hz

Single Degree of freedom model - parameters

3.1.9 that as

$$f \rightarrow 0 \quad \text{so} \quad S^0(z, f) \rightarrow \infty$$

Also, it is worth noting that after resonance the response falls off sharply at 12 dB/octave and thus the characteristic shape of the acceleration response spectrum (figure 12) will be white when remote from resonance.

The mean square response in both cases will increase linearly with velocity,  $v$ . The effect of varying the model parameters is of little interest with the exception of the damping factor,  $\zeta$ , which has the effect of reducing the mean square acceleration response/...

response. (This parameter has been suggested by some authors [31,34] [35] as providing a ride comfort index). Figures 13 and 14 show how  $\tilde{\sigma}_z$  and  $\tilde{\sigma}_z$  vary with damping and a minimum mean square acceleration (optimum comfort) is realised.

It was shown by DINCA (1969) [31] who was aided by the author, that in a parametric study of this vehicle - road model, and using as input data various specified forms of road spectra, (see Chapter 4, Section 4.2) there did exist a value of  $\zeta$  between 0.2 and 0.3 for which the mean square acceleration response was a minimum, thus reinforcing the general result of figure 13.

This type of optimisation procedure was advanced by THOMPSON [36] (1969) who using the same evaluation criterion, optimised suspension damping in a more complex vehicle model with both linear and non-linear damping.

### 3.2 Single degree of freedom, double input case

To appreciate the effects of a second input subjected to the same random excitation as the first, but separated by a constant lag, consider now the vehicle model shown in figure 10, which is symmetric front and rear. It will be subjected to symmetric inputs with the same form of excitation as in the previous case, with spectral density given by

$$S(n) = \frac{S_1}{4\pi^2 n^2} \quad 3.2.1$$

The response spectrum, given by equation 2.3.8 for the general case of a vehicle with two inputs, reduces to (equation 2.4.7)

$$S^0(z, f) = 2\alpha_1^* \alpha_1 (1 + \cos 2\pi \frac{fa}{v}) \frac{S_1 v}{4\pi^2 f^2} \quad 3.2.2$$

when

$$\alpha_1 = \alpha_2$$

The response  $z(t)$  of this model is related to the excitations  $z_1(t), z_2(t)$  by the differential equation

$$\ddot{z} + 2\zeta\omega_n\dot{z} + \omega_n^2 z = \zeta\omega_n(\dot{z}_1 + \dot{z}_2) + \frac{1}{2}\omega_n^2(z_1 + z_2) \quad 3.2.3$$

from which we obtain

$$\begin{aligned} \alpha(z, z_1, f) &= \frac{\frac{\omega_n^2}{2} + i\zeta\omega\omega_n}{(\omega_n^2 - \omega^2) + i2\zeta\omega\omega_n} \\ &= \frac{1}{2} \cdot \frac{f_n^2 + i2\zeta ff_n}{(f_n^2 - f^2) + i2\zeta ff_n} \\ &= \alpha(z, z_2, f) \end{aligned} \quad 3.2.4$$

Combining equation 3.2.2 and 3.2.4 we obtain the response spectral density

$$S^o(z, f) = \frac{1}{2} \cdot \frac{f_n^4 + 4\zeta^2 f^2 f_n^2}{(f_n^2 - f^2)^2 + 4\zeta^2 f^2 f_n^2} \left(1 + \cos 2\pi \frac{fa}{v}\right) \frac{\int_1^v}{4\pi^2 f^2} \quad 3.2.5$$

which if the wheelbase,  $a$ , is zero corresponds to the single input spectrum given by equation 3.1.9.

The acceleration spectrum is given by

$$S^o(\ddot{z}, f) = 16\pi^4 f^4 S^o(z, f) \quad 3.2.6$$

which can be related to that obtained from the single input case

by/...

by

$$S^0(\ddot{z}, f) = \left[ S^0(\ddot{z}, f) \right]_{\text{Single}} \times \frac{1}{2} (1 + \cos 2\pi \frac{fa}{v}) \quad 3.2.7$$

It is clear by examination of figures 6 and 12 that by a suitable choice of speed or wheelbase we can eliminate or reduce the resonance in the response spectrum (3.2.7). For example, to eliminate the resonance at 1.5 Hz in figure 12 we could choose from figure 6

$$\left[ \frac{v}{af} \right] = 2 \quad 3.2.8$$

(f = 1.5)

$$\Rightarrow \frac{v}{a} = 3 \quad 3.2.9$$

and the new response spectrum would peak when (equation 2.4.8)

$$\frac{v}{af} = 1, 0.5 \dots \quad 3.2.10$$

$$\text{i.e. at } f = 3 \text{ Hz, } 6\text{Hz} \dots \quad 3.2.11$$

This is shown in figure 15.

Although in general the receptances,  $\alpha_1$  and  $\alpha_2$  will not be equal, the case considered here will not be far removed from the practical problem, and has demonstrated a method by which the wheelbase of a vehicle can be chosen to avoid major resonances in the vehicle. It was shown by BOGDANOFF and KOZIN [37] that the wheelbase,  $a$ , is an important variable in determining limiting vehicle velocity if the limit on driver comfort is set by the maximum value of  $S^0(z, f)$ .

The variation of the mean square response with speed will not be linear for low speeds, but as speed increases

$$\cos 2\pi \frac{fa}{v} \longrightarrow 1 \quad 3.2.12$$

and linearity is approached (figure 16).

### 3.3 Two-degree of freedom - single input model

In an attempt to obtain a more realistic vehicle model consider now the simple linear system of figure 17, which will represent a single wheel-suspension unit, subjected to a single random displacement excitation imposed by the road. The response spectra, are given by the general relationship of equation 3.1.1 and the interest in this more realistic model is the effect on the response of varying the model parameters.

This model has been extensively used to represent the basic dynamic properties of a vehicle suspension system, [26, 28, 29, 34, 36] and it is not the object of this thesis to dwell at great length on its characteristics. A recent parametric study of this model may be found in MITSCHKE'S "Dynamik der Kraftfahrzeuge" [38] (1972). However, to maintain continuity and aid understanding of the experimental work which will follow in a subsequent chapter the main results of the author's study will be presented. (They are in broad agreement with MITSCHKE'S work).

The model shown in figure 17 is governed by the differential equations

$$\begin{bmatrix} m_{u_1} & 0 \\ 0 & m_{s_1} \end{bmatrix} \begin{bmatrix} \ddot{z}_1 \\ \ddot{z}_{s_1} \end{bmatrix} + \begin{bmatrix} c_{T_1} + c_1 & -c_1 \\ -c_1 & c_1 \end{bmatrix} \begin{bmatrix} \dot{z}_1 \\ \dot{z}_{s_1} \end{bmatrix} + \begin{bmatrix} k_{T_1} + k_1 & -k_1 \\ -k_1 & k_1 \end{bmatrix} \begin{bmatrix} z_1 \\ z_{s_1} \end{bmatrix} = \begin{bmatrix} c_{T_1} \dot{z} + k_{T_1} z \\ 0 \end{bmatrix} \tag{3.3.1}$$

which may be solved for the various receptances -

- $\alpha(z_{s_1}, z, f)$  : displacement of mass  $m_{s_1}$
- $\alpha(z_{u_1}, z, f)$  : displacement of mass  $m_{u_1}$
- $\alpha(z_{s_1} - z_{u_1}, z, f)$  : relative displacement of spring  $k_1$
- $\alpha(\ddot{z}_{s_1}, z, f)$  : acceleration of mass  $m_{s_1}$

The relationship between the model parameters and a real vehicle is given in Table 2.

TABLE 2

PARAMETER	VEHICLE COMPONENT
$m_{s_1}$	proportion of vehicle sprung mass (i.e. body) carried by single suspension system
$m_{u_1}$	proportion of vehicle unsprung mass (i.e. axle, etc.) carried by single suspension system
$k_{T_1}, c_{T_1}$	tyre stiffness and damping parameters
$k_1, c_1$	suspension spring rate and linear damping coefficient

Description of Model Parameters

It is the object of this paragraph to examine these parameters in order to gain a measure of their relative importance on the response to base excitation of the model. This will give a guide to the accuracy which must be attained in assessing their values for a real vehicle so as to enable successful prediction of vehicle response to be carried out.

The system parameters are defined as:

$$\text{body natural frequency } f_{n_1} = \frac{1}{2\pi} \sqrt{\frac{k_1}{m_{s_1}}} \quad 3.3.2$$

$$\text{axle natural frequency } f_{T_1} = \frac{1}{2\pi} \sqrt{\frac{k_{T_1}}{m_{u_1}}} \quad 3.3.3$$

$$\text{suspension damping factor } \zeta_1 = \frac{c_1}{2\sqrt{k_1 m_{s_1}}} \quad 3.3.4$$

$$\text{tyre damping factor } \zeta_{T_1} = \frac{c_{T_1}}{2\sqrt{k_{T_1} m_{u_1}}} \quad 3.3.5$$

The subscript (1) is used to denote that these parameters refer to a single suspension unit (e.g. front) and corresponding definitions with subscript (2) will be used when we consider a vehicle with two inputs. Natural frequency and damping parameters discussed throughout this work will be defined in the general terms of equations 3.3.2 to equations 3.3.5, (i.e. uncoupled frequencies).

3.3.1. Analysis of body lifting acceleration,  $\ddot{z}_{s_1}$ : As previously mentioned this parameter is used as a ride comfort index. Solving equation 3.3.1 for  $\alpha(\ddot{z}_{s_1}, z, f)$  and using parameter values typical of modern British vehicles we can plot the receptance against frequency/...

frequency, varying the sprung mass  $m_{s_1}$ , suspension spring stiffness  $k_1$ , suspension damping and tyre damping.

It is obvious from figures 18-21 that an increase in  $m_{s_1}$  decreases the acceleration response and, of course, lowers the natural frequency. Thus an empty vehicle has poorer ride comfort, according to the criterion, than a laden vehicle. Variation of the suspension spring rate,  $k_1$ , causes a decrease in the receptance for a decrease in  $k_1$ , especially at the first, body bounce, natural frequency. Change in suspension damping yields, as one would expect, the characteristic effect at body resonance. However, at the axle resonance ( $f_n \sim 10$  Hz), body acceleration at first decreases with higher suspension damping, but increases again as  $\zeta_1$  increases further. There is thus a minimum at a relatively low damping factor.

The tyre parameters,  $k_T$ ,  $\zeta_T$ , have little effect on  $\alpha(\ddot{z}_{s_1}, z, f)$  noting that tyre damping is of the order  $\zeta_T < 0.1$  [39].

3.3.2 Analysis of the displacement  $z_{s_1}$ : This tends to be a relatively uninteresting parameter from the analytical side and it is questionable whether it would be useful practically due to the difficulty of measurement. It is worth noting, however, that as suspension damping tends to be moderately high ( $\zeta_1$  in the range 0.15 - 0.4) the receptance  $|\alpha(z_{s_1}, z, f)|$  predominates at the first natural frequency and behaves in a like manner to that of a single degree of freedom model.

3.3.3. Analysis of relative suspension movement  $z_{s_i} - z_i$  : This parameter will determine the force in the suspension spring as

$$F_i = k_i(z_{s_i} - z_i) \quad 3.3.6$$

and this force is one of the measurements taken on a real vehicle and compared with the theoretical predicted force in Chapter 4. Plotting  $\alpha(z_{s_i} - z_i, z, f)$  against frequency (figures 22 to 24) it can be seen that the variation of mass,  $m_{s_i}$ , and suspension spring rate have the obvious effects on this parameter i.e. lowering or raising the natural frequency respectively. Lowering of suspension damping will increase the magnitude of the first resonance peak and if sufficiently low ( $< 0.125$ ) allow the axle resonance to become visible.

Variation of axle mass,  $m_{u_i}$ , or tyre hardness  $k_i$ , has little effect on any of the above receptances, but it should be mentioned that any effects of variation of these parameters only becomes noticeable in the axle resonance region.

In an attempt to summarise the above results we shall restrict our comments to the determination of  $\alpha(\ddot{z}_{s_i}, z, f)$  and  $\alpha(z_{s_i} - z_i, z, f)$  as body acceleration and spring force will be the parameters finally measured by experiment. It is abundantly clear (figures 20,24) that for a successful prediction of vehicle response, based on this model, determination of a suspension damping parameter is of primary importance. Vehicle sprung mass, is liable to be accurately known/...

known, but a small variation on  $m_{s_1}$ , (figure 18, insert) will produce a proportional change on the receptance. It will be necessary to obtain an accurate estimate of spring rate (figures 19,23) because of its noticeable effect at body resonance. Tyre and axle parameters need only be in the correct range for the vehicle under consideration and are of secondary importance.

### 3.4 Double-input models

The single input model considered in paragraph 3.3 lends itself well only to the consideration of response in components which are particularly dependent on the excitation of a single wheel. We shall require, however, a more sophisticated model if we hope to consider components which are not so conveniently situated.

We shall next consider a two input model as shown in figure 25. It is assumed that each pair of wheels moves together, but that the rear wheel follows the same profile  $z(x)$  as the corresponding front wheel. The dynamic model must now include front and rear suspensions, and the moment of inertia of the body must be explicitly included.

It was shown in 2.3.8 that the response spectrum is given by

$$s^o(f) = \frac{1}{v} [A(f) + B(f) \cos 2\pi na + C(f) \sin 2\pi na] \mathcal{J}(n)$$

3.4.1

where/...

where

$$\left. \begin{aligned} A(f) &= \alpha_1^* \alpha_1 + \alpha_2^* \alpha_2 \\ B(f) &= 2 \operatorname{Re}[\alpha_1^* \alpha_2] \\ C(f) &= 2 \operatorname{Im}[\alpha_1^* \alpha_2] \end{aligned} \right\}$$

and we will examine the behaviour trends peculiar to this model which will affect response. (Changing the basic mass, spring and damper parameters has a similar effect on response to that exhibited by the single input model discussed in Section 3.3).

The equations of motion for the model shown in figure 25 can be written in matrix form as

$$[M] \ddot{\underline{z}} + [C] \dot{\underline{z}} + [K] \underline{z} = [I] \quad 3.4.2$$

where  $\ddot{\underline{z}}$ ,  $\dot{\underline{z}}$  and  $\underline{z}$  are column matrices. The coefficient matrices are

$$[M] = \begin{bmatrix} m_{u_1} & \cdot & \cdot & \cdot \\ \cdot & m_g & \cdot & \cdot \\ \cdot & \cdot & I_p & \cdot \\ \cdot & \cdot & \cdot & m_{u_2} \end{bmatrix} \quad 3.4.3$$

$$[C] = \begin{bmatrix} c_{T_1} + c_1 & -c_1 & -l_1 c_1 & 0 \\ & c_1 + c_2 & c_1 l_1 - c_2 l_2 & -c_2 \\ & & c_1 l_1^2 + c_2 l_2^2 & c_2 l_2 \\ & & & c_{T_2} + c_2 \end{bmatrix} \quad 3.4.4$$

(symmetric matrix)

and  $[K]$  is identical to  $[C]$  with  $k_r$  replacing  $c_r$ . The input matrix  $[I]$  will depend on the receptance under consideration e.g.

$$\text{for } \alpha_1(\text{if}) \quad [I] = \begin{bmatrix} c_{T_1} \dot{z} + k_{T_1} z \\ 0 \\ 0 \\ 0 \end{bmatrix} \quad 3.4.5$$

and

$$\text{for } \alpha_2(\text{if}) \quad [I] = \begin{bmatrix} 0 \\ 0 \\ 0 \\ c_{T_2} \dot{z} + k_{T_2} z \end{bmatrix} \quad 3.4.6$$

These may be solved for the two receptances,  $\alpha_1(\text{if})$  and  $\alpha_2(\text{if})$ . Since the overall transfer function  $|\bar{T}(f)|^2$  is dependent on vehicle speed where

$$|\bar{T}(f)|^2 = A(f) + B(f) \cos 2\pi \frac{fa}{v} + C(f) \sin 2\pi \frac{fa}{v} \quad 3.4.7$$

(See Sections 2.4 and 3.2) consideration of these individual terms  $A(f)$ ,  $B(f)$  and  $C(f)$  which are independent of speed, will provide an understanding of the effects of the second input on overall vehicle response. It is obvious that for components in close proximity to a single wheel (e.g. suspension spring) one would expect the contribution from the other input to be small and hence  $|\bar{T}(f)|^2$  would vary only slightly with speed. In figure 26 three cases are considered, and in each case the receptance is evaluated for displacement at various points on the chassis frame. At the point/...

point directly above the suspension the main contribution to  $|\bar{T}(f)|^2$  comes from the  $A(f)$  term with a negligible contribution from the receptance  $\alpha_2(if)$  whereas at the centre of gravity contributions from  $A(f)$  and  $B(f)$  equally combine to yield a transfer function  $|\bar{T}(f)|^2$  heavily dependent on vehicle speed  $v$ .

In order that realistic conclusions may be drawn from further consideration of this vehicle model the response analysis was performed using data pertaining to test vehicle A (See Appendix 3) which is a typical modern Continental passenger car. The responses will be evaluated in terms of

- i) the force in the suspension spring  $k_s$
- ii) accelerations on the chassis frame.

The various parts of the transfer function  $|\bar{T}(f)|^2$  for the response at the front suspension spring are shown in figure 27 and it is noted that changes in velocity will affect  $|\bar{T}(f)|^2$  only in the region of the first (body) natural frequency. The contribution to the response from the rear input,  $\alpha_2(if)$  is negligible. Because of the general trend in the form of the road input spectrum ( $1/f^2$ ) the response spectrum of this component will predominate in the frequency range around 1 Hz, and the axle resonance at 10 Hz will be reduced by about 20 dB.

The acceleration responses at various points along the vehicle chassis are of interest for two reasons:

- i) due to the relative ease of measurement at these points they are ideal for comparing experimental response with analytical predicted response
- ii) the mean square acceleration response has been shown to agree with ride comfort.

For this vehicle model the response spectra were calculated from equation 3.4.1 substituting the road spectrum under consideration. The mean square response was evaluated at 6 points along the chassis beam (figure 28) and plotted as a function of its position on the chassis. A minimum r.m.s. acceleration occurs in the region of the driver's seat (position 3). This has been confirmed by experiment.

The transfer function for some of the positions are shown in figures 29 to 32 for various speeds  $v$ , and emphasise the two points discussed above -

- 1) the importance of the speed  $v$  in determining resonance and
- 2) the response position in relation to the front and rear inputs in determining the basic shape of the transfer function and its dependence on speed (figures 29,31).

Although this model has inherently four natural frequencies consisting of two unsprung mass frequencies and a coupled pitch and bounce frequency of the sprung mass, the transfer function for spring force (figure 27) exhibits only 2 of these: the first peak at 1 Hz being a combination of the pitch and bounce frequencies.

### 3.5 Models with four inputs

To enable accurate prediction of vehicle response may require a mathematical model in which all four inputs are considered. The dynamics of the vehicle can be as complex as we like and the general equation for the harmonic response analysis for the individual determination of the  $\alpha$ 's will be

$$[M]\ddot{z} + [C]\dot{z} + [K]z = [I_r]$$

$$r = 1,2,3,4.$$

3.5.1

where the matrices are of the general form to those in equations 3.4.3 to 3.4.6 and the layout of the inputs is described in figure 7. The  $\alpha$ 's can then be combined and if we consider the response analysis to be performed using the simplified response equation 2.5.26 the two transfer functions  $[\Gamma_D(f)]^2$  and  $[\Gamma_X(f)]^2$  can be evaluated. (See equation 2.5.22).

The response spectrum at any point on the model is given by

$$S^0(f) = \frac{1}{v} \left\{ [\Gamma_D(f)]^2 + g_v(f) [\Gamma_X(f)]^2 \right\} J_D(n) \quad 3.5.2$$

and it was discussed in Section 2.6 that the effects of lateral out-of-phase road irregularities on the vehicle oscillations would be dependent on the form of the coherency function  $g(n)$  noting that

$$g_v(f) = g_v(nv) = g(n) \quad 3.5.3$$

We shall therefore restrict our discussion of this general model to an examination of the two transfer functions  $[\Gamma_D(f)]^2$  and  $[\Gamma_X(f)]^2$  for the particular case of vehicle B, (British saloon car; parameters given in Appendix 3) and we shall consider the effects on the response when they are combined and coupled with the coherency function in the response equation 3.5.2

The model chosen was one with seven degrees of freedom (figure 33): four independent vertical oscillations of the unsprung masses and the bounce, pitch and roll modes of the vehicle body. The responses were evaluated in terms of the force in the front coil spring and the accelerations at various points on the rigid body.

The direct and cross transfer functions for the force in the front coil spring are shown in figure 34 for a fixed speed  $v$ , together with the transfer function evaluated for the two input model (figure 25) with the same parameters. Suspension damping was of the order of  $\zeta = 0.35$ , and even although tyre damping was very small ( $\zeta_{\text{T}} = 0.04$ ), this ensures that the transfer function predominates at the first resonant condition (Section 3.3). It can be seen from figure 34 and by examination of equation 3.5.2 that if the coherency function  $g(n) = 1$  then the two functions plotted are additive and become equal to the transfer function for the double-input, single track case. In the more general case,  $g(n) \neq 1$ , and since it was shown that

$$\left. \begin{array}{l} g(n) \rightarrow 1 \quad \text{as} \quad n \rightarrow 0 \\ g(n) \rightarrow 0 \quad \text{as} \quad n \rightarrow \infty \end{array} \right\} 3.5.4$$

and

$$g_v(f) = g_v(nv) = g(n)$$

it becomes important to know the frequency range for which  $g_v(f) \approx 1$ .

For example, if

$$\left. \begin{array}{l} g(n) \approx 1 \quad \text{for} \quad n \leq 0.2 \text{ c/m} \\ g_v(f) \approx 1 \quad \text{for} \quad f (=nv) < 0.2v \end{array} \right\} 3.5.5$$

and for the case shown in figure 34 when  $v = 13.3 \text{ m/s}$  (30 mph)

this implies that

$$g_v(f) \approx 1 \quad \text{for} \quad f < 2.7 \text{ Hz} \quad 3.5.6$$

and/...

and that the response in the frequency range  $0 < f < 2.7$  Hz will be identical to that produced by the single track, double-input model. Moreover, remembering that the profile excitation decreases at around 6 dB/octave, then any changes in the response due to the difference between the direct and cross transfer functions in this model at frequencies greater than 2.7 Hz, will produce a negligible difference between the mean square response evaluated from the single track vehicle model and that evaluated from the double track, four input model. In consideration of the response of this component, increased complexity of the road-vehicle model to attempt to reproduce a more accurate response picture may not be justified. It will be shown in Chapter 4 that the assumptions concerning the values of the coherency function, equations 3.5.4 and 3.5.5, are perfectly reasonable for normal roads. However, there will be some cases, in particular when the vehicle is traversing a very rough surface (e.g. pavé) when the coherency function falls very quickly to zero and the roll input to the vehicle becomes important. Finally, from the results in the previous section, change of vehicle speed will produce only small changes in the transfer functions for this component.

If we now consider the acceleration response of the body (figure 35) and choose any point along the centre line, which in a symmetrical vehicle model will bisect the centre of gravity, then it is obvious from equation 2.5.15 that by putting

$$\left. \begin{aligned} \alpha_1 &= \alpha_3 \\ \alpha_2 &= \alpha_4 \end{aligned} \right\} \quad 3.5.7$$

the direct and cross transfer functions are equal and both equal to one half of the transfer function of the double-input, single track case. Variation of vehicle velocity will again produce similar effects on these functions, as was obtained in the previous Section (figure 29).

However, this new model will enable us to examine the response of points on the chassis which are off-centre and figure 36 shows the acceleration response of a point on the vehicle sill in line with the centre of gravity. It is still true that

$$[\Gamma_D(f)]^2 + [\Gamma_X(f)]^2 = \{|\Gamma(f)|^2\} \text{ double input} \quad 3.5.8$$

and it can be seen that the response depends heavily on the form of  $g_v(f)$ . But the response spectrum, because of the nature of the profile excitation, will predominate in the region of the first resonance at 1.5 Hz and any changes in the spectrum due to roll oscillations in the frequency range 12-15 Hz will be 20 dB down and thus have little effect on the mean square response.

In attempting to summarise the effects on response that result from increasing the complexity of the road-vehicle model from the single-input, single-track, single degree of freedom model to the four wheeled two track multi-degree of freedom model discussed above, we must bear in mind two important facts.

i) The excitation provided by the road has a spectrum which is typically of the form

$$S^i(f) \propto \frac{1}{f^w} \quad \text{with} \quad w \approx 2 \quad 3.5.9$$

ii) the coherency function for normal roads will for a certain range of frequencies be approximately 1. Only for frequencies greater than about 5Hz will  $g_v(f)$  tend to zero.

Hence response will tend to predominate at the low frequency end of the spectrum and thus a single track road model will be sufficient to reproduce in most instances a form of excitation accurate enough to base vehicle response prediction. However, there will be roads where  $g_v(f) \rightarrow 0$  for very low values of frequency and there will be cases when we will be interested in the high frequency response (e.g. laboratory simulation for endurance testing, see Chapter 5) where a true picture of vehicle response can only be obtained from accurate vehicle models and a more complete form of road surface description than is provided by a single track profile. Moreover, there will be components whose situation in the vehicle will require the more complex four input model for analysis, if only to maintain their geometric compatibility with the remainder of the vehicle.

## CHAPTER 4

### THE RESPONSE OF VEHICLE COMPONENTS TO RANDOM ROAD SURFACE IRREGULARITIES

The theory of vehicle response to random displacement excitation has been developed and it has been applied to a series of analytical vehicle models whose response characteristics have been examined. It is the object of this Chapter to investigate the statistical properties of road surface roughness in order to justify the road descriptions proposed in Chapter 1 and based on random process theory. Also, experimental response spectra taken from a test vehicle will be examined and the validity of the response analysis checked. Finally the response spectra of selected components will be compared with predicted response spectra derived from the analytical models discussed in Chapter 3 and using as input data the spectral descriptions of one of the measured road surfaces.

#### 4.1 Road surface description

In Chapter 2 it was shown that the road surface undulations along a single track  $z(x)$  could be considered as a member function of a stationary Gaussian process  $\{z(x)\}$ . It was pointed out that using this single function to characterise the road surface implies consideration of its properties as a random cylindrical surface. It is not in fact comprised of such a surface, and we do expect its probability characteristics to change not only in the longitudinal/...

longitudinal direction but also in the lateral direction across the road. Hence, for a more complete analysis of the probability characteristics of the road surface, it must be examined as a random function of two variables, the length  $x$  and the width  $y$ . If we assume that this surface can be expressed as a random, stationary function with a zero mean value then a two dimensional correlation function serves as its exhaustive probability characteristic and to determine these latter functions the surface profile recordings relative to a fixed plane are required throughout every possible longitudinal road surface section, so forming a surface matrix of points  $(x_r, y_r)$ . This can then be analysed to obtain the general autocorrelation functions

$$\rho(x_r y_r; x_s y_s) = E [z(x_r, y_r) \cdot z(x_s, y_s)] \quad 4.1.1$$

The establishment of these autocorrelation functions (4.1.1) will be an extremely laborious operation both in data acquisition and computing time and it is doubtful if any useful analysis could be based on them. Thus we are put into a position whereby we must seek a simplified road surface description, and as mentioned at the outset treat a single longitudinal track with homogeneous properties along the direction of measurement. Historically we are on firm ground as this is the descriptive process employed by the majority [10, 12, 13, 22, 24, 25, 26, 27, 28, 30, 31] of workers in this field.

If we consider the surface irregularities to be represented by a member function  $z(x)$  of a random process  $\{z(x)\}$  then for the analysis in Chapter 2 to be applicable the measured length of

road/...

road  $z(x)$  must conform to the requirement of stationarity and have its amplitude levels governed by a Gaussian distribution. If these requirements are satisfied then the surface irregularities can be defined by their second order moments and in effect by the spectral density function  $J(n)$ , from which the autocorrelation function, mean square value and distribution can be defined:

$$R(\delta) = \int_{-\infty}^{\infty} \frac{1}{2} J(n) e^{i2n\delta} dn \quad 4.1.2$$

$$\sigma^2 = \langle z^2(x) \rangle = \int_0^{\infty} J(n) dn \quad 4.1.3$$

$$p(z) = \frac{1}{\sigma \sqrt{2\pi}} e^{-\frac{z^2}{2\sigma^2}} \quad 4.1.4$$

The next step in the descriptive process must be to consider the properties of two parallel tracks  $z_R(x)$  and  $z_L(x)$  (figure 8a) under the same conditions assumed for the single track. In this case the surface is being treated as a separately homogeneous surface in the  $x$  and  $y$  directions and the correlation function given by equation 4.1.1 can be expressed as

$$R(\xi, \eta) = \langle z(x, y) \cdot z(x + \xi, y + \eta) \rangle \quad 4.1.5$$

which for the particular case under consideration when

$$\left. \begin{aligned} y &= y_1 \\ y + \eta &= y_2 \end{aligned} \right\} \quad 4.1.6$$

and/...

and writing

$$\left. \begin{aligned} z_R(x) &= z(x, y_1) \\ z_L(x) &= z(x, y_2) \end{aligned} \right\} 4.1.7$$

reduces to, for the case of the cross-correlation function between the two tracks:

$$R_{RL}(\xi) = R(\xi, y_2 - y_1) \quad 4.1.8$$

Although the complete surface has not been defined, as to do so would require a sufficient set of values of  $\eta$ , we have obtained a road surface model, based on two measured longitudinal tracks which will provide the necessary data in terms of spectra and cross spectra to enable response analysis to be performed, based on equation 2.5.15, for a vehicle of fixed track,  $2b$ .

If the track width is changed to  $2b'$  then to evaluate the response of this new vehicle necessitates the measurement of a new track

$z(x, y_3)$  such that

$$z(x, y_3) - z(x, y_1) = 2b' \quad 4.1.9$$

Although we may hope that the autocorrelation functions of the tracks  $z(x, y_1)$ ,  $z(x, y_2)$  and  $z(x, y_3)$  will be the same there is no justification for

$$R(\xi, y_2 - y_1) = R(\xi, y_3 - y_1) \quad 4.1.10$$

An approach for simplifying this form of road surface description was suggested by PARKHILOVSKI [14] and from his hypothesis a simplified response analysis has been derived in Chapter 2 (Section 2.5). Verification of this hypothesis requires the stationary properties of the two random tracks  $z_R(x)$  and  $z_L(x)$  to conform to certain rules:

- i) the cross-correlation function between the mean track and the slope between the two tracks must be zero (equations 2.5.16, 2.5.17).
- ii) the autocorrelation functions of both tracks must be equal. (Equation 2.5.18). If these conditions can be satisfied then a response analysis based on equation 2.5.20 or on equation 2.5.26 may be performed.

However although some form of surface description has been achieved in utilising Parkhilovski's hypothesis, i.e. a random longitudinal signal with a randomly varying constant lateral slope across the track for each longitudinal increment (figure 8a), it is clearly not as realistic as we would desire. It does permit response analysis to be performed utilising equation 2.5.26 and will permit a complete description, albeit intuitively suspect, of the road surface. Hence the coherency function obtained and required by equation 2.5.26 to define the relationship between the tracks  $z_R(x)$  and  $z_L(x)$  would in fact define the relationship between any pair of longitudinal tracks, and the response equation 2.5.26 would be effective for any vehicle, with any track width, traversing the road.

Finally, a complete surface descriptive process is presented in Section 2.7 in which the road surface is characterised by a completely homogeneous surface in both the  $x$  and  $y$  directions. It was shown that, in this case, the surface properties can be obtained from measurements taken from a single track along the road. If the response analysis is performed according to equation 2.5.26 a different coherency function would result when the track width,  $2b$ , is varied since the cross-correlation function between the two tracks was shown to be a function of the track width.

These three road-surface models have been presented by the author in an effort to obtain an increasingly more accurate description of the road surface, yet comply with the requirements of a simple response analysis. The spectral density  $S(n)$  of any single track along the road is common to all of them and the complexity arises from a need to describe the cross-properties between the two tracks along which the vehicle will travel. It is not expected that any of the above models will completely define every road surface, but if permitted to describe suitable surfaces will allow for verification of the analysis presented in Chapter 2.

#### 4.2 The surface as a single realisation of a random process

$$\{z(x)\}.$$

The total published work on vehicle response to road surface undulations has, up to the presentation of this thesis, been founded on this premise, and measured road profile spectra are now available for a wide and varied range of motor roads [12,13].

Discounting related work on aircraft runways, road profile spectra were first presented by QUINN and THOMPSON [40] in 1962 who obtained their data from a series of surveyed points. This was followed by work done by PEVZNER and TIKHONOV [30] (1964) who surveyed the surface profiles of various types of road in the USSR and from the data established analytical expressions for the spectral density. These are presented in Table 3 in terms of a normalised spectral density defined as

$$\bar{S}(\omega) = \frac{S(\omega)}{R(0)}$$

which represents the displacement-time spectrum of the road as viewed from the vehicle at any given speed  $v$ . ( $R(0)$  is of course the mean square value and the units are  $\text{cm}^2$ ; the units of  $v$  are  $\text{m/s}$ ).

The optimisation work carried out by DINCA [31] and mentioned above in Chapter 3, Section 3.1, was performed using these spectra as typifying road surface undulations. If we examine some of these spectra it is obvious from the form of the equations in Table 3 that a resonant condition can be achieved by driving the vehicle at a speed such that the natural frequency of the vehicle coincides with the "resonance" in the spectrum. This phenomenon is likely to be observed on poorly made-up roads, where a periodic component has been superimposed on the surface roughness due to the vibration characteristics of heavy vehicles traversing the road. It has not been observed on road spectra presented by other authors [12,13].

Table 3/...

TABLE 3

TYPE OF ROAD SURFACE	EQUATION FOR SPECTRAL DENSITY
Cobbles of satisfactory quality	$\bar{S}(\omega) = \frac{0.143v}{\omega^2 + 0.2 v^2}$
Cobbles with holes and ridges	$\bar{S}(\omega) = \frac{0.135v}{\omega^2 + 0.25 v^2} + \frac{0.0096v (\omega^2 + 4.04 v^2)}{(\omega^2 - 3.96v^2)^2 + 0.64 v^4}$
Asphalted	$\bar{S}(\omega) = \frac{0.54v}{\omega^2 + 0.04 v^2} + \frac{0.0024v (\omega^2 + 0.36 v^2)}{(\omega^2 - 0.36 v^2)^2 + 0.0036 v^4}$
Cement Concrete	$\bar{S}(\omega) = \frac{0.048v}{\omega^2 + 0.0225 v^2}$

Analytical expressions for the normalised spectral density for various types of surface profile after PEVZNER and TIKHONOV [30]

Attempts to speed up the profile measurement technique resulted in mechanical profilometers being developed by MIRA [10,11,12] and BRAUN [13] who presented, independently, a wide range of road profile spectra taken from a single track measured along the road. Braun summarised his results by assuming that road spectra could be approximated by an equation of the type

$$J(n) = \frac{J(n_0)}{n^w} \quad 4.2.2$$

and listed corresponding averaged values for  $J(n_0)$  (a roughness coefficient) and  $w$  (waviness) for various types of surface.

These are given in Table 4.

TABLE 4

<u>Type of Road</u>	<u>Condition</u>	<u>Mean Values</u>	
		<u>w</u>	<u><math>J(n_0)</math> cm<sup>3</sup></u>
Cement-Concrete	Very Good	2.29	0.6
	Good	1.97	4.5
	Medium	1.97	8.7
	Bad	1.72	56.3
Asphalt-Concrete	Very Good	2.20	1.3
	Good	2.18	6.0
	Medium	2.18	22.3
Macadam	Good	2.26	8.9
	Medium	2.26	20.8
	Bad	2.15	42.9
	Very Bad	2.15	158
Cobble Stone	Good	1.75	13.7
	Medium	1.75	22.8
	Bad	1.81	36.4
	Very Bad	1.81	323
Unsurfaced	Good	2.25	31.8
	Medium	2.25	155
	Bad	2.14	602
	Very Bad	2.14	16300

Spectrum parameters of test routes according to BRAUN [13]

$(S(n_0))$  is the value of the spectrum at  $1/2\pi$  c/m or  $10^{-2}$  radian /cm).

The MIRA road survey programme was carried out during the period of the present work and the MIRA profilometer recordings and analogue spectral analysis techniques were compared with results obtained by the author utilising geodesic measurement of the road surface and a digital approach to the spectral analysis techniques. The comparison of the spectra so obtained (figures 37 , 38 ) placed a fair degree of reliability on the profilometer measurements taken by MIRA.

If we perform a similar analysis on the road spectra produced by MIRA as was carried out by Braun we find that these spectra can be approximated by an equation of the form

$$\left. \begin{aligned} S(n) &= S(n_0) \left(\frac{n}{n_0}\right)^{-w_1} & n \leq n_0 \\ &= S(n_0) \left(\frac{n}{n_0}\right)^{-w_2} & n \geq n_0 \end{aligned} \right\} 4.2.3$$

where  $S(n_0)$  is the "roughness coefficient" (value of the spectrum) at the frequency  $n_0$ . The measurements can be classed into various groups and the parameter values for each group are given in Table 5. (The range of road sections covered is given in Appendix 1).

From the spectra presented by MIRA a wavelength of 20 ft. averaged out as the dividing line between the two slopes. It is worth noting that this happens to be one of the standard lengths used in road construction techniques and corresponds to approximately  $\frac{1}{2\pi}$  c/m, which was chosen as the standard value of  $n_0$ .

Table 5/...

TABLE 5

$$n_o = \frac{1}{2\pi} c/m$$

ROAD CLASS		$\mathcal{J}(n_o)$ RANGE	$w_1$		$w_2$	
			Mean	Standard Deviation	Mean	Standard Deviation
Motorways	Very Good	2 - 8	1.945	.464	1.360	.221
	Good	8 - 32				
Principal Roads	Very Good	2 - 8	2.05	.487	1.440	.266
	Good	8 - 32				
	Average	32 - 128				
	Poor	128 - 512				
Minor Roads	Average	32 - 128	2.28	.534	1.428	.263
	Poor	128 - 512				
	Very Poor	512 - 2028				

$\mathcal{J}(n)$  measured in units of  $10^{-6} m^3/c$   
(note: to compare directly with table 4 requires division by  $2\pi$ )

Classification of Roads  
based on road spectra presented by MIRA [12]

Classification of road spectra by this means is proposed by the author, and although much work is still needed to confirm the parameters in table 5, it is felt that this could form a sound basis for future road classification.  $\mathcal{J}(n_o)$  is simply the basic roughness coefficient. Since it is expressed in terms of the spectral density the ratio of amplitude roughness between two roads is proportional to the square root of the ratio of their respective  $\mathcal{J}(n_o)$  values. The exponents  $w_1$  and  $w_2$  have completely contradictory significance. For a given  $\mathcal{J}(n_o)$  a high value of  $w_1$  indicates a road with increase in proportional roughness at the longer wavelengths. Conversely a road with a high  $w_2$  exponent suggests a road with a decrease in proportional roughness at shorter/...

at shorter wavelengths. As a road's state of repair deteriorates, a decrease in the exponent  $w_2$  is to be anticipated (figure 39).

The results of these various surveys and others [41,42] are presented in the form of spectra in figure 40. It can be assumed that as these spectra cover a wide range of road surfaces from motorways to pavé test tracks then the whole range of input spectra to which road vehicles are exposed in normal use has been covered. The spectra follow the same general trend with the exception of the Russian ones [30] which deviate at the low frequency end. This is due to the analysis technique employed by these authors who evaluated the autocorrelation function of the route, approximated to it by a mathematical function of the type

$$A_1 e^{-a_1 |\delta|} + A_2 e^{-a_2 |\delta|} \cos \beta \delta \quad 4.2.4$$

where  $A_1$ ,  $A_2$ ,  $a_1$ ,  $a_2$  and  $\beta$  are constants and then calculated the profile spectrum by Fourier transform of this function. The low frequency cut off is inherent in the structure of the approximate spectral density equation so obtained and presented in Table 3.

#### 4.3 The Probability characteristics of three test routes

The geodesic surveys carried out by the present author were taken on three different types of surface:

- 1) a motorway; black top on concrete;
- 2) a country road; black top
- 3) a pavé test track; stone set in concrete

and are tabulated as Routes A,B and C respectively. The measurements are taken at equispaced points/...

at equispaced points in the longitudinal direction on two parallel tracks, a distance 4 ft. (1.2m) apart. The measurement and spectral analysis techniques developed are discussed in Appendix 2.

These measurements were taken for the following reasons:

- 1) As there are some discrepancies in the particular form of spectra presented by other authors, an independent check as to their validity would be valuable.
- 2) There is no published evidence on the probability characteristics of the road surface undulations and in particular the probability density function.
- 3) With the exceptions of the work published by PARKHILOVSKI [14] in 1968 who considered the cross properties of two tracks along a single road in support of his hypothetical surface, no other evidence is available to support his theory although both BRAUN [13] and KANESHIGE [15] both supported the premise that the same road spectrum resulted from measurements taken on any track along the road.
- 4) It would be desirable to check the theory presented in Section 2.7 in which the road was treated as a 2-D random process with completely homogeneous properties.

In this Section we shall discuss the results of this work with reference to points(1) and(2) above. The cross-properties of the various surfaces are discussed in Section 4.4 and finally in Section 4.5 we investigate the possibility of treating the road surface undulations in terms of a completely homogeneous surface in both the x and y directions.

The form of the signal obtained directly from the survey levels for route B is shown in Figure 41 . This is typical of the others, in that data pertaining to the surface irregularities is superimposed on a linear or low frequency trend. Since the length of data sample will determine the lower limit on frequency resolution, it would not be possible to prove stationarity from a data sample of finite length. Any component of the signal with a frequency less than the lower cut-off value would appear as a trend or non-stationary component that will contaminate the power spectral density estimates computed from this "raw" data.

We must therefore separate this trend from the components of surface roughness likely to affect the vehicle dynamics. This is achieved by processing the data through a high-pass filter. Two types of filter were tried by the author, the first based on a linear moving average which has a frequency characteristic shown in figure 42 , and given by

$$|\alpha(\text{in})|^2 = \left(1 - \frac{\sin \Delta n}{\Delta n}\right)^2 \quad 4.3.1$$

for  $\Delta = 150\text{ft} (45.7\text{m})$

It can be seen that this filter has the undesirable characteristic of contaminating the data in the range of interest. The second filter was derived from a filtering technique suggested by MARTIN [43] where each data point was modified as follows

$$\tilde{z}_r = z_r - \sum_{s=-k}^k b_s z_{r+s} \quad 4.3.2$$

and the  $b_k$ 's were based on a series of weights given by Martin. The frequency characteristic of this filter is shown in figure 43 and it should be noted that the function is within 2% of being a perfect filter over most of the frequency range.

Using either of these filters to remove the non-stationary trends in the data resulted in a detrended profile which exhibited the property of a zero mean value. Moreover if the analysis had been performed on the original data, while it might appear that the trend would only alter the low frequency components of the signal it does in fact alter all frequency components (figure 44 ) (BLACKMANN and TUKEY [4] discuss the reasons for this anomaly).

Having satisfied one of the conditions for stationarity in road surface data, the major hurdle which remains is the assumption of a Gaussian distribution for the road heights. The probability density function was evaluated from the filtered data for the three roads surveyed and a Gaussian distribution curve for the given mean square value superimposed on the measured distribution. It can be seen from figure 45 that the data appear to have a Gaussian distribution noting, however, that the data values obtained for class intervals greater than three standard deviations, is, as expected, exceedingly small due to the finite data length examined. The probability density curves computed from the other profiles of tracks B and C were also Gaussian in nature.

The spectral densities of the three tracks were computed and these are shown in figure 46 . Comparison with those obtained by other authors tends to favour the MIRA results and an approximate equation/...

equation of the form 4.2.3:

$$\begin{aligned}
 f(n) &= f(n_0) \left(\frac{n}{n_0}\right)^{-w_1} & n \leq n_0 \\
 &= f(n_0) \left(\frac{n}{n_0}\right)^{-w_2} & n \geq n_0
 \end{aligned}
 \quad \left. \vphantom{\begin{aligned} f(n) &= f(n_0) \left(\frac{n}{n_0}\right)^{-w_1} \\ &= f(n_0) \left(\frac{n}{n_0}\right)^{-w_2} \end{aligned}} \right\} 4.3.3$$

with the parameters  $f(n_0)$ ,  $w_1$  and  $w_2$  given in table 6 for  $n_0 = 1/2\pi$  c/m.

TABLE 6

ROUTE	$f(n_0)$ cm <sup>3</sup> /c	$w_1$	$w_2$
A, Motorway	13.0	2.10	1.42
B, Minor Road	28.4	3.30	1.48
C, Pavé Test Track	870.0	1.80	0.57

Spectrum parameters for the three surveyed tracks

It can be seen that the parameter values fall roughly within the limits imposed by our analysis of the road spectra presented by MIRA with the exception of route C which has an extremely low value of  $w_2$ . This implies a very rough surface at short wavelengths, which is to be expected on a route which was specially built for accelerated endurance testing. This then confirms the proposed classification method for road description based on a knowledge of the spectral density for a single track. Moreover, since the surface undulations were Gaussian, then this will provide the complete description of the surface as a single track profile.

#### 4.4 Consideration of the properties of two parallel tracks along the direction of travel.

To obtain a more complete description of the road input to a real vehicle requires a knowledge of the direct and cross-properties of two random tracks. Both BRAUN [13] and KANESHIGE [15] concluded that the same spectrum was obtained independently of the track  $z(x, y_r)$  measured. It can be seen from figures 47, 48 and 49, that for routes A, B and C this conclusion can be drawn. Further evidence in support of this was obtained privately by the author from VOLVO (Göteborg, Sweden, 1972) who had surveyed two parallel tracks of one of their endurance test surfaces and computed their individual spectra (figure 50).

Although we have not measured every track  $z(x, y_r)$  it seems reasonable to infer from the above evidence that

$$R(\xi, y_r) = R(\xi) \quad r = 1, 2, 3, \dots \quad 4.4.1$$

and the spectral density of the road surface profile in the longitudinal direction is independent of the track taken for measurement. (From practical considerations it may be wise to modify this and exclude any measurements taken on tracks in close proximity to the kerbs which may contain a slightly higher short wavelength content in the spectrum).

The cross-spectra between the two measured tracks  $z(x, y_1)$  and  $z(x, y_2)$  for the routes A, B and C were found to be real (the imaginary part being of the order of 20 dB down on the real part and hence/...

and hence we conclude that

$$R(\xi, y_2 - y_1) = R_{RL}(\xi) \quad 4.4.2$$

is even in  $\xi$  for a given  $(y_2 - y_1)$ . The cross-correlation function for route B is shown in figure 51 and is seen to be even in  $\xi$ .

This latter conclusion from the measured data is certainly one which is not generally true of cross-spectra, but PARKHILOVSKI [14] had derived this conclusion, from a set of measurements taken on a test surface. He assumed that the road surface could be described by

$$z(x) = \frac{z_R(x) + z_L(x)}{2} \quad 4.4.3$$

which would represent the mean heights along the road and

$$\psi(x) = \frac{z_R(x) - z_L(x)}{2b} \quad 4.4.4$$

which would represent a constant slope across the road and varying for each longitudinal increment. He hypothesised that

$$R_{\psi}(\xi) = 0 \quad 4.4.5$$

from which if the autocorrelation functions of the two original tracks are equal then as was shown in Section 2.5 it was concluded that  $R_{LR}(\xi)$  is even in  $\xi$  (i.e. the cross-spectrum between the tracks is a real valued quantity).

Parkhilovski's hypothesis which has been confirmed by the analysis of the three roads surveyed (see for example figure 52 ), greatly simplifies the response analysis and it was shown/...

shown in Chapter 2 that the response of a four input vehicle in this case was given by (equation 2.5.26):

$$S^o(f) = \frac{1}{v} \left\{ [T_D(f)]^2 + \epsilon_v(f) [T_\lambda(f)]^2 \right\} \mathcal{K}(n) \quad 4.4.6$$

Thus for complete surface description a knowledge of  $\mathcal{K}(n)$  and the coherency function  $g(n)$  would suffice. If a constant angular slope across the road was assumed then  $g(n)$  would be independent of the track width  $2b$ , otherwise for a vehicle of different track a new profile measurement would be required. The coherency functions for the three test tracks are presented in figure 53 and it can be seen that they conform to the restrictions imposed on them in Chapter 2 (Section 2.6).

$$\begin{array}{l} \text{i.e.} \quad 0 < g(n) < 1 \\ \\ g(n) \rightarrow 1 \quad \text{as} \quad n \rightarrow 0 \\ \\ g(n) \rightarrow 0 \quad \text{as} \quad n \rightarrow \infty \end{array} \quad \left. \vphantom{\begin{array}{l} \\ \\ \\ \end{array}} \right\} \quad 4.4.7$$

It can be seen that whereas on the motorway type surface (route A)  $g(n) \approx 1$  for wavelengths as low as 5m, the coherency falls off rapidly on the specially built track (route C) indicating that in the latter case a severe roll oscillation would be imposed on the vehicle.

#### 4.5 The road surface as a completely homogeneous random surface

Treatment of the road surface properties as forming part of a completely homogeneous random surface was shown in Chapter 2 (Section 2.7) to lead to a simple relationship between the cross-correlation function of any pair of longitudinal tracks and the autocorrelation function of either one of them:

$$R_{RL}(\xi) = R(\sqrt{\xi^2 + 4b^2}) \quad 4.5.1$$

where  $2b$  is the track width. It is implied by equation 4.5.1 that

$$R_{RL}(\xi) = R_{LR}(\xi) \quad 4.5.2$$

Thus from a knowledge of  $R(\xi)$  we can establish  $R_{RL}(\xi)$  for any given track,  $2b$ , and by Fourier transform the corresponding direct and real cross-spectrum, from which the coherency function can be obtained. This will provide perhaps a more realistic description of the surface irregularities than was provided by the assumptions due to Parkhilovski, since it allows the surface to contain random fluctuations in the lateral direction without imposing any restrictions on their respective heights as was imposed by Parkhilovski's assumption of a constant lateral slope for each longitudinal increment.

However, to establish the validity of the assumption of complete homogeneity requires measurements to be made in any direction to establish the uniformity of  $R(\xi)$ . Roads in general do not extend in a direction perpendicular to the direction of travel, but if we are prepared to consider that the surface could be extended in all directions then, since similar constructional techniques would be used throughout, the assumption of complete homogeneity could/...

could reasonably be applied. We must of course ignore the camber effect which will not contribute to the vibrational input to any vehicle travelling in the longitudinal direction and consider the road surface as consisting of a plane surface in the lateral direction (figure 54 ).

From the autocorrelation functions of routes A, B and C the cross-correlation functions were derived for various values of  $2b$  and it can be seen from figures 55 and 51 that remarkable agreement is obtained between  $R_{RL}(\xi)$  computed from equation 4.5.1 and that obtained from the measured data of two parallel tracks. Further, it is observed that as the track width decreases so

$$R_{RL}(\xi) \longrightarrow R(\xi) \quad 4.5.3$$

and as  $2b \longrightarrow \infty$

$$\text{so } R_{RL}(\xi) \longrightarrow 0 \quad 4.5.4$$

The coherency functions for the three measured surfaces were computed by this means and are compared with those obtained by computation from direct measurements in figure 56 for the measured track width  $2b$ . Agreement is good considering the errors which must be induced in this type of analysis.

Figure 57 shows the effect of a varying track width on the coherency function for route B and confirms the intuitive result expected.

This then confirms that, for the limited data available, treatment of the road surface as a completely homogeneous random surface is possible and that a single measurement of the auto-correlation function of any longitudinal track will serve as the exhaustive probability characteristic required to describe the surface.

#### 4.6 An examination of vehicle response spectra, vehicle model parameters and testing technique

Before proceeding to predict vehicle response spectra from a knowledge of the vehicle dynamics and road surface properties it will be useful to examine typical vehicle response spectra to ensure the applicability of the previous analysis and in particular that the general response equations given in Chapter 2:

$$S^o(f) = \alpha_1(if) \alpha_1^*(if) \frac{1}{v} J(n) \quad 4.6.1$$

and

$$S^o(f) = \frac{1}{v} \left[ A(f) + B(f) \cos 2\pi na + C(f) \sin 2\pi na \right] J(n) \quad 4.6.2$$

apply to the present problem.

Whether component response requires analysis based on a single or double input vehicle model (equation 4.6.1 and 4.6.2 respectively) is irrelevant if we invert equations 4.6.1 and 4.6.2 and examine the transfer function so obtained for any given speed,  $v$ , on a range of road surfaces:

$$\frac{vS^o(f)}{J(n)} = |T(f)|^2 \quad 4.6.3$$

where  $|\bar{T}(f)|^2 = \alpha_1 \alpha_1^*$  for the single input model

$$= A(f) + B(f) \cos 2\pi na + C(f) \sin 2\pi na$$

for the double input model.

A rigorous analytical treatment of the problem demands that  $|\bar{T}(f)|^2$  should be constant for any given speed  $v$  over a range of roads whose direct spectrum is given by  $\hat{d}(n)$ . Using experimental response spectra supplied by MIRA [44] for vehicle B (see Appendix 3) the transfer function for the force in the front spring was evaluated according to equation 4.6.3 for a variety of measured road surfaces.

Figures 58 and 59 show the spread of results for two given speeds; the response spectra being taken on widely differing surfaces from motorway to country class B type roads. The maximum variance on the mean result is 27%, but when we consider the measurement and analysis task involved this represents a surprisingly consistent result.

Evaluating mean square response for the same component yields an interesting and yet not unexpected result. If the experimental mean square values are plotted against vehicle speed (figure 60) it is clear that for smooth roads (motorways) a linear variation is obtained, suggesting that a negligible pitch motion is induced in the vehicle whereas for roads with a rougher surface the variation of mean square response is similar to that observed in Chapter 3, Section 3.2, when we considered the response of a double-input model (figure 16).

Effects due to vehicle roll motion were not expected to contribute to any of the above response spectra and hence the assumption of a single track vehicle model was taken to be valid.

Similar results were obtained for the transfer functions for the response at various other points on the vehicle with a similar speed. It was noticed, however, that roads with approximately the same roughness coefficient (see Section 4.2) yielded almost identical transfer functions (figure 58) suggesting that some of the variance in the results may be due to vehicle non-linearity and in particular, in the case of vehicle B, the suspension shock absorbers.

Tests were carried out on the shock absorbers of vehicle B to evaluate their force-displacement receptance and it can be seen from figure 61 that this is heavily dependent on the piston stroke. Thus while the other parameters for the vehicle models were evaluated from manufacturers drawings and specifications, or from examination of the actual test vehicle, the dampers were tested independently and a linear approximation to viscous damping obtained, based on a foreknowledge of the roughness coefficient of the test route.

The experimental response spectra were computed from pre-recorded data taken from transducers situated at the various measuring points on vehicle B. Strain gauges were fitted to the suspension components and accelerometers placed on the chassis. The signals were amplified and recorded on a frequency modulated tape recorder.

On arrival at the test route, the car was allowed to roll to a standstill, without braking, on a level surface. This allowed a zero signal (representing the static strain in the strain gauged components) to be recorded. The car then accelerated to the required speed, and the/...

the recordings initiated by utilisation of a voice channel. Constant speed was maintained throughout the test run over the selected surface of about 0.5 - 1 mile in length.

Although the author did take part in some of the data acquisition, the vast majority of this work was carried out by MIRA who supplied all of the experimental response spectra and the test vehicle. Some of the vehicle parameters (e.g. roll and pitch moment of inertias) were obtained on experimental apparatus available at MIRA.

#### 4.7 Comparison between experimental and predicted vehicle response

In this Section we shall treat a typical problem - the determination of response in a particular component of one vehicle running on one of the measured test routes, route B - using a sequence of analytical models of increased sophistication. The analysis relevant to each model has been presented in Chapter 3 and the test route parameters in Section 4.3 of the present Chapter. Comparison with the experimental results at each stage will enable the value of increased sophistication to be assessed.

We shall concentrate our attention on the response of the front coil spring of vehicle B, running along the given stretch of route B on two parallel tracks, a track width apart.

##### 4.7.1 Single input model

We shall initially consider an exceedingly simple analytical model in which the vehicle is taken to be represented by the simple linear system of figure 17, and subjected to a single random displacement - excitation imposed by the road profile. It was shown in

Chapter 2, Section 2.2 that the response spectral density of the system when travelling at constant speed,  $v$ , over the profile  $z(x)$  was given by

$$S^o(f) = \frac{1}{v} \alpha_1^* (if) \alpha_1(if) \mathcal{J}(n) \quad 4.7.1$$

The properties of a front spring system of the test vehicle were simulated (as indicated in Appendix 3) by allocating to the parameters of the system of Figure 17 values derived from the parameters of the actual vehicle. These original parameters were mainly taken from the manufacturer's drawings, or in a few cases from direct measurements on the test vehicle; it was found difficult to obtain damper parameters and these were obtained from special tests on the individual dampers and discussed in the previous Section. It was thus possible to determine the receptance of the force in the spring  $k_1$  with respect to imposed displacement at the point of contact. For the frequency range 0-30 Hz which is relevant to ride and stressing a simple linear type model is justified: tyre parameters can be determined [39] if tyre type, pressure, and vehicle speed are known.

Using the known spectral density  $\mathcal{J}(n)$  of the profile of Route B, and the calculated receptance  $\alpha_1(if)$  of the force in the spring  $k_1$ , it was therefore possible by using Equation 4.7.1 to predict the spectral density  $S^o(f)$  of the force in the spring due to traversing the profile at any speed  $v$ .

Figure 62 shows the predicted response spectrum, together with the experimental spectrum obtained by analysis of a strain-gauge record for the actual spring. Agreement is remarkably good considering the simplicity of the vehicle model, but clearly leaves something to be desired.

There are other reasons too for believing that a single input model is inadequate. Evaluation of the quantity  $a_1^*(if) a_1(if)$  in equation 4.7.1 in terms of the model in figure 17 yields an expression which is dependent only on frequency and the constants of the system. It was shown that equation 4.7.1 could be rewritten as

$$|\Gamma(f)|^2 = v S^0(f) / \mathcal{J}(n) \quad 4.7.2$$

and using equation 4.7.2 the quantity  $|\Gamma(f)|^2$  which for the single-input case is identical to the square of the modulus of complex receptance, was evaluated from experimental measurements of response and road spectra. Examination of these results for one component, on a variety of roads at various speeds, shows the function  $|\Gamma(f)|^2$  not independent of velocity. It may be inferred therefore either that receptance is velocity-dependent or that the single input model is not valid.

Furthermore the single input model lends itself well only to the consideration of response in components which are particularly dependent on excitation of a single wheel. As the spectra of Figure 62 concern such a component, reasonable agreement was perhaps to be expected: we shall however require a more sophisticated model if we hope to consider components which are not so conveniently situated.

#### 4.7.2 Double input model

We shall next consider the model (two input model) as shown in figure 25, which includes both front and rear suspensions. It

was/...

was shown in Section 2.3 that the response spectral density  $S^{\circ}(f)$  of any variable of such a two input system was given by

$$S^{\circ}(f) = \frac{1}{v} [A(f) + B(f) \cos 2\pi na + C(f) \sin 2\pi na] \cdot f(n) \quad 4.7.3$$

It has been demonstrated that this transfer function is speed dependent and fulfils the requirements lacking in the single input case.

Again properties of the test vehicle (as defined by the manufacturers) were simulated by allocating suitable parameters to the system of Figure 25 as explained in Appendix 3; this enabled receptances  $\alpha_1(\text{if})$ ,  $\alpha_2(\text{if})$  allowing the force in the front spring  $k_1$  due to excitation at front and rear wheels to be determined. Use of equation 4.7.3 then gave the response spectral density of the force in  $k_1$ . The predicted spectrum is compared with the experimentally obtained spectrum in Figure 63. Comparison with the predicted spectrum of Figure 62 shows that prediction has been improved.

The more complex model permits the prediction of other response spectra, and Figures 64 and 65 show the spectral densities respectively of the acceleration of the centre of gravity of the body, and of the force in a rear spring. Comparison with experimental spectra shows that agreement here is quite good although the model is not yet good enough for precise prediction. It seems desirable to consider a four-input model, although an improved dynamical model might also prove effective.

#### 4.7.3 Four input model

For the vehicle shown in Figure 33 it has been shown that the response spectrum (under certain assumptions discussed in Chapters 2 and 4) reduces to

$$S^o(f) = \frac{1}{v} \left\{ [T_D(f)]^2 + \epsilon_v(f) [T_X(f)]^2 \right\} J_D(n) \quad 4.7.4$$

and the general form of these new transfer functions has been presented in Chapter 3 (Section 3.5).

It remains to see how the predicted response spectra are affected by the adoption of this new road vehicle model.

The coherency function  $g(n)$  for Route B is shown in Figure 53. It will be seen that  $g(n) \doteq 1$  for  $n < 0.17$ , and it follows that  $\epsilon_v(f) \doteq 1$  for  $f (= nv) < 0.17v$ . Thus for  $v = 48$  km/h, i.e. 13.3 m/s,  $\epsilon_v(f) \doteq 1$  for  $f < 2.3$  Hz.

As the receptance for a front spring has its peak value well within this frequency range, it can be assumed that at all frequencies contributing significantly to response  $J_X(n) \doteq J_D(n)$ , and in fact that approximately  $Z_L(x) = Z_R(x)$  as far as the relevant frequency is concerned. Differences between  $Z_L(x)$  and  $Z_R(x)$  cannot therefore significantly affect the response of our test vehicle on this road and no purpose would therefore be served by computing response for this case.

This is in agreement with our conclusions drawn at the end of Chapter 3 when we considered vehicle response based on this four-input model and the effects of various forms of coherency function  $g(n)$  on this response.

A similar analytical procedure was applied to predict the response of similar components in a third vehicle whose suspension characteristics varied slightly with those of vehicle B. The comparison between predicted and response spectra was good with characteristics of a similar nature to those presented above, and no useful purpose can be served by presenting the results.

## CHAPTER 5

### THE LABORATORY SIMULATION OF VEHICLE SERVICE STRESSES

To reproduce in the laboratory the response of a vehicle, or vehicle component, to a given road at a given speed for a sufficient variety of different roads and speeds has long been the goal of vehicle development engineers. Achievement of this goal requires a complete road surface description, a road classification technique and indications of the proportion of its life each vehicle spends on each class of road. Moreover, a reliable response analysis must be achieved before component testing can be introduced without recourse to prototype vehicle testing.

It is the object of this Chapter to show how the theory developed in Chapter 2 coupled with the response analysis of Chapter 3 and the road description and classification methods proposed in Chapter 4 can form the basis of developing the only reliable simulation test of vehicle service stress. It will be demonstrated that a laboratory simulated test based on recordings taken from a prototype vehicle has very limited scope, whereas the test based on the work presented in this thesis shows definite promise and is currently being developed for the industrial testing of vehicles.

The simulation test method proposed does not describe the complete vehicle environment and may seem only a limited objective in comparison to complete testing, but such a test would itself form a very powerful tool, besides offering the first step towards eventual complete simulation testing.

## 5.1 The nature of the problem

The term Simulation Testing embodies an attractively simple idea - the reproduction in the laboratory of service conditions - but even when restricted to the vehicle field embodies a great variety of different types of test. The ultimate objective of this test may be to define vehicle durability criteria which is in itself a work of major importance. We will confine our attention on one particular test, that of reproducing in the laboratory the response of a vehicle to road surface undulations. We will assume that the vehicle travels at constant speed and hence we can draw on the response analysis and results presented in Chapter 2 to 4.

It was shown that successful response prediction required a knowledge only of the spectral density of a single track along the road. But, to design a simulation technique for a complete vehicle based on symmetrical inputs to both off-side and near-side wheels is undesirable, especially when the final objective of the work may be durability testing. Thus, we must endeavour to produce a test which will correctly simulate the four input signals, together with their related inter-dependence, which can be applied to the four wheels of the vehicle.

It will be shown in Section 5.3 that it is possible to obtain these signals, with the same spectra and cross spectra, as would have been measured on the road. Although we are considering only the simulation of spectra, i.e. we shall be satisfied if at the wheels of the test vehicle all possible direct and cross-spectral densities are identical to those obtained on the road, if we ensure that our simulation signals are Gaussian, then the simulation

technique based on spectra will be a complete simulation of the excitation. It was shown in Chapter 4, Section 4.3 that the road surface undulations were governed by a Gaussian distribution.

The method outlined in Section 5.3 for the simulation testing of complete vehicles may be applied to discrete components since the input spectra to any component in the vehicle may be obtained with recourse to the analysis of Chapter 3. It may not, at first sight, be obvious why one should adopt this technique for testing individual components and it is shown in Section 5.2 that the more obvious form of testing, using prerecorded data, contains some major drawbacks in its application.

The equipment necessary to perform either type of simulation test is now generally available and consists basically of four or more servo-hydraulic actuators which can be driven from any external source. There are yet many problems to be considered in the specification of such equipment and in the conditions of its use, but these will not generally concern us here. We will examine the two possible methods of supplying the external signal sources - the random excitation which the test vehicle or component will 'see' as a simulation of the road surface roughness.

## 5.2 Prototype-based testing

The most obvious form of simulation test is to measure displacements or stresses in a component which forms part of a prototype vehicle under service conditions, and to apply such forces as will reproduce similar effects in a similar component in the laboratory.

This technique, although simple in principle, has three major drawbacks.

i) Before any test can be carried out, a prototype vehicle has to be constructed, instrumented, and then driven over a series of test tracks to record a stress history of the various components under test.

ii) The application of the requisite forces and constraints to an isolated component can impose serious practical difficulties.

iii) If it should prove necessary to modify any part of a component under test (e.g, to stiffen a structural component), then it is only by installing the modified component in the original vehicle and obtaining new stress histories that a properly modified test can be established. Testing the modified system with the original excitations could lead to serious errors in stress simulation.

This last difficulty is an important one and can be illuminated by analytical treatment of the problem. Consider for example the system shown in Figure 66 where system  $\alpha$  represents a particular component to be tested and system  $\lambda$  the remainder of the system in service including the vehicle suspension. Suppose that  $F_0$  causes a displacement  $z_0$  at the point 0 on system  $\lambda$  and that we are interested in the response  $z_2$  at the point 2 on  $\alpha$ . The systems are connected at the point 1 where they have a common displacement  $z_1$  and experience equal and opposite forces  $F_1$ . To provide a suitable test for the system  $\alpha$  in isolation it is necessary to ensure that  $z_2$  is properly simulated, and so that the proper force  $F_1$  is applied to it.

Then the responses and excitations are related by

$$\left. \begin{aligned}
 z_0 &= \chi_{00} F_0 + \chi_{01} F_1 \\
 z_1 &= \chi_{10} F_0 + \chi_{11} F_1 \\
 z_1 &= \alpha_{11} (-F_1) \\
 z_2 &= \alpha_{21} (-F_1)
 \end{aligned} \right\} 5.2.1$$

where  $\alpha_{rs}$ ,  $\chi_{rs}$  are receptances (or transfer functions) representing the response at  $r$  to unit harmonic excitation at  $s$ .

Solving 5.2.1 for  $z_2$  in terms of  $z_0$  we obtain

$$z_2 = \frac{\alpha_{21} \chi_{10}}{\alpha_{11} \chi_{00} - \chi_{10} \chi_{01} + \chi_{11} \chi_{00}} z_0 \quad 5.2.2$$

This is the response which must be excited when the component  $\alpha$  is tested alone, and this will require imposing a force  $F_1$  which correctly simulates that in the combined system.

Let us now consider instead of  $\alpha$  a modified system  $\beta$  (figure 67) and determine its response when the force  $F_1$  is applied to it. Let the response  $z_2$  in this test be denoted by  $z_2^{(\beta)}$ .

From equations 5.2.1 the force  $F_1$  is given by

$$F_1 = - \frac{\chi_{10}}{\alpha_{11} \chi_{00} - \chi_{10} \chi_{01} + \chi_{11} \chi_{00}} z_0 \quad 5.2.3$$

whence the response of system  $\beta$  alone is given by

$$z_2^{(\beta)} = \frac{\beta_{21} \chi_{10}}{\alpha_{11} \chi_{00} - \chi_{10} \chi_{01} + \chi_{11} \chi_{00}} z_0 \quad 5.2.4$$

However, by making the necessary changes in 5.2.2 it is clear that if system  $\beta$  had replaced  $\alpha$  in our original model the response  $z_2$  would instead have been given by

$$z_2^{(\chi + \beta)} = \frac{\beta_{21}\chi_{10}}{\beta_{11}\chi_{00} - \chi_{10}\chi_{01} + \chi_{11}\chi_{00}} z_0 \quad 5.2.5$$

The ratio

$$\frac{z_2^{(\beta)}}{z_2^{(\chi + \beta)}} = \frac{\beta_{11}\chi_{00} - \chi_{10}\chi_{01} + \chi_{11}\chi_{00}}{\alpha_{11}\chi_{00} - \chi_{10}\chi_{01} + \chi_{11}\chi_{00}} \quad , \quad 5.2.6$$

relates the response of the system  $\beta$  to a test based on the service behaviour of  $\alpha$  to that in a correctly prescribed test: it will not in general be unity, and the extent of its departure from unity will be a measure of the error which has arisen.

Unless  $\alpha_{11} = \beta_{11}$ , the ratio given by equation 5.2.6 will be effectively unity only if

$$|\alpha_{11}| \quad \text{and} \quad |\beta_{11}| \ll \left| \frac{\chi_{11}\chi_{00} - \chi_{01}^2}{\chi_{00}} \right| \quad 5.2.7$$

The difficulty is best illustrated by means of an example. Suppose that the system  $\alpha$  (and  $\beta$ ) is a chassis frame, and that  $\chi$  is the vehicle suspension, represented by figure 68.

It can be shown that

$$\Lambda(f) = \frac{\chi_{11}\chi_{00} - \chi_{10}^2}{\chi_{00}} = \frac{m\omega^2 - (p_T + p_1)}{p_1(m\omega^2 - p_T)} \quad , \quad 5.2.8$$

where/...

where  $p_{\Gamma} = k_{\Gamma} + i\omega c_{\Gamma}$

$p_1 = k_1 + i\omega c_1$ .

Clearly the magnitude of  $|\Lambda(f)|$  will be frequency dependent, and there are ranges of frequency where it may be expected to be small. Figure 69 shows how  $|\Lambda(f)|^2$  varies with frequency for a particular set of parameter values taken from a public service vehicle. Particularly for high values of frequency this must limit the stiffnesses of alternative chassis frames to which a single specified test will apply.

In this simple case where only a single excitation is involved, it is an easy matter to compensate the force which was obtained from the  $(\alpha+\chi)$  test so as to make it applicable to the new  $(\alpha+\beta)$  test. Further complexities arise, however, when two or more inputs have to be considered.

The analysis was carried out for the case when two inputs were considered and force compensation was also achieved. It was found that it required not just the simple multiplication of equation 5.2.6 but a complex algebraic manipulation of the various receptances in the system.

### 5.3 Test based on road profile spectra

The difficulties of prototype-based testing are avoided by a testing technique which uses as input, data based on the road itself. Now that adequate road profile data is available it is possible to produce synthesised signals which represent the vertical displacements imposed by the road at the vehicle tyres. This type of input can be applied to a prototype vehicle, or indeed to a component in the

vehicle provided the data is modified to allow for the filtering action of the remainder of the vehicle.

Consider a test rig consisting of 4 electro-hydraulic actuators which apply controlled vertical displacements to the 4 wheels of a complete vehicle under test. It is in fact possible to devise a means of imposing suitable displacements at the four wheels without the necessity of making the vibrators follow actual point-by-point road data, as the following analysis will show.

Suppose that two parallel tracks on a given road have profiles  $z_L(x)$  and  $z_R(x)$  for which the spectral densities  $S_R(n)$ ,  $S_{RL}(n)$ ,  $S_{LR}(n)$  and  $S_L(n)$  are known. Then if we define new variables

$$\begin{aligned} z(x) &= [z_R(x) + z_L(x)] / 2, \\ \psi(x) &= [z_R(x) - z_L(x)] / 2b, \end{aligned} \quad 5.3.1$$

where  $2b$  is the track width, and let  $S^z(n)$  and  $S^\psi(n)$  be the spectra of the two new signals defined by equation 5.4.1 then it was shown in Chapter 2 (Section 2.6) that

$$\left. \begin{aligned} S^z(n) &= \frac{1+g(n)}{2} S_D(n) \\ S^\psi(n) &= \frac{1-g(n)}{2b^2} S_D(n) \end{aligned} \right\} 5.3.2$$

where  $S_D(n) = S_L(n) = S_R(n)$

$$g(n) = \frac{S_X(n)}{S_D(n)}$$

and  $S_X(n) = S_{RL}(n) = S_{LR}(n)$

It is then possible to synthesise uncorrelated signals  $z(x)$  and  $\psi(x)$  which have spectral densities given by 5.3.2.

It remains only to combine these signals to give the required displacements at the wheels of the vehicle. If  $z_1(x), z_2(x), z_3(x), z_4(x)$  are the required displacements at the several wheels as numbered in Figure 7 these are related to  $z(x)$  and  $\psi(x)$  by the equations

$$\left. \begin{aligned} z_1(x) &= z(x) + b\psi(x) \\ z_2(x) &= z(x+a) + b\psi(x+a) \\ z_3(x) &= z(x) - b\psi(x) \\ z_4(x) &= z(x+a) - b\psi(x+a) \end{aligned} \right\} 5.3.3$$

If the signals  $z(x), \psi(x)$  are stored on tape or are digitally generated the translations such as that from  $z(x)$  to  $z(x+a)$  and the transfer from  $z(x)$  to  $z(t)$  are easily enough accomplished.

The definition of the four imposed displacements by 5.3.3 completes the specification of the test. The imposition of the desired displacement at each wheel is then accomplished by suitable control systems.

Where it is not possible to test a complete vehicle a test on the same principle can be devised, at least in the case where the behaviour of a constant velocity vehicle is to be simulated, in which the analysis, presented in Chapter 3, is used to replace some part of the complete test specification. The test must now consist of displacements imposed at the points at which the component to be tested is in contact with the remainder of the vehicle. The spectral densities of these imposed displacements must be determined by analysis and signals having these spectral densities must then

be applied.

#### 5.4 Some practical considerations in the simulation of road surface undulations.

A simulation test based on the analysis of Section 5.3 can be applied through the wheels of any four wheeled vehicle irrespective of vehicle wheelbase or track width. The input signals which represent the imposed displacements and are expressed in equation 5.3.3 can be defined from a knowledge of the direct spectral density of the road and the coherency function. Moreover, if we are prepared to assume that the road surface roughness is characterised by a completely homogeneous two-dimension Gaussian random process, and this seems to be a reasonable assumption in the cases of the routes considered in this thesis, then a complete road simulation, complete, that is, in the present context, can be performed with only a knowledge of the autocorrelation function of any longitudinal track along the road. For it was shown in Chapter 2 (Section 2.7) that the coherency function describing the relationship between two parallel tracks a width  $2b$  apart could be obtained from the autocorrelation function through the relationship:

$$\mathcal{R}_{RL}(\xi) = \mathcal{R}_{LR}(\xi) = \mathcal{R}(\sqrt{\xi^2 + 4b^2}) \quad 5.4.1$$

Thus the method of road description and classification proposed in Chapter 4 (Section 4.2) in which road surface spectra were approximated by the simple power law relationship

$$\left. \begin{aligned} \mathcal{J}(n) &= \mathcal{J}(n_0) \left(\frac{n}{n_0}\right)^{-w_1} && \text{for } n \leq n_0 \\ &= \mathcal{J}(n_0) \left(\frac{n}{n_0}\right)^{-w_2} && \text{for } n \geq n_0 \end{aligned} \right\} \quad 5.4.2$$

(with the proposed parameter values given in Table 5) is sufficient material on which to found the proposed simulation test.

Generation of the imposed displacement signals presents no major difficulty. SHINOZUKA [45] has shown that a Gaussian random stationary process with a zero mean value whose spectrum is given by  $S(\omega)$  can be simulated by the way of the series

$$z(t) = \sigma \left(\frac{2}{N}\right)^{\frac{1}{2}} \sum_{r=1}^N \cos(\omega_r t + V_r) \quad 5.4.3$$

where  $\sigma^2 = \langle z^2(t) \rangle$ ; and  $\omega_r$  ( $r = 1, 2, \dots, N$ ) are independent random variables identically distributed with the density function  $p(\omega) = p(\omega_r)$  given by

$$p(\omega) = S(\omega)/\sigma^2 \quad 5.4.4$$

and  $V_r$  are independent random variables identically distributed with the uniform density  $1/(2\pi)$  between 0 and  $2\pi$ .

The input signals to the vehicle have their complete spectral information contained in equation 5.4.2. The simulation technique is to generate the signals  $z(x)$  and  $\psi(x)$ , with spectra given by equation 5.3.2, using the method outlined above and then add these two uncorrelated signals to obtain the required input signal, e.g.

$$z_1(x) = z(x) + b\psi(x) \quad 5.4.5$$

An alternative method used to provide the four imposed displacements can be achieved by means of applying analogue (or digital) filters to the uncorrelated outputs of two random white noise generators: Identical high pass and low pass filters with fall-off rates ranging from 3dB to 9 dB per octave can be applied to each noise generator to establish the two basic uncorrelated signals  $\zeta(x)$  and  $\psi(x)$  required for the test. The varying fall-off rates enable spectra with any exponent  $w$  to be realised, and the coherency function to be approximately reproduced by a low pass filter.

Basic testing equipment requirements can be simply established. For complete vehicle simulation, with inputs applied directly through the tyres the vibrator stroke, velocity and acceleration requirements can be evaluated as follows.

The signal applied to each vibrator is given by, for example, from equation 5.3.3

$$\zeta_1(x) = \zeta(x) + b \psi(x) \quad 5.4.6$$

The spectrum  $S_1(n)$  can be obtained:

$$\begin{aligned} S_1(n) &= S_{\zeta}(n) + b^2 S_{\psi}(n) \\ &= \left[ \frac{1 + q(n)}{2} + b^2 \cdot \frac{1 - q(n)}{2b^2} \right] S_D(n) \end{aligned}$$

from equation 5.3.2

$$= S_D(n) \quad 5.4.7$$

with the expected result.

Hence the input spectrum to the vehicle can be evaluated by combining equations 5.4.7 and 5.4.2, and this will represent the displacement spectrum of the vibrator stroke,  $S_h(f)$ .

$$\begin{aligned}
 S_h(f) &= v^{w_1-1} J(n_o) \left[ \frac{f}{n_o} \right]^{-w_1} & n \leq n_o \\
 &= v^{w_2-1} J(n_o) \left[ \frac{f}{n_o} \right]^{-w_2} & n \geq n_o
 \end{aligned}
 \tag{5.4.8}$$

The mean square value is given by

$$\begin{aligned}
 \tilde{\sigma}_h^2 &= \int_{f_2}^{f_1} S_h(f) df \\
 &= J(n_o) v^{w_1-1} n_o^{w_1} \int_{f_2}^{f_m} f^{-w_1} df \\
 &+ J(n_o) v^{w_2-1} n_o^{w_2} \int_{f_m}^{f_1} f^{-w_2} df
 \end{aligned}$$

where  $f_m = n_o v$

$$\begin{aligned}
 &= J(n_o) v^{w_1-1} n_o^{w_1} \frac{1}{1-w_1} (f_m^{1-w_1} - f_2^{1-w_1}) \\
 &+ J(n_o) v^{w_2-1} n_o^{w_2} \frac{1}{1-w_2} (f_1^{1-w_2} - f_m^{1-w_2})
 \end{aligned}
 \tag{5.4.9}$$

The maximum piston stroke is then given by  $2\lambda\sigma_h$  where  $\lambda$  is the number of standard deviations. A similar analysis will yield the maximum velocity and acceleration requirements.

This simple form of analysis shows how basic information can be obtained regarding test equipment specification, and could easily be expanded, utilising the response analysis of Chapter 3, to provide the complete equipment specification necessary to provide an accurate simulation of road surface roughness.

## CHAPTER 6

### CONCLUSIONS

The major findings of this work are:

1) Road surface undulations may be treated and analysed by consideration of their statistical properties as member functions of a stationary random Gaussian process. Three road surface models have been proposed and their properties analysed and presented using standard techniques based on the existing theory of random vibration.

In the first instance, it was shown that the road could be considered as a cylindrical surface with random properties in the longitudinal direction. Complete description was thus provided by the spectral density of a single track along the road in the direction of traverse.

Secondly, a more realistic picture was obtained by consideration of the surface as consisting of a mean random track with a randomly varying, constant lateral slope for each longitudinal increment. Specification of this form of surface required either a knowledge of the two uncorrelated spectra of the mean track and lateral slope variations, or, as was demonstrated in Chapter 2, the direct spectrum of any track along the road together with the coherency function between two parallel tracks. The surface format suggested must preclude any variation in either the direct spectrum or in the form of the coherency function for varying track width.

Finally, consideration of the road surface as part of a two dimensional completely homogeneous random process was shown not only to provide a practical and plausible description of the actual surface, but also to allow for its complete description to be provided by a single autocorrelation function; this latter function being evaluated from any longitudinal track. It was shown that the coherency function for any pair of longitudinal tracks could be derived, with characteristics which varied with track width. Hence a single direct spectral density function serves as the exhaustive probability characteristic required to define road surfaces, and a new road classification method is proposed based on this function.

2) The theory of random vibration has been applied to the problem of determining the response of vehicle components to road surface excitation. A response theory has been developed in which the various forms of road surface description specify the excitation environment. Simple relationships between the response and excitation spectral densities were obtained not only for the case of a single input system, but also for a system with four inputs and a vehicle model with as sophisticated dynamics as may be necessary.

However, it was shown that a very simple road-vehicle model gave surprisingly good prediction of the response of a given vehicle component; a more sophisticated vehicle model with two inputs gave even better results. A model with four inputs was examined and found to give virtually no improvement for the particular component considered. It was suggested that unless the component of interest requires a four input model for geometric compatibility, or unless the coherency function

of the excitation departs from unity at a very low frequency, increased sophistication of the vehicle model to a case with four inputs could not be justified. Vehicle response to road surface undulations must always predominate at the lower frequency end of the spectrum.

3) A novel technique for the laboratory simulation of vehicle response to road surface roughness has been developed which is based on the statistical properties of the road surface and hence independent of the dynamic characteristics of the vehicle. It was shown that this has a major advantage over other methods and, if properly developed, seems likely to provide a very good simulation of vehicle response to road profile undulations.

No simulation can be perfect, and there are of course certain factors which have not been considered here. The effect of rolling tyres cannot easily be reproduced: certain components will be heavily stressed due to cornering or acceleration: a stationary random process cannot exactly reproduce the profiles of a real road since occasional large irregularities as potholes have been removed from the analysis. But certainly the founding of a test specification on basic road properties does seem likely, even in its basic form, to offer a meaningful type of test which has not previously been available.

While every effort has been made to provide experimental verification of the theoretical analysis of road surface roughness and vehicle response, it is recognised that this must be limited. The results of this work must therefore be taken as providing a sound theoretical treatise of the problem, and, although the results may not be applicable in every case, it has been shown that there

is sound justification that the proposed theory of profile excited vehicle response, based on the theory of random vibration, can be applied to provide sufficient information about road surface description, accurate vehicle response prediction and a basic form of simulation test. It must be remembered, however, that this forms only part of the overall problem of vehicle response. Much work needs to be done to provide the complete response or complete simulation of a vehicle's excitation environment.

## REFERENCES

1. ROBSON, J.D.                   An Introduction to Random Vibration  
E.U.P. (1963).
2. CRANDALL, S.H.                Random Vibration - Volume 1  
(Editor)                        Technology Press/Wiley 1958.
3. CRANDALL, S.H.                Random Vibration - Volume 2  
(Editor)                        M.I.T. Press 1963.
4. BLACKMAN, R.B.                The Measurement of Power Spectra  
TUKEY, J.W.                     from the Point of View of Communications  
                                   Engineering  
                                   Dover 1959.
5. BENDAT, J.S.                  Measurement and Analysis of Random Data  
PIERSOL, A.G.                    Wiley 1966.
6. CRANDALL, S.H.                Random Vibration in Mechanical Systems  
MARK, W.D.                       Academic Press 1963
7. LIN, Y.K.                     Probabilistic Theory of Structural  
                                   Dynamics  
                                   McGraw-Hill 1967
8. COOLEY, J.W.                  An algorithm for the Machine Calculation  
TUKEY, J.W.                     of Complex Fourier Series.  
                                   Mathematics of Computation 19 pp 297-301  
                                   (1965)
9. MACAULAY, M.A.                Measurement of Road Surfaces: Advances  
                                   in Automobile Engineering  
                                   Granfield International Symposium Series  
                                   4 pp 93-112 (1963).

10. CRAGGS, A.  
COLLEDGE, R.B.      Vehicle Service Loads - Part II - Random  
Vibration Analysis applied to Road  
Surface Measurements and Vehicle  
Suspension Performance  
MIRA report No. 1964/9 (1964)
11. ANDREW, S.      A Device for Rapid Measurement of  
Road-Surface Roughness  
MIRA Bulletin No. 1 (1968)
12. LABARRE, R.P.  
FORBES, R.T.  
ANDREW, S.      The Measurement and Analysis of  
Road Surface Roughness  
MIRA Report No. 1970/5 (1969)
13. BRAUN, H.      Untersuchungen über Fahrbahnebenheiten  
Deut.Kraft.No. 186 (1966)
14. PARKHILOVSKI, I.G.      Investigations of the Probability  
Characteristics of the Surfaces of  
Distributed Types of Roads  
Avtom.Prom. 8 pp 18-22 (1968)
15. KANESHIGE, I.      Application of the Probability Theory  
to the Design Procedure of an  
Endurance Test Track Surface  
SAE Paper No. 690111 (1969)
16. DODDS, C.J.  
ROBSON, J.D.      Road Simulation  
J.A.E. 3 No. 4 (1972)
17. VIRCHIS, V.J.  
ROBSON, J.D.      The Response of an Accelerating Vehicle  
to Random Road Undulation  
J. Sound Vib. 18 (3) pp 423 - 427  
(1971)

18. ELLIS, J.R. An Introduction to the Dynamic  
Properties of Vehicle Suspensions  
Proc. I. Mech. Eng. 179 (2A) (1964-5)
19. ELLIS, J.R. Vehicle Dynamics  
Business Books (1969)
20. BARSON, C.W. Tyre and Vehicle Vibration  
et al Proc. I. Mech. Eng. 179 (2A) (1964-5)
21. HALES, F.D. The Assessment of Vehicle Ride  
et al and Handling  
Proc. Auto. Div. I. Mech. Eng. 182 (3B)  
(1967/8)
22. KOZIN, F. On the Statistical Properties of  
BOGDANOFF, J.L. the Ground Contour and its Relation  
to the Study of Land Locomotion  
Land Locomotion Laboratory, Michigan  
(1962)
23. LONGUET-HIGGINS, M.S. The Statistical Analysis of a Random  
Moving Surface  
Phil. Trans. of Royal Soc. London,  
Series A. Math. and Phys. Sci. pp 321  
249 No. 966 (1957)
24. BIENIEK, M.P. Suspension Dynamics  
Automobile Engineer (1960)
25. RAPIN, P. Une application à l'automobile de  
la technique des vibrations aléatoires  
Rev. Franç. de Méc. No. 7 (1963)

26. RAPIN, P. Comportement d'un véhicule automobile soumis à des excitations aléatoires Rev. Franc. de Mec. No. 14 (1965)
27. VAN DEUSEN, B.D. Analytical Techniques for designing Riding Quality into Automotive Vehicles SAE paper No. 670021 (1967)
28. ROSSINI, L.R. Applicazione di criteri statistici allo studio delle vibrazioni verticali delle sospensioni A.T.A. (1969)
29. DODDS, C.J.  
ROBSON, J.D. The Response of Vehicle Components to Random Road Surface Undulations Proc. 13 F.I.S.I.T.A. Congress, paper 17.2D, Brussels (1970)
30. PEVZNER, Ya M.  
TIKHONOV, A.A. An Investigation into the Statistical Properties of the Microprofile of the Main Types of Motor Road Avtom. Prom. 30 (1) pp 15-18 (1964)
31. DINCA, F.  
TEODOSIU, C. Vibratii Neliniare si Aleatoare Editura Academiei Republicii Socialiste Romania, (1969)
32. DAVENPORT, W.B.  
ROOT, W.L. Random Signals and Noise McGraw Hill Book Co. (1958)
33. DOOB, J.L. Stochastic Processes John Wiley and Sons (1953)
34. MITSCHKE, M. Schwingempfinden von Menschen um fahrenden Fahrzeug Proc. 12 F.I.S.I.T.A. Congress paper 2-11 (1968)

35. VAN DEUSEN, B.D. Ride Evaluation  
Automobile Engineer December (1963)
36. THOMPSON, A.G. Optimum Damping in a Randomly Excited  
Non-linear Suspension  
Proc.I. Mech.E. 184 (2A) (1969)
37. BOGDANOFF, J.L. On the Statistical Analysis of the  
KOZIN, F. Motion of Some simple Vehicles moving  
on a Random Track  
Land Locomotion Report No. 65
38. MITSCHKE, M. Dynamik der Kraftfahrzeuge  
Springer-Verlag (1972)
39. LOEBICH, R. Untersuchungen zum Abrall-und  
Federungs - Verhalten von Pkw - Reifen  
Dt. Kraft. StrassVerk.Tech. No. 189  
(1967)
40. QUINN, B.E. Effect of Pavement Conditions upon Dynamic  
THOMPSON, D.R. Vehicle Reactions  
Purdue Univ. Dept. of Maths.  
Report BPR - 611004
41. WALLS, J.H. Some Measurements and Power Spectra  
et al of Runway Roughness  
N.A.C.A. T.N. 3305
42. WENDEPORN, J.O. Description of Road Profile by  
means of the Spectral Density of the  
Irregularities  
A.T.Z. 69 No. 5 (1967)

43. MARTIN, M.A. Digital Filters for Data Processing  
Tech. info. Ser. No. 62SD484 G.W.C.  
Missile and Space Div. (1962)
44. ANDREW, S. Vehicle Service Loads - Suspension  
WHITTAKER, M.W. Component Loads in Four Passenger  
Cars  
MIRA Report 1969/10
45. SHINOZUKA, M. Fatigue Life of Simple Bridges;  
KOBORI, T. A Sensitive Study  
Columbia U.Tech. Report No. 8  
NSF-GK 3858

APPENDIX 1

A Range of Road Sections Measured by M.I.R.A.

The reference letters and locations are taken from M.I.R.A. Report No. 1970/5. The subjective ratings vary from 'a' (very smooth) to 'f' (very rough) and are the rating given to the road by several M.I.R.A. engineers.

The roads are given in three sections

- Motorways;
- Principal Roads;
- Minor Roads.

They are arranged in ascending order of their  $f(n_0)$  value,

$$\text{with } n_0 = \frac{1}{2\pi} \text{ c/m.}$$

MOTORWAYS

M.I.R.A. Ref.	Location	Subjective Rating	Road Spectrum at Spatial Frequency		Upper Slope $W_1$	Lower Slope $W_2$
			FT <sup>3</sup> /C	CM <sup>3</sup> /C		
BK	High Speed Circuit M.I.R.A. Proving Ground	b	0.000078	2.20	2.89	1.43
AU	Ostend-Brussel Autobahn Jabbeke	a	0.00009	2.55	2.86	1.53
BF	Autoroute Al. 25 Km N. of Paris	a	0.00014	4.00	1.87	1.46
U	Ml. Leicestershire	a	0.00016	4.53	1.75	1.44
AW	Cologne-Bonn Autobahn 8 Km S. of Cologne.	a	0.00016	4.53	1.66	1.11
V	M6. Staffordshire	b	0.00043	12.18	1.70	1.08
AL	Ostend-Brussels Autobahn Ghent	b	0.00044	12.45	1.80	1.06
BL	Horizontal Twin Track Straight. M.I.R.A. Proving Ground	b	0.00069	19.59	2.03	1.57
BZ	Ostend-Brussels Autobahn Bruges	b	0.00079	22.49	1.84	1.28
BA	Autoroute du Sud 31 Km S. of Paris	a	0.00081	23.02	1.52	1.80
AZ	Cologne-Frankfurt Autobahn Wiesbaden 2	c	0.00096	27.04	1.96	1.27
AY	Cologne-Frankfurt Autobahn Wiesbaden	c	0.00174	49.21	1.46	1.29

PRINCIPAL ROADS

I.T.R.A. Ref.	Location	Subjective Rating	Road Spectrum at Spatial Frequency		Upper Slope $W_1$	Lower Slope $W_2$
			$Ft^3/C$	$CM^3/C$		
BP	E. Horndon Essex	b	0.00017	4.92	2.89	1.57
BE	N20 N. of Etampes 47 Km S. of Paris		0.00030	6.55	2.57	1.61
AC	A5 High Cross Warwickshire	b	0.00039	11.02	2.82	1.13
AS	Mons-Brussels N7 13 Km N. Of Soignes	b	0.00049	13.87	2.10	1.55
AD	A5 Rugby Warwickshire	b	0.00085	24.10	1.18	1.33
AE	A5 Weedon Northants	b	0.00096	27.04	2.41	1.49
AB	A5 Atherstone Warwickshire	b	0.00132	37.33	1.81	2.09
Z	Coleshill Warwickshire	c	0.00162	45.92	1.67	1.17
BU	Luton Bedfordshire	c	0.00166	46.99	1.77	1.36
BH	N347 1.5 Km E. of Les Moeres		0.00178	50.36	1.63	1.39
BG	N16 W. of St. Pol Sur Ternoise	d	0.00263	74.48	2.07	1.15
BB	N191 0.4 Km S. of Ballancourt		0.00302	85.92	1.70	1.00
BC	D17 W. of Ballancourt 35 Km. S. of Paris		0.00372	105.21	2.34	1.61
BJ	N347 0.4 Km W. of Les Moeres		0.00417	118.04	2.25	1.42
BD	D17 W. of Le Bouchet 35 Km. S. of Paris	d	0.00479	135.53	2.16	1.73
AA	Coventry Warwickshire	d	0.00510	141.92	1.43	1.44

MINOR ROADS

M.I.R.A. Ref.	Location	Subjective Rating	Road Spectrum at Spatial Frequency		Upper Slope	Lower Slope
			Ft <sup>3</sup> /C	CM <sup>3</sup> /C	W <sub>1</sub>	W <sub>2</sub>
BM	Dunton Essex		0.00026	7.36	2.72	1.46
BM	Gladbach-Elrp 30 Km S.W. of Cologne		0.00026	7.36	1.54	1.20
BW	Beeley Derbyshire		0.00081	23.02	2.67	1.60
BR	Private Drive Essex	c	0.00085	24.10	1.96	1.42
H	Hednesford Staffordshire	d	0.00112	31.71	3.08	1.52
BN	E. Horndon Essex	c	0.00120	34.04	2.19	1.41
C	Huntingdon Staffordshire	c	0.00123	34.84	2.30	1.24
W	Fosseway Warwickshire	d	0.00166	46.99	2.40	1.21
BQ	E Horndon Essex		0.00234	66.38	2.23	1.96
AP	10 Km N. of Mons		0.00234	66.38	2.10	1.26
B	Gailey Staffordshire	d	0.00234	66.38	2.38	0.95
Y	Slaley Derbyshire	e	0.00288	81.67	2.48	1.58
BS	Private Drive Bedfordshire	d	0.00288	81.67	2.56	1.23
BV	Luton Bedfordshire.		0.00331	93.72	2.90	1.47
AH	Market Bosworth Leicestershire		0.00347	98.18	1.66	1.04
X	Fosseway Leicestershire	d	0.00398	112.73	2.11	1.44
AG	Upton Leicestershire	d	0.00447	126.49	2.14	1.55
BT	Luton Bedfordshire	d	0.00457	129.43	2.40	1.43
AN	6 Km N. of Mons		0.00724	205.14	1.48	1.46
BX	Beeley Derbyshire	f	0.00955	270.42	2.16	1.64
AM	2 Km S.W. of Ghent	f	0.01202	340.44	1.63	1.39
J	Pave M.I.R.A. Proving Ground	f	0.01738	492.09	3.49	1.17
AQ	5 Km. E. of Mons	f	0.02239	633.93	2.14	1.18
AV	Ghlin 5 Km N. of Mons	f	0.03802	1076.57	3.15	1.88
AR	4 Km E. of Mons	f	0.2138	6054.02	1.34	2.01

## APPENDIX 2

### The Measurement and Analysis of Road Surface Undulations

A brief description of the measurement and analysis techniques developed during the course of this work, and used to estimate road and response spectra, is given.

#### A2.1 Measurement of road surface undulations

The surface undulations of the routes A, B and C presented in Chapter 4, Section 4.3, were measured by the same survey technique. Reduced levels were obtained for two parallel tracks, 4 ft. (1.2m) apart, and running for distances of the order of 0.5 to 1 mile (0.8 - 1.6 km). The levels were recorded in three sets with a different longitudinal spacing  $\Delta x$ :

- 1) the complete distance at  $\Delta x = 4$  ft. (1.2m)
- 2)  $3/4$  of the complete distance at  $\Delta x = 2$  ft. (0.6m)
- 3) 2 separate lengths of around  $1/8$  of the complete distance at  $\Delta x = 1$  ft. (0.3m).

This would ensure that the complete frequency range of the spectrum was covered with a minimum time spent on the field measurement.

Typical progress was in the region of 130 levels per hour.

The levels were read to 0.01 ft. (3mm) with an allowable error of  $\pm 0.005$  ft (1.5 mm). This in turn would produce typical errors in the spectrum of around 10% at wavelengths of 10 ft. (3m) and 1% at wavelengths greater than 25 ft. (7.5m).

The data so obtained to represent the random process  $\{z_j(x)\}$  was thus in the form of discrete samples of finite length, and consideration of the analysis techniques developed to obtain an estimate of the "true" road spectrum  $f(u)$ , is given in Section A2.2. Prior to this analysis, however, preliminary filtering was carried out on the data as explained in the text, Section 4.3.

## A2.2 Analysis of road surface roughness

The definitions for the correlation function,  $R(\delta)$ , and the road spectrum,  $f(n)$  given in the text, have been based on a continuous (in)finite signal with the Fourier transform of the correlation function defined for all lag values,  $\delta$ . In order to evaluate these functions, however, we must introduce the idea of discrete, finite data, i.e. we must be prepared to carry out our analysis work on the series of discrete sampled values which represent the signal of finite length characterising the road. That is, we have a signal  $z(x)$  in the interval  $0 \leq x \leq x_{\max}$  and we sample values of  $z(x)$  at equidistant intervals  $\Delta x$  to obtain a sequence of  $N$  discrete observations  $z_1 z_2 \dots z_N$ .

Before proceeding further it is necessary to state without proof some theorems and ideas related to the handling of discrete data. The sampling theorem attributed to SHANNON [A1] states that if the power in  $z(x)$  is limited to a band less than  $\frac{1}{2\Delta x}$ , then sampling at an interval of  $\Delta x$  enables one to reconstruct the signal uniquely.

Secondly, if  $A(in)$  and  $z(x)$  are an integral Fourier transform pair

$$\text{i.e.} \quad \left. \begin{aligned} A(in) &= \int_{-\infty}^{\infty} z(x) e^{-i2\pi nx} dx \\ z(x) &= \int_{-\infty}^{\infty} A(in) e^{i2\pi nx} dn \end{aligned} \right\} \quad \text{A2.1}$$

and we define the discrete Fourier transform to be

$$A(r) = \sum_{k=0}^{N-1} z(k) e^{-i2\pi kr/N} \quad r = 0, 1, 2, \dots, N, \quad A2.2$$

then provided  $z_k$  is sampled from  $z(x)$  at equally spaced points (Nyquist samples) then  $A(r)$  is closely related to  $A(\omega)$ . It is beyond the scope of this note to expand on this point and further information can be obtained from COCHRAN [A2] (1967) and COOLEY [A3] (1969).

Lastly, all the theorems relating to the integral transform e.g., convolution, are applicable to the discrete case.

#### A2.2.1 Standard Method or BLACKMAN-TUKEY Method of Spectral Analysis [A4]

The correlation function is evaluated from the sampled data and the spectrum through its Fourier transform. Since the correlation function is an even function of  $\delta$ , we can define the "one-sided" spectrum to be

$$S(\omega) = 4 \int_0^{\infty} R(\delta) \cos 2\pi\omega\delta d\delta \quad A2.3$$

where

$$R(\delta) = \lim_{x_{\max} \rightarrow \infty} \frac{1}{x_{\max}} \int_{-\frac{x_{\max}}{2}}^{\frac{x_{\max}}{2}} z(x) z(x+\delta) dx \quad A2.4$$

The continuous signal,  $z(x)$ , with zero mean value, is sampled at equal intervals,  $\Delta x$ , to obtain the finite series  $z_k$  for  $k = 0, 1, 2, \dots, N-1$ . The choice of  $\Delta x$  must be such that the largest frequency

in the record

$$n_c = \frac{1}{2 \Delta x} \quad A2.5$$

It is obvious that whereas the correlation function defined by equation A2.4 is evaluated for all lag values,  $\delta$ , in the discrete case of  $N$  samples, it will not be possible to obtain an infinite number of lag values, and moreover, it is usually not desirable to use lag values longer than about 5% ~ 10% of the record length [A4.]

We therefore replace equation A2.4 by an apparent correlation function for the discrete case. One common estimator of this function, and used in this present work is given by

$$\tilde{R}(r) = \frac{1}{N-r} \sum_{k=0}^{N-r} z_k z_{k+r} \quad A2.6$$

for  $r = 0, 1, 2, \dots, m$ , with  $\delta = r \Delta x$

The number of lag values,  $m$ , decides the equivalent frequency bandwidth of the spectrum in the frequency interval  $(0, n_c)$

$$B_e = \frac{2n_c}{m} = \frac{1}{m \Delta x} \quad A2.7$$

and for small statistical uncertainty in the spectrum estimates we should choose  $m \ll N$  since the maximum number of degrees of freedom is  $2N/m$ . But, unfortunately, high resolution will result when  $m$  is large, and a compromise situation has developed.

Because the apparent correlation function A2.6 has no value for  $\delta > \delta_{\max}$ , we must replace this function by a modified correlation function  $\hat{R}(\delta)$  which is defined for all  $\delta$ . This is achieved by

multiplying the apparent correlation function  $\tilde{R}(\delta)$  by a prescribed even function of  $\delta$ ,  $P(\delta)$  subject to the restriction that

$$\left. \begin{aligned} P(0) &= 1 \\ P(\delta) &= 0 \quad \delta > \delta_{\max} \end{aligned} \right\} \quad \text{A2.8}$$

i.e. 
$$\hat{R}(\delta) = \tilde{R}(\delta) \cdot P(\delta) \quad \text{A2.9}$$

This new function may not be a good estimate of the true correlation function  $R(\delta)$ , but its Fourier transform gives a very respectable estimate of the true spectrum  $S(n)$  [A4].

The function used for  $P(\delta)$  is the lag window, whose use is called "Hamming"

$$\begin{aligned} P(\delta) &= 0.54 + 0.46 \cos \frac{\pi\delta}{\delta_{\max}} & |\delta| < \delta_{\max} \\ &= 0 & |\delta| > \delta_{\max} \end{aligned} \quad \text{A2.10}$$

Further functions for  $P(\delta)$  may be found in references [A4, A5, A8.]

However, one of the advantages of the digital technique is that instead of modifying the apparent correlation function as in equation A2.9 it is possible to evaluate a "rough" spectrum,  $\tilde{f}(n)$ , from the apparent correlation function and then linearly "smooth" or convolve this spectrum with the spectral window  $Q(n)$  corresponding to  $P(\delta)$ . (The transform of a product of two signals yields the convolution of the transforms of each signal). Moreover, if the rough spectrum is evaluated for a frequency interval

$$\frac{1}{2\delta_{\max}} = \frac{1}{2m \Delta x} \quad \text{A2.11}$$

this provides for  $m/2$  independent spectral estimates (since those at points less than  $\frac{2n}{m} = B_e$ , apart will be correlated), and the spectral window simplifies to smoothing adjacent points with the weights 0.23, 0.54, 0.23.

We can now evaluate the "rough" spectrum by means of the discrete Fourier transform which for the case of a real even function can be written as [A3].

$$J(n_r) = 2 \Delta x \left[ \tilde{Q}(0) + 2 \sum_{k=1}^{m-1} \tilde{Q}(k) \cos \beta + (-1)^r \tilde{Q}(m) \right] \quad A2.12$$

where  $\beta = 2\pi \delta n_r = 2\pi (k \Delta x) \cdot \frac{r}{2m \Delta x} = \pi \frac{kr}{m}$  }  
 $r = 0, 1, 2, \dots, m$  }

The final "smoothed" estimates of the spectrum are obtained by

$$\hat{J}(n_r) = 0.23 \tilde{J}(n_{r-1}) + 0.54 \tilde{J}(n_r) + 0.23 \tilde{J}(n_{r+1}) \quad A2.13$$

and  $\hat{J}(n_r)$  is our sampled estimate of the true spectrum  $J(n)$ , which is used in the main body of the text.

A2.2.2 Direct method using the Fast Fourier Transform of COOLEY and TUKEY [A6]

If  $y_k$  is our sampled signal of  $N$  points we can evaluate using the F.F.T. algorithm the discrete Fourier transform for the  $N$  point sequence.

$$A_r = \sum_{k=0}^{N-1} y_k e^{-i2\pi kr/N} \quad A2.14$$

for  $r = 0, 1, 2, \dots, N - 1$

Forming the modulus squared of the complex  $A_r$  coefficients we evaluate the periodogram  $I(n)$  which is not, unfortunately, a good estimate of the spectrum.

$$I(n_r) = \frac{2 \Delta x}{N} |A_r|^2 \quad A2.15$$

where  $n_r = \frac{r}{N \Delta x}$   $r = 0, 1, \dots, N/2$

(It is worth noting that although  $N$  real data points were transformed to  $N-2$  complex frequency values ( $A_0$  and  $A_n$  are real), due to the property that  $A_r = A_{-r}^* = A_{N-r}^*$  (i.e. sequence  $\{z_k\}$  is real) and since our maximum frequency in the record is  $n_c = \frac{1}{2 \Delta x}$  values of  $A_r$  and  $I(n_r)$  are redundant for  $\frac{N}{2} < r < N$ ).

It remains now a matter of smoothing the spectrum with an appropriate window, or multiplying the original data by a prescribed function defined for all values of distance,  $x$ . Examples of smoothing functions may be found in reference [A7].

Programs based on both of these analysis techniques were developed by the author and used to establish the estimate of the road spectrum,  $\hat{J}(n)$ . The latter technique, based on the F.F.T. algorithm, was used mainly for the response analysis, since a narrower analysis bandwidth could more readily be obtained.



A8. BENDAT, J.S.  
PIERSOL, A.G.

Random Data: Analysis and Measurement  
Procedures  
Wiley Interscience (1971)

## APPENDIX 3

### Test Vehicle Parameters

The parameters of the two test vehicles A and B are given in Tables A1 and A2 respectively. The following notes apply to both sets of parameters.

1. The total mass was assumed distributed between front and rear suspension in such a way that the position of the centre of gravity, G, was maintained.
2. A half-width model was considered; all masses are equal to half those of the test vehicle.
3. Equivalent spring and damping rates in the vertical direction, at wheel centres.
4. These are estimates of the damping rate, in the vertical direction, obtained from a knowledge of the roughness coefficient of the test route, and from individual tests on dampers.
5. Tyre parameters obtained from a knowledge of tyre type, pressure and vehicle speed [39].
6. Test vehicle mass includes personnel and testing equipment.

TABLE A1

Test Vehicle Parameters - Vehicle A

PARAMETER	SYMBOL	NOTE NO.	VALUE IN BRITISH UNITS	VALUE IN S.I. UNITS
Front near-side mass	$m_{s_1}$	1, 6		
Front unsprung mass	$m_{u_1}$	2	2.4 lbf sec <sup>2</sup> /ft	35 kg
Rear unsprung mass	$m_{u_2}$	2	3.5 lbf sec <sup>2</sup> /ft	51 kg
Front suspension spring	$k_1$	3	680 lbf/ft	9.8 kN/m
Rear suspension spring	$k_2$	3	1300 lbf/ft	18.9 kN/m
Mass at centre of gravity	$m_g$	2, 6	39.1 lbf sec <sup>2</sup> /ft	573 kg
Pitch moment of inertia	$I_p$	2, 6	670 lbf sec <sup>2</sup> ft	910 kg m <sup>2</sup>
Front damping	$c_1$	3, 4	68.5 lbf sec/ft	1 kN s/m
Rear damping	$c_2$	3, 4	68.5 lbf sec/ft	1 kN s/m
Length G to front	$l_1$		4.33 ft	1.31 m
G to rear	$l_2$		4.37 ft	1.32 m
Track	2b			
Tyres: front stiffness	$k_{T_1}$	5	8400 lbf/ft	122.5 kN/m
damping	$c_{T_1}$	5	12.6 lbf sec/ft	0.184 kN s/m
rear stiffness	$k_{T_2}$	5	8400 lbf/ft	122.5 kN/m
damping	$c_{T_2}$	5	12.6 lbf sec/ft	0.184 kN s/m

TABLE A2

Test Vehicle Parameters - Vehicle B

PARAMETER	SYMBOL	NOTE NO.	VALUE IN BRITISH UNITS	VALUE IN S.I. UNITS
Front near-side mass	$m_{s_1}$	1, 6	12.28 lbf sec <sup>2</sup> /ft	180 kg
Front unsprung mass	$m_{u_1}$	2	1.66 lbf sec <sup>2</sup> /ft	24.3 kg
Rear unsprung mass	$m_{u_2}$	2	1.72 lbf sec <sup>2</sup> /ft	25.2 kg
Front suspension spring	$k_1$	3	1214 lbf/ft	17.8 kN/m
Rear suspension spring	$k_2$	3	1788 lbf/ft	26.0 kN/m
Mass at centre of gravity	$m_g$	2, 6	32.5 lbf sec <sup>2</sup> /ft	475 kg
Pitch moment of inertia	$I_p$	2, 6	324 lbf sec <sup>2</sup> ft	440 kg m <sup>2</sup>
Front damping	$c_1$	3, 4	85 lbf sec/ft	1.24 kN s/m
Rear damping	$c_2$	3, 4	95 lbf sec/ft	1.39 kN s/m
Length G to front	$l_1$		4.25 ft	1.3 m
G to rear	$l_2$		2.58 ft	.785 m
Track	2b		4.0 ft	1.22 m
Tyres: front stiffness	$k_{T_1}$	5	7500 lbf/ft	110 kN/m
damping	$c_{T_1}$	5	9 lbf sec/ft	0.131 kN s/m
rear stiffness	$k_{T_2}$	5	11800 lbf/ft	172 kN/m
damping	$c_{T_2}$	5	1.1 lbf sec/ft	0.161 kN s/m

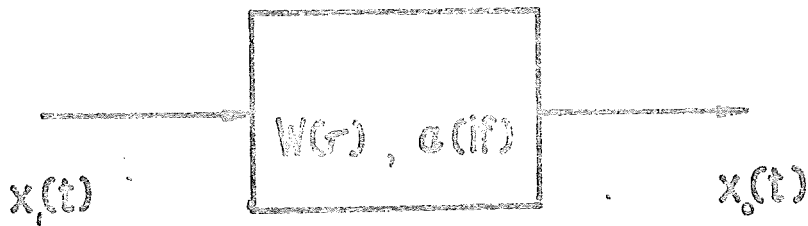


FIGURE 1

Single point excitation and response

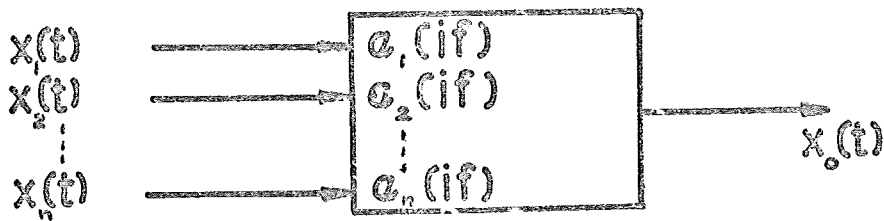


FIGURE 2

Multiple point excitation system

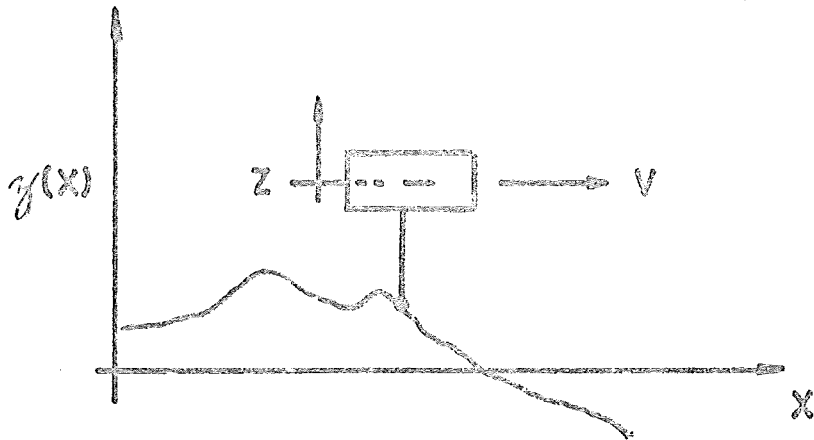


FIGURE 3

Single point follower on a random track

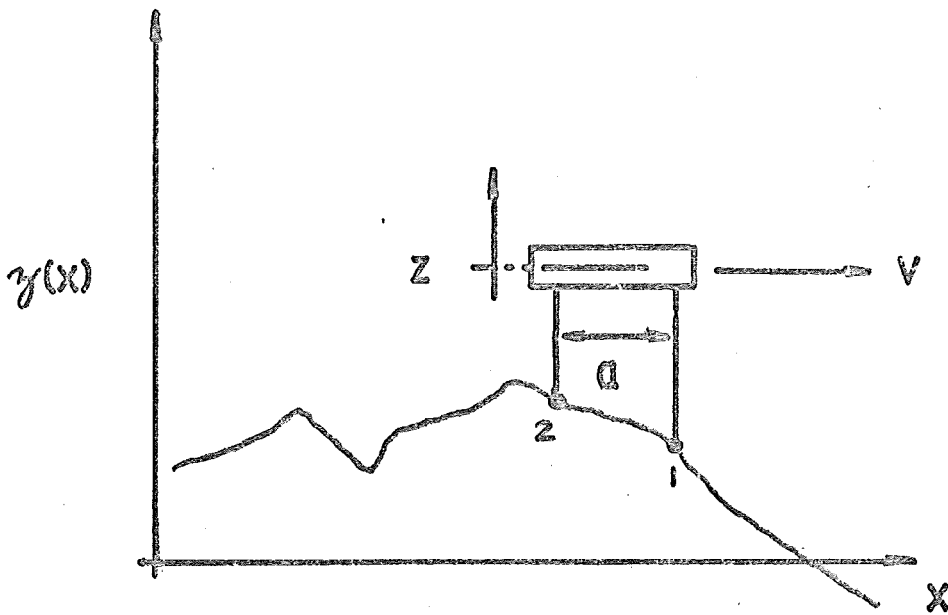


FIGURE 4

Two point follower on a random track

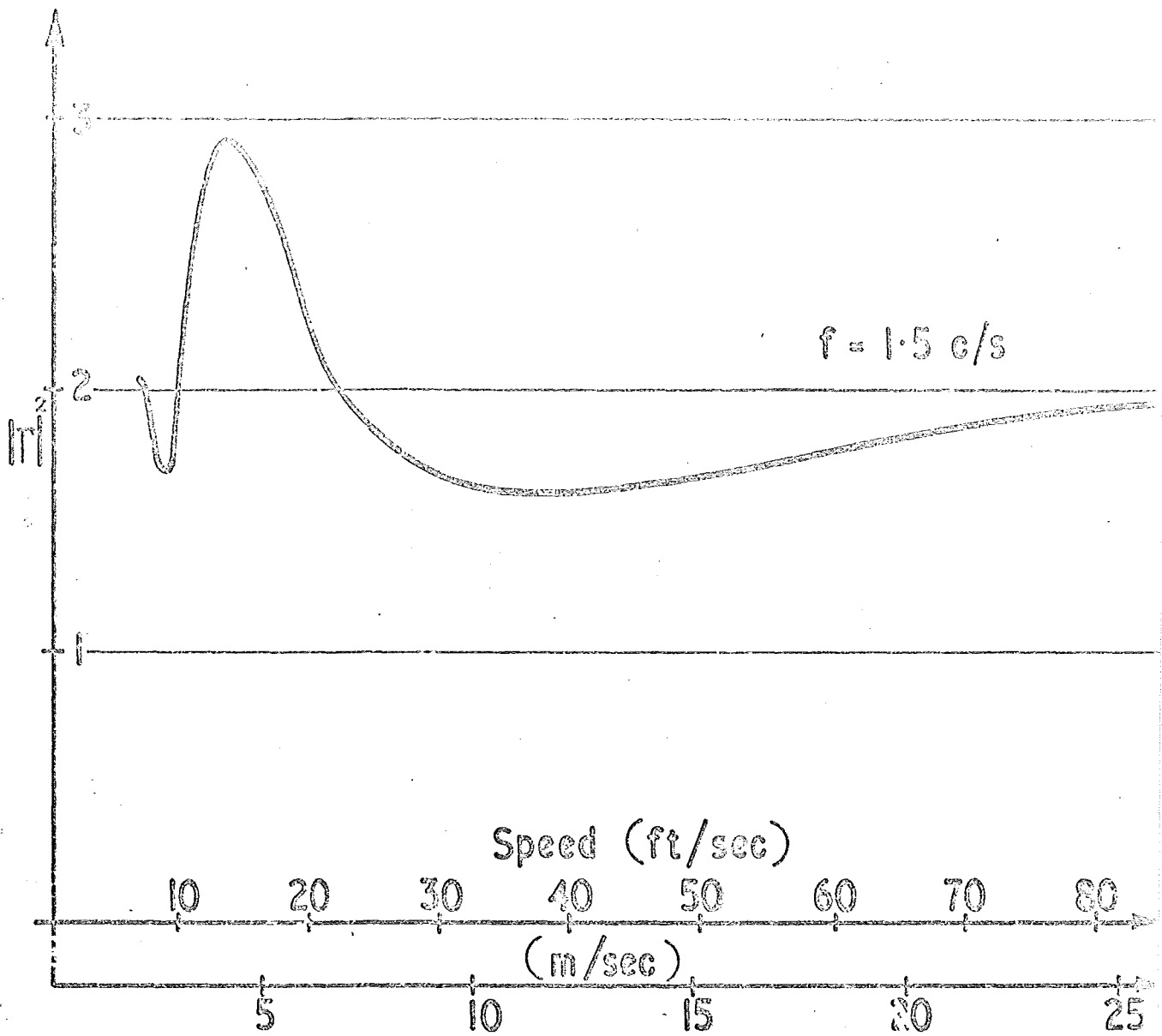


FIGURE 5

Relationship of  $|T|^2 = \frac{vS^0(f)}{\delta(n)}$  against speed  $v$ .

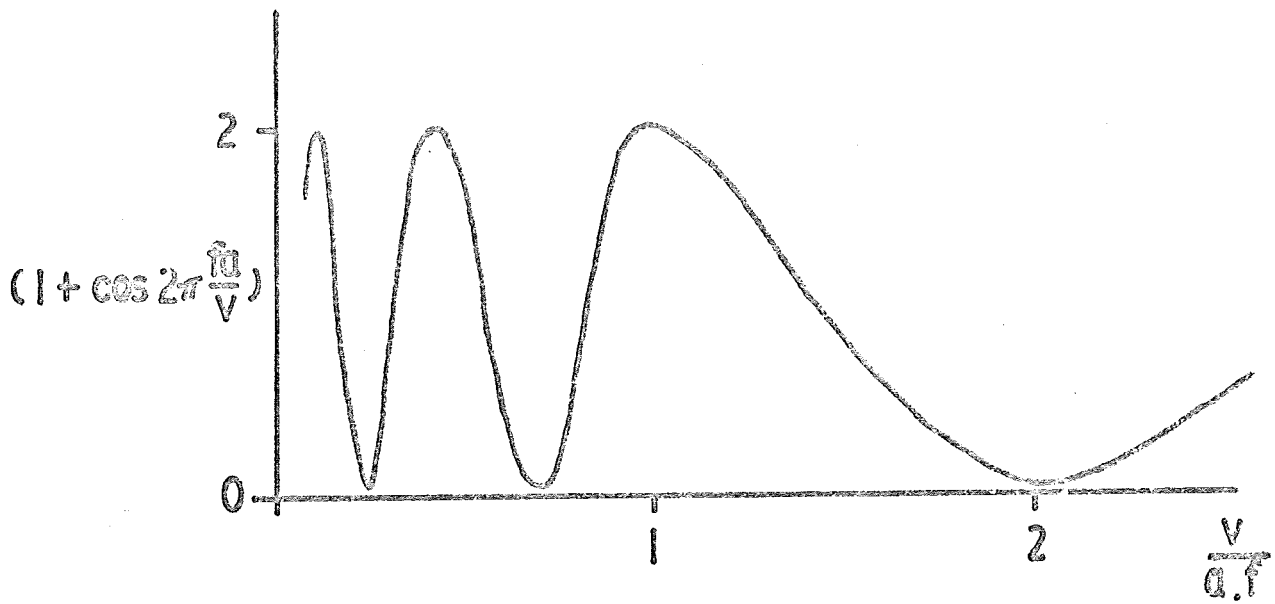


FIGURE 6

Function  $(1 + \cos 2\pi \frac{f_0}{v})$  against  $\frac{v}{a.f}$

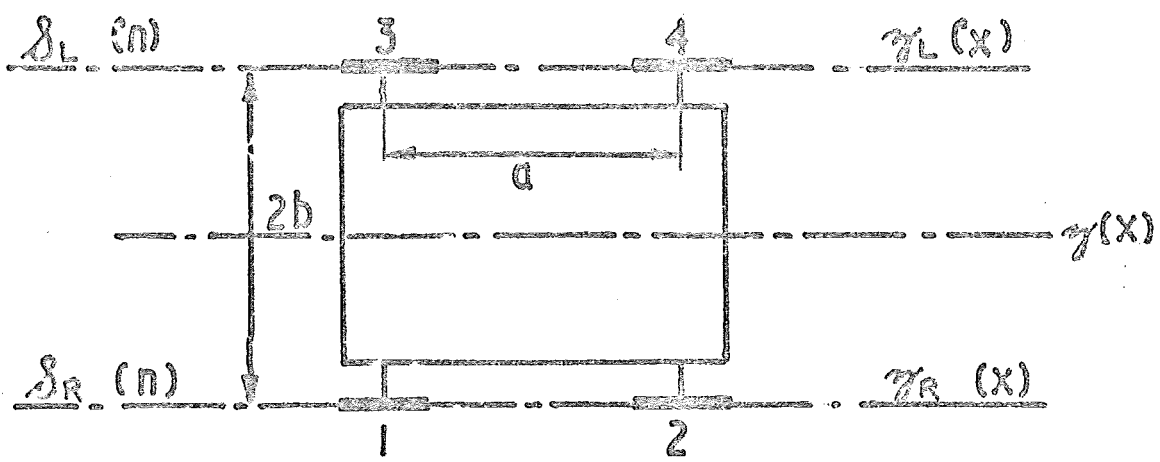


FIGURE 7

4 - input model - layout of inputs

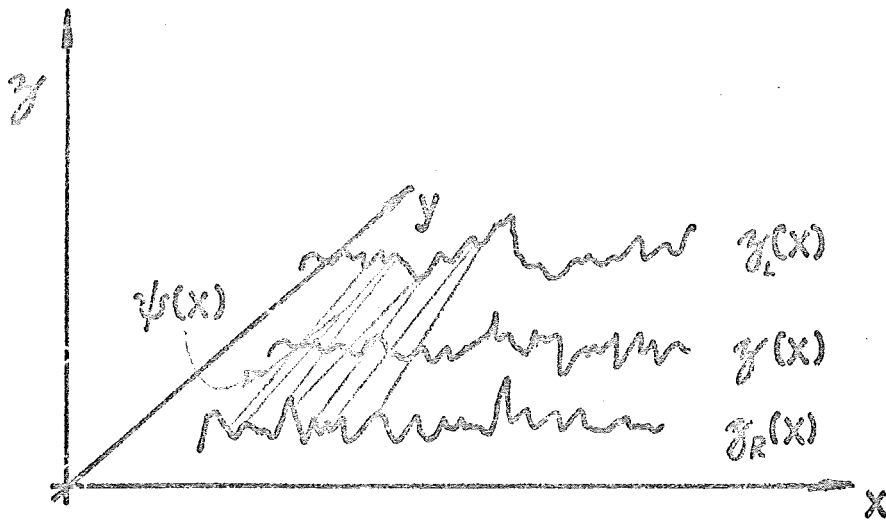


FIGURE 8a

3-D characterisation of road surface roughness

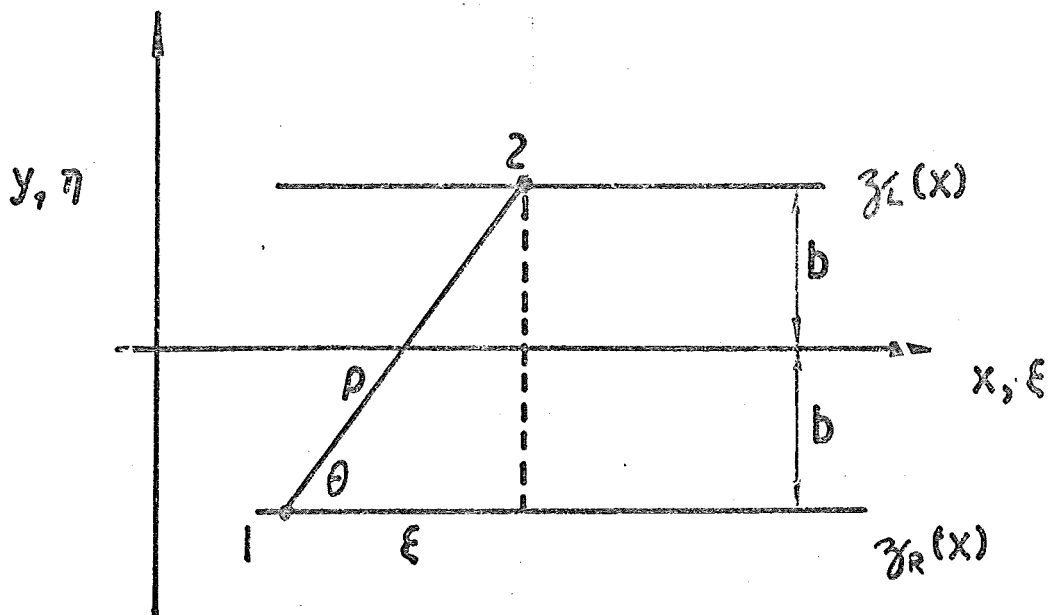


FIGURE 8b

2-D road surface parameters

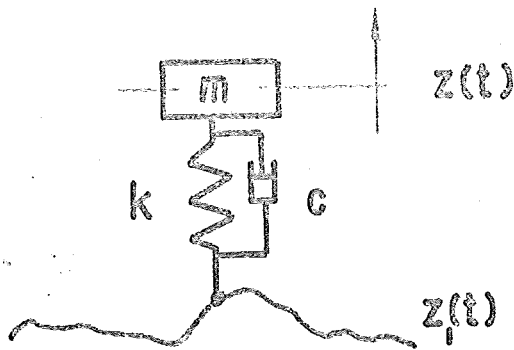


FIGURE 9

Single input, single degree of freedom vehicle model

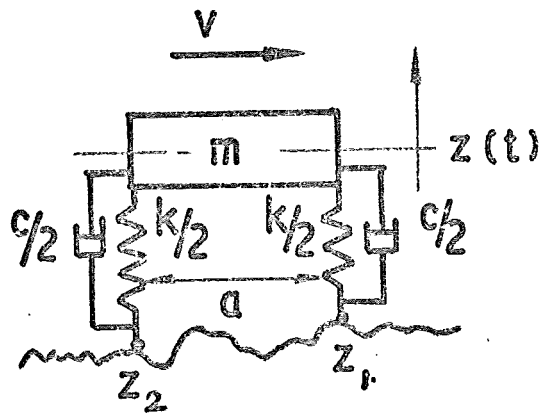


FIGURE 10

Double input, single degree of freedom vehicle model

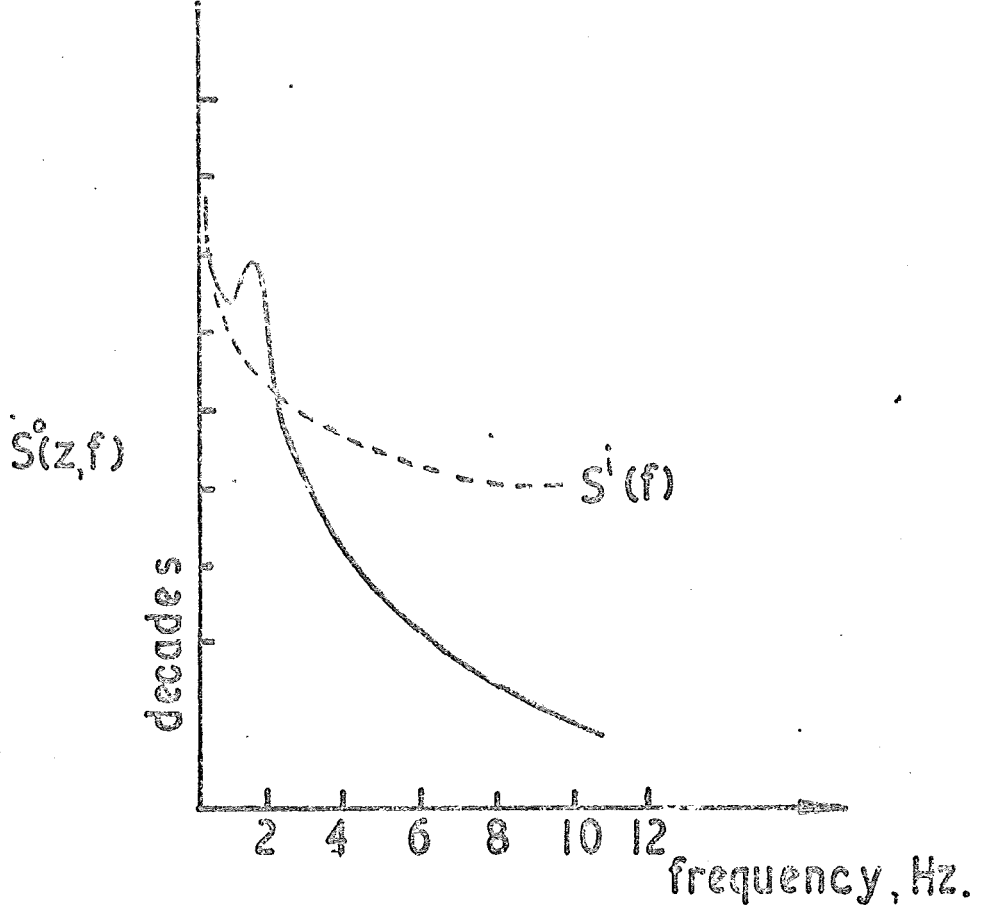


FIGURE 11

Response spectrum - displacement of mass, m

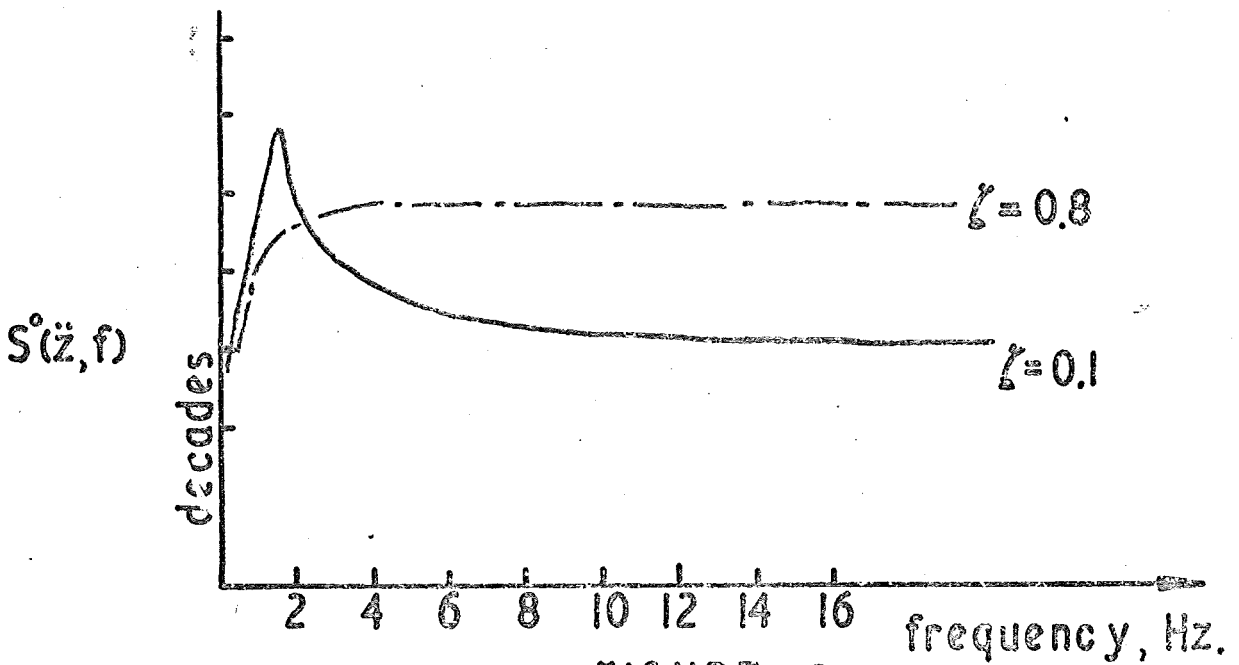


FIGURE 12

Response spectrum - acceleration of mass, m

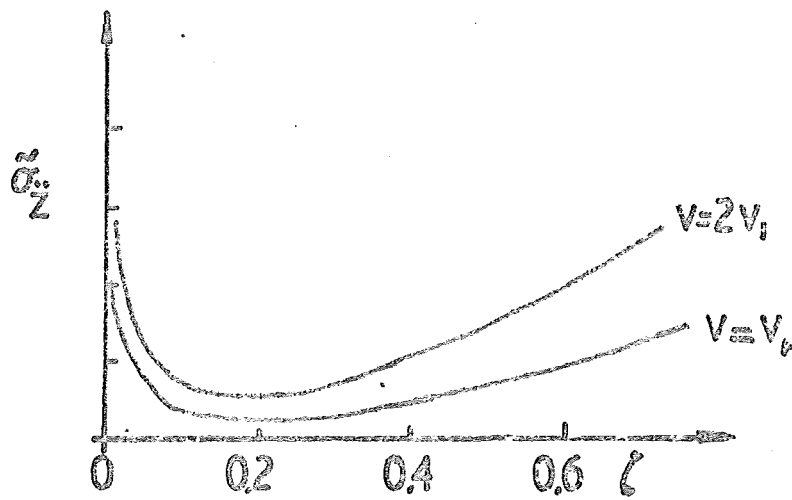


FIGURE 13

Variation of mean square acceleration response with damping

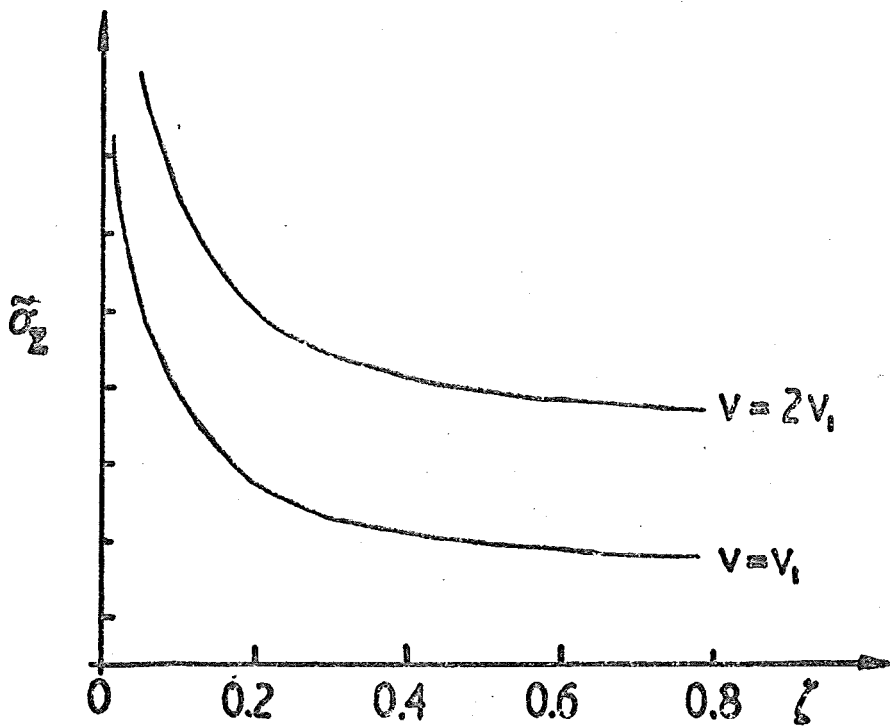


FIGURE 14

Variation of mean square displacement response with damping

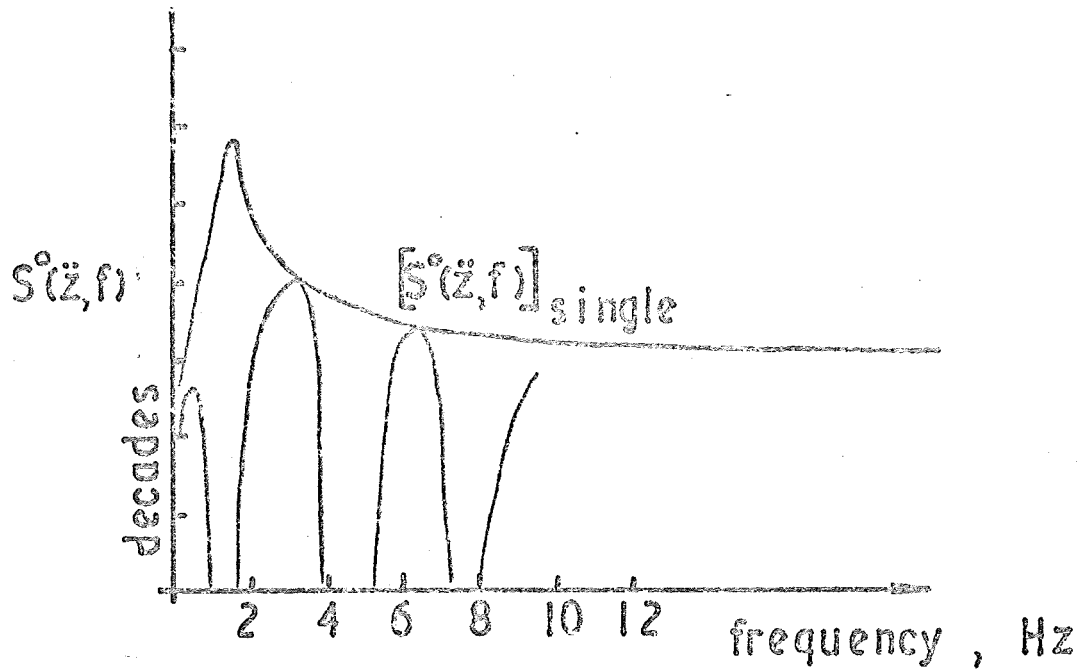


FIGURE 15

Acceleration response spectrum, double input vehicle model

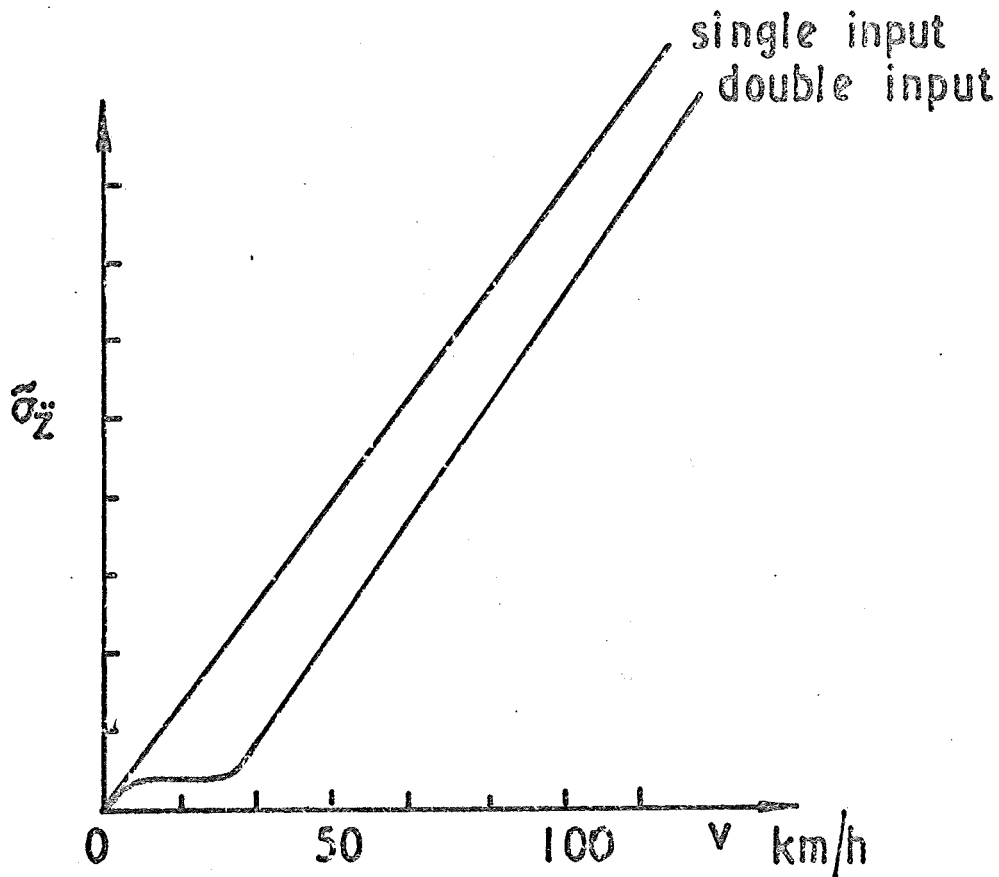


FIGURE 16

Variation of mean square acceleration response with speed

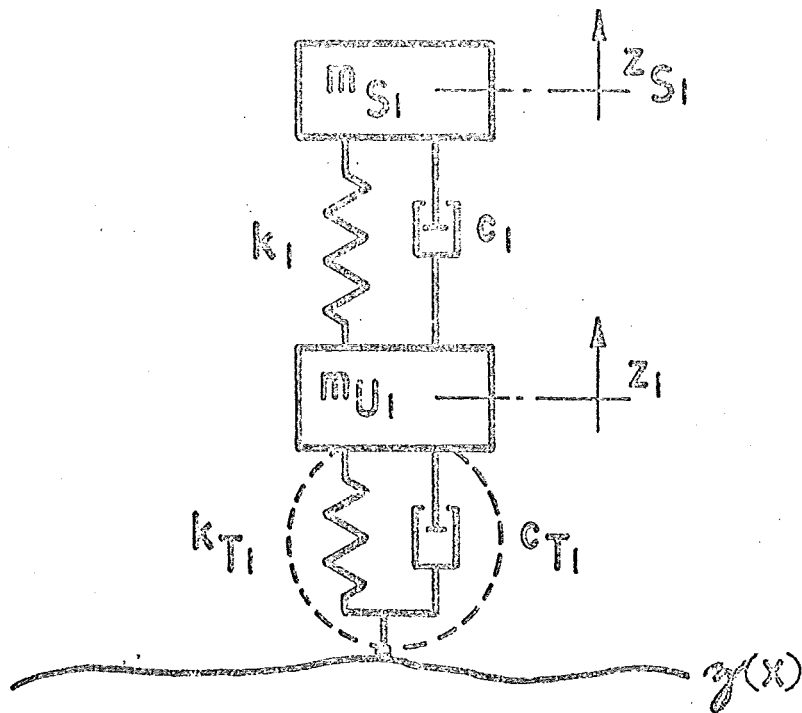
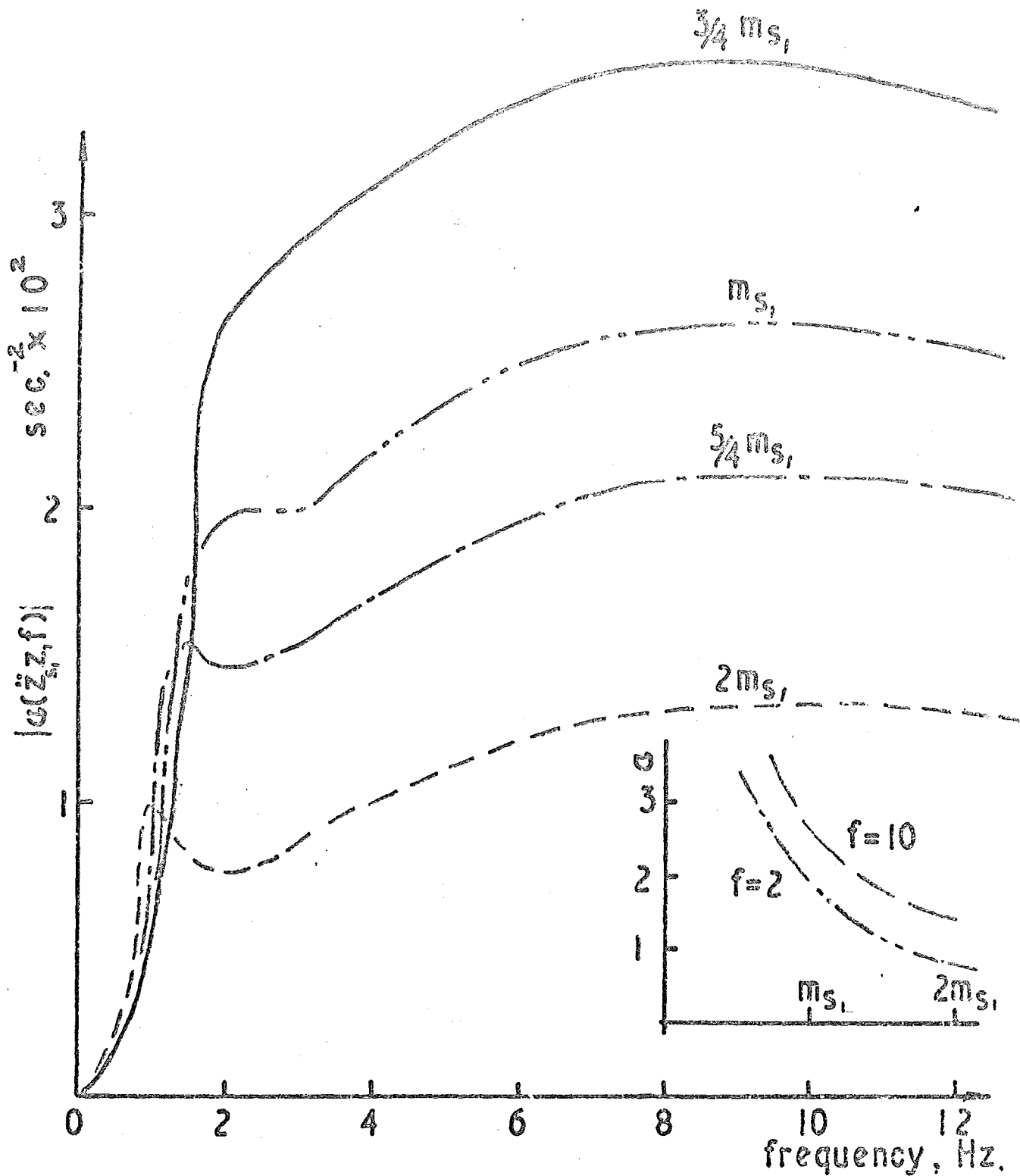


FIGURE 17

Single input, 2-degree of freedom, linear vehicle model  
(front suspension)



**FIGURE 18**

Effects of varying  $m_s$  on body lifting acceleration

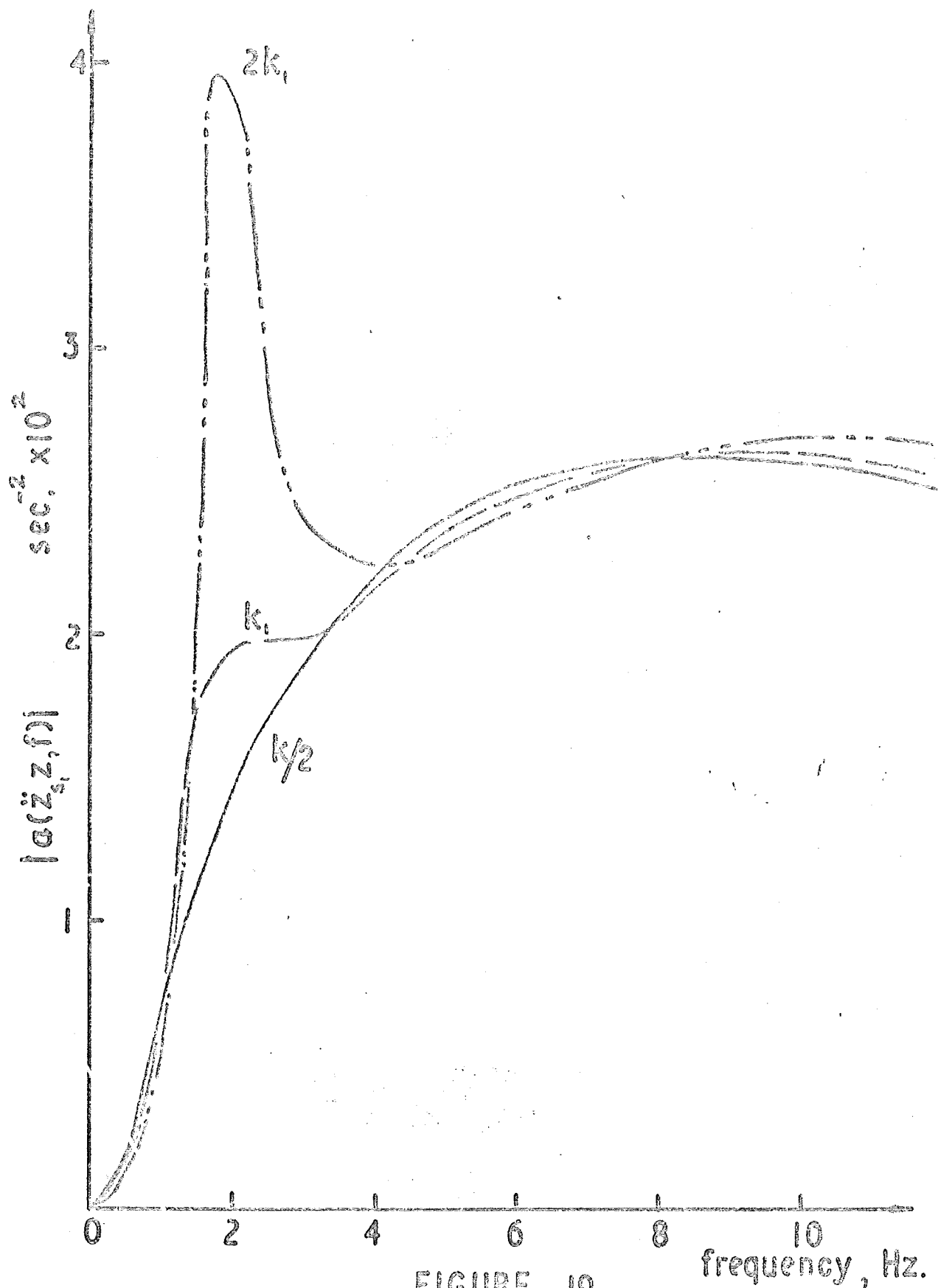
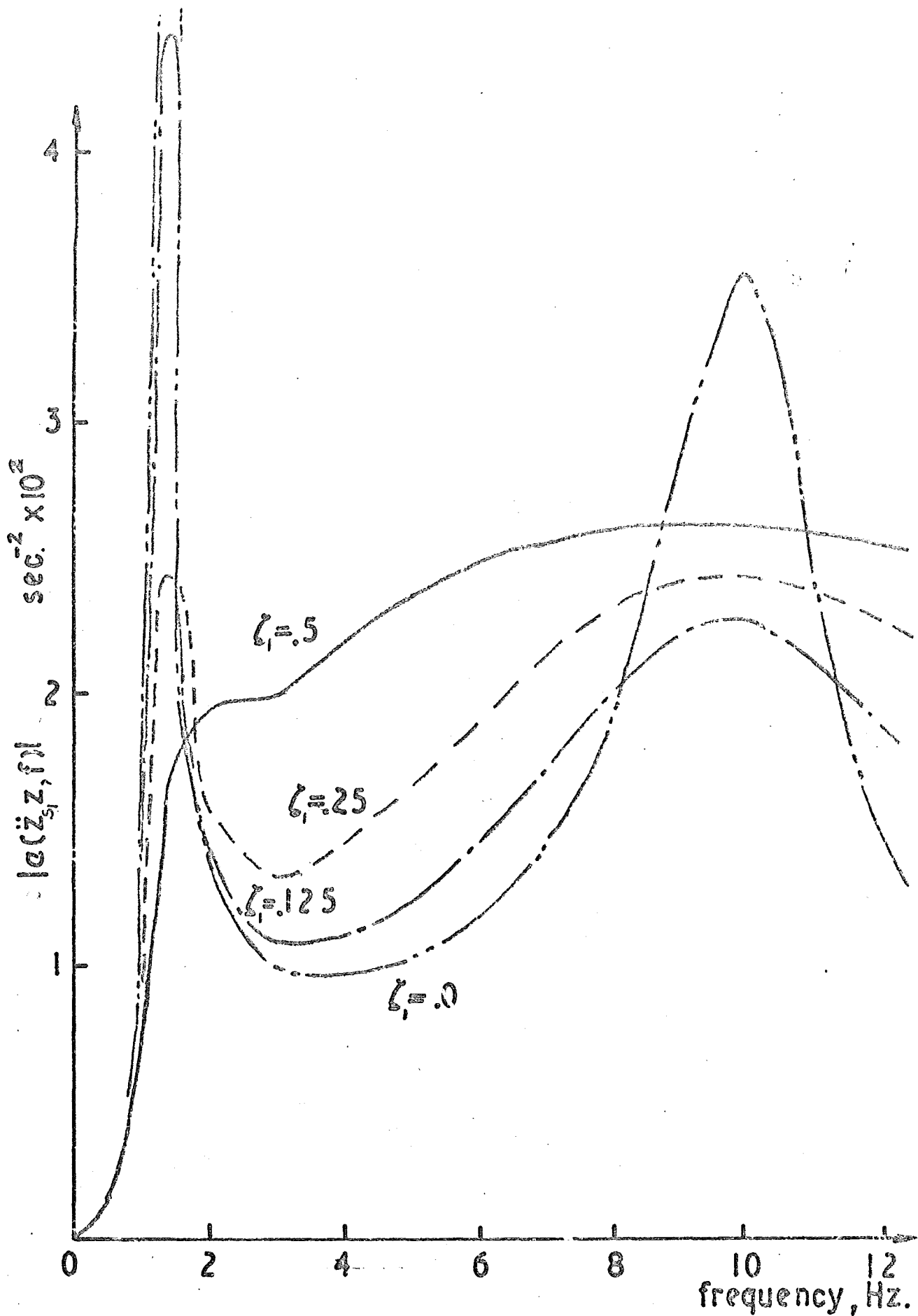


FIGURE 19

Effects of varying  $k$ , on body lifting acceleration



**FIGURE 20**

Effects of varying  $\zeta_1$  on body lifting acceleration

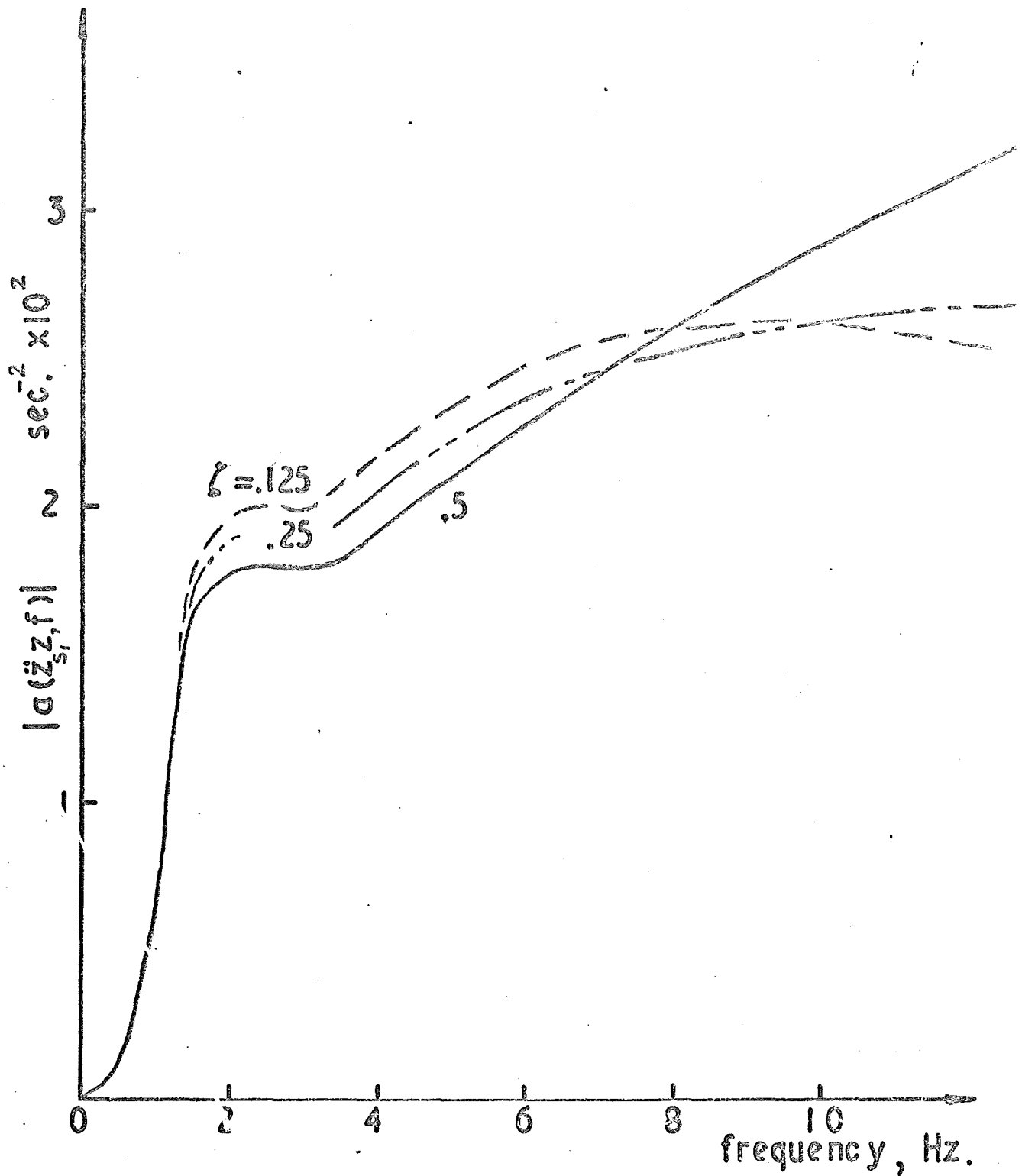


**FIGURE 21**

Effects of varying  $\zeta_T$  on body lifting acceleration

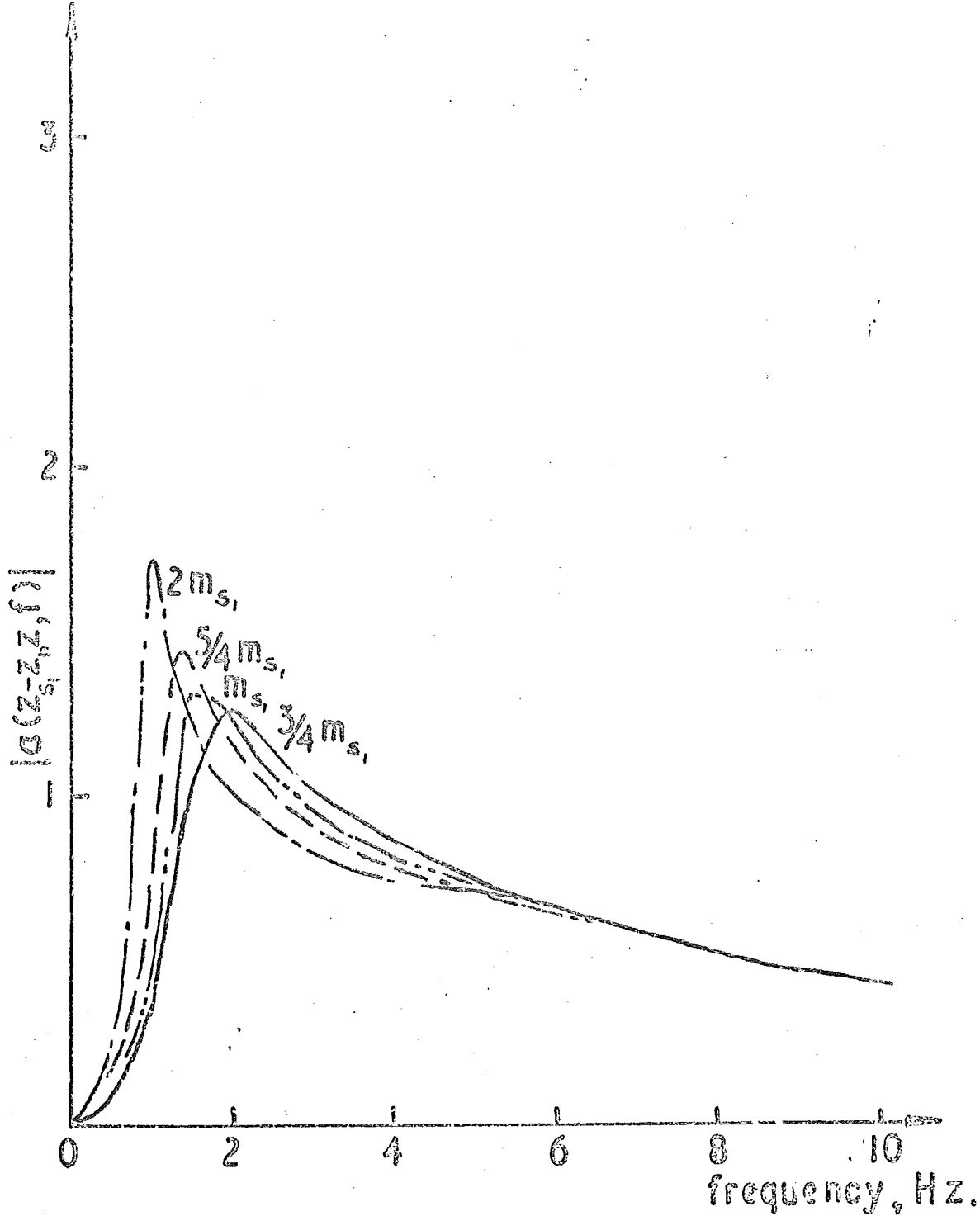


FIGURE 22

Effects of varying  $m_s$  on relative suspension movement

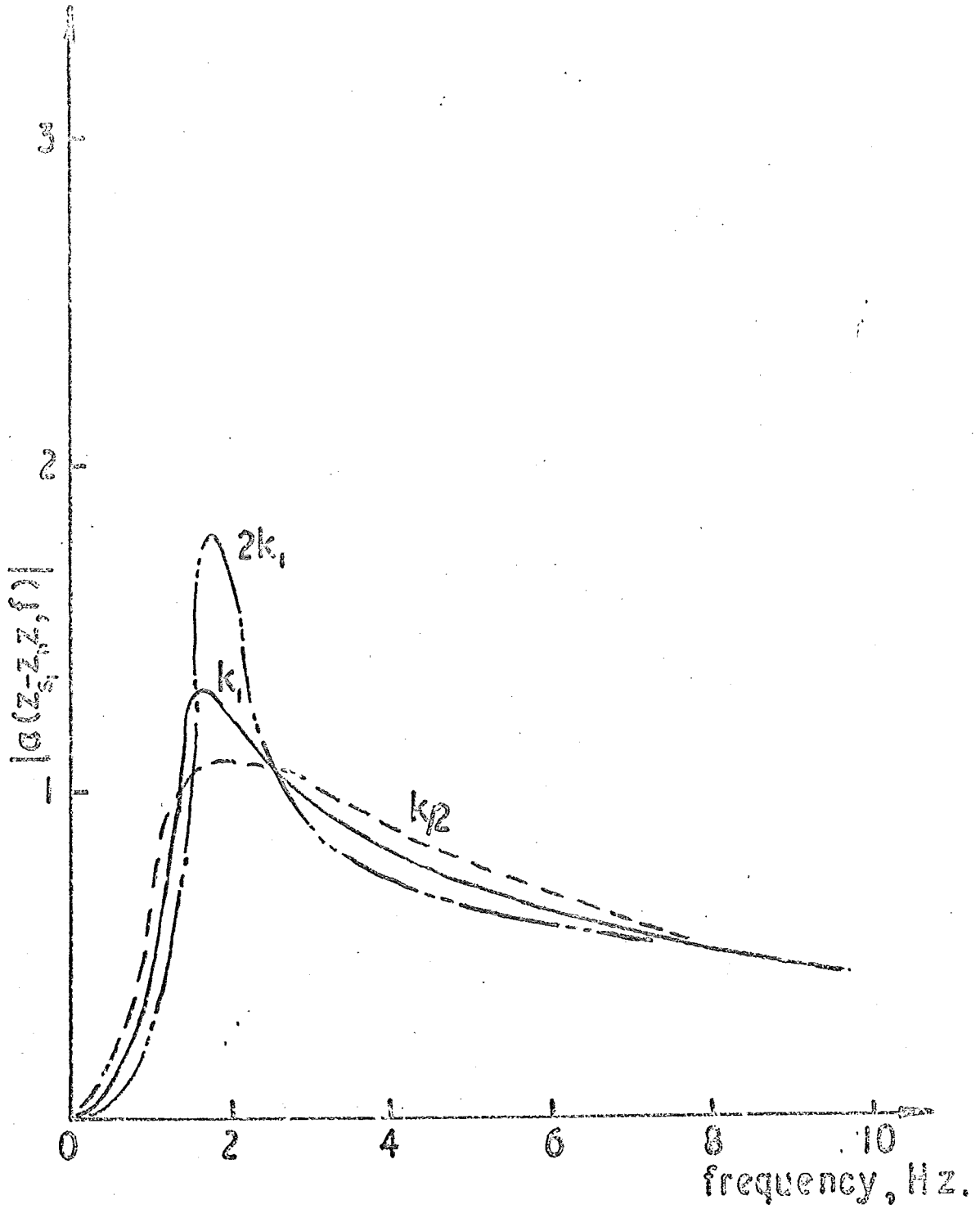
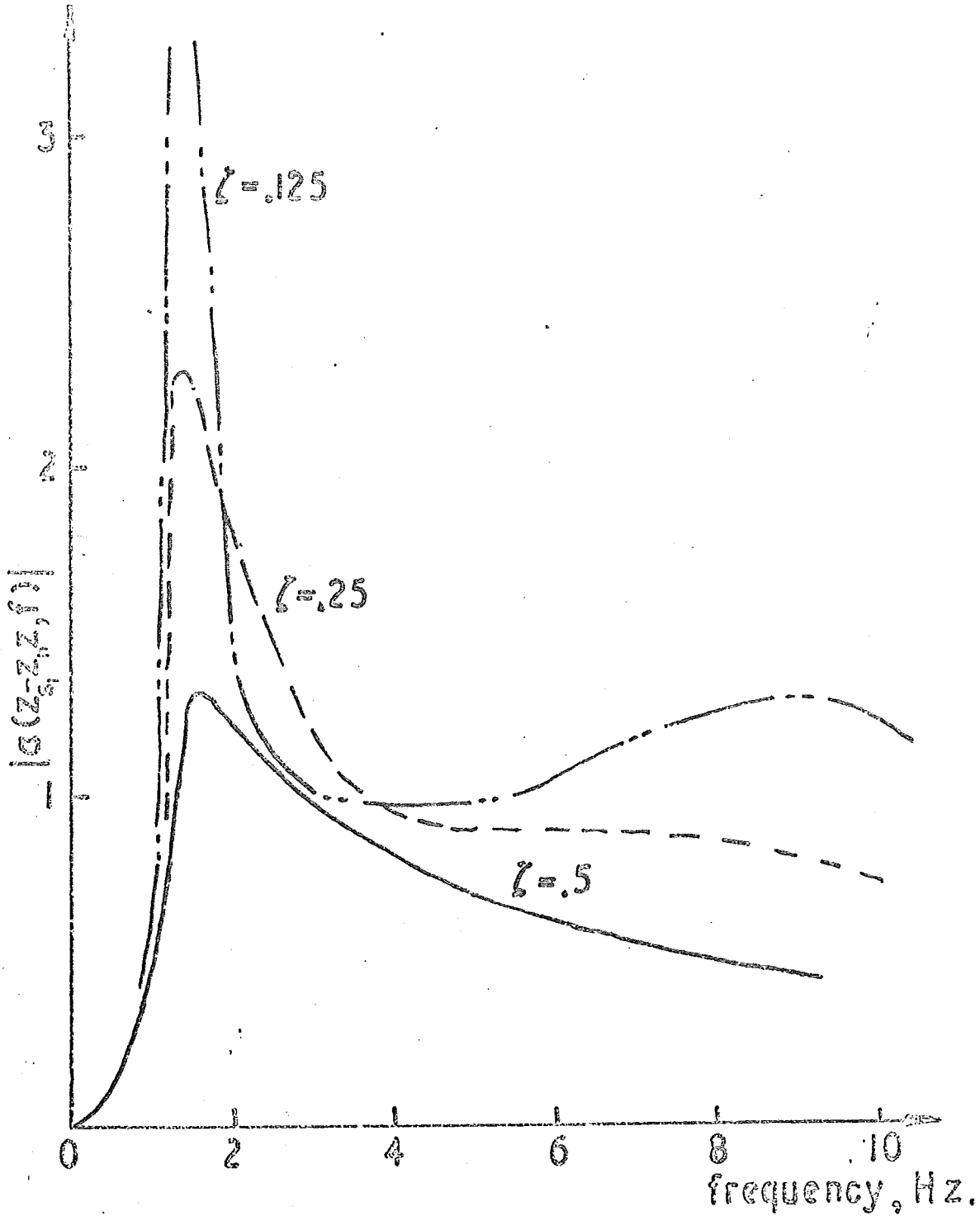


FIGURE 23

Effects of varying  $k$ , on relative suspension movement



**FIGURE 24**

Effects of varying  $\zeta_1$  on relative suspension movement

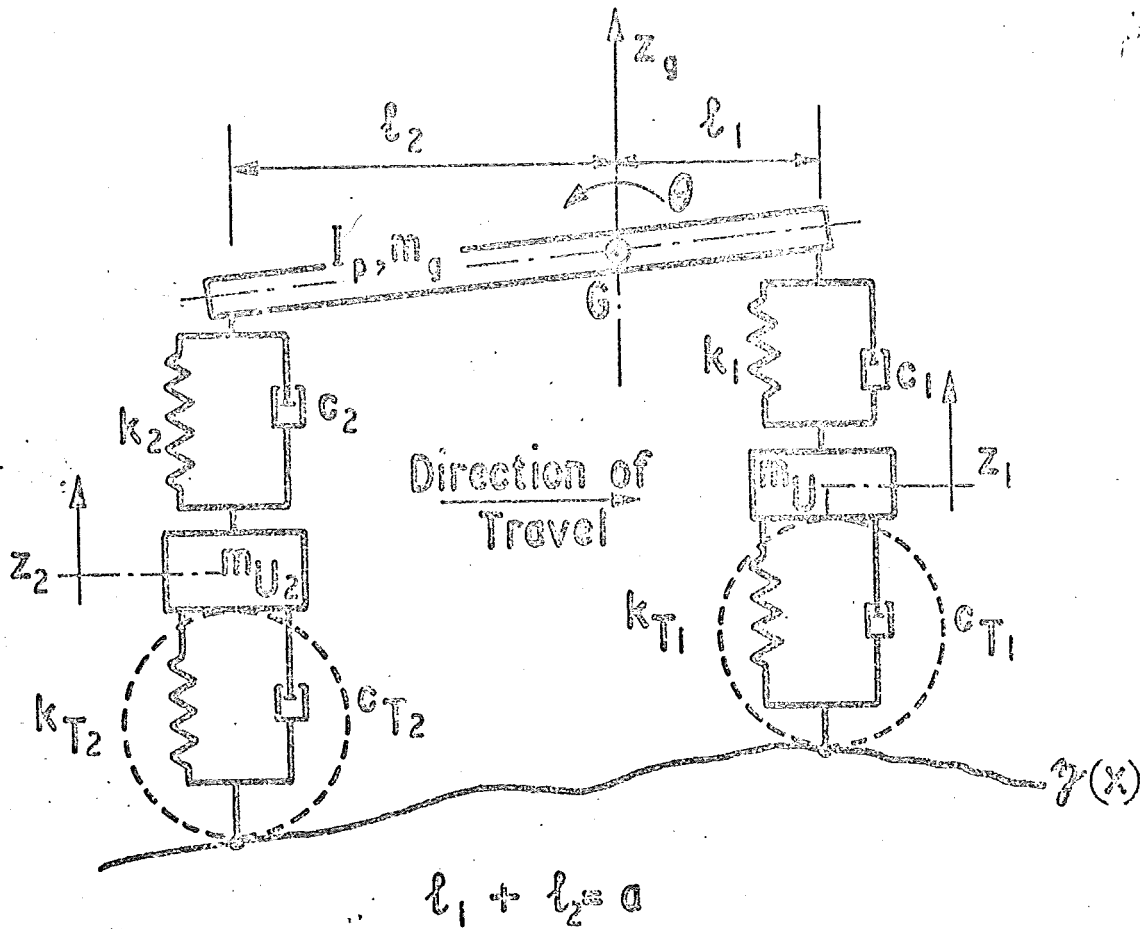


**FIGURE 25**

Double input, 4-degree of freedom, linear vehicle model.

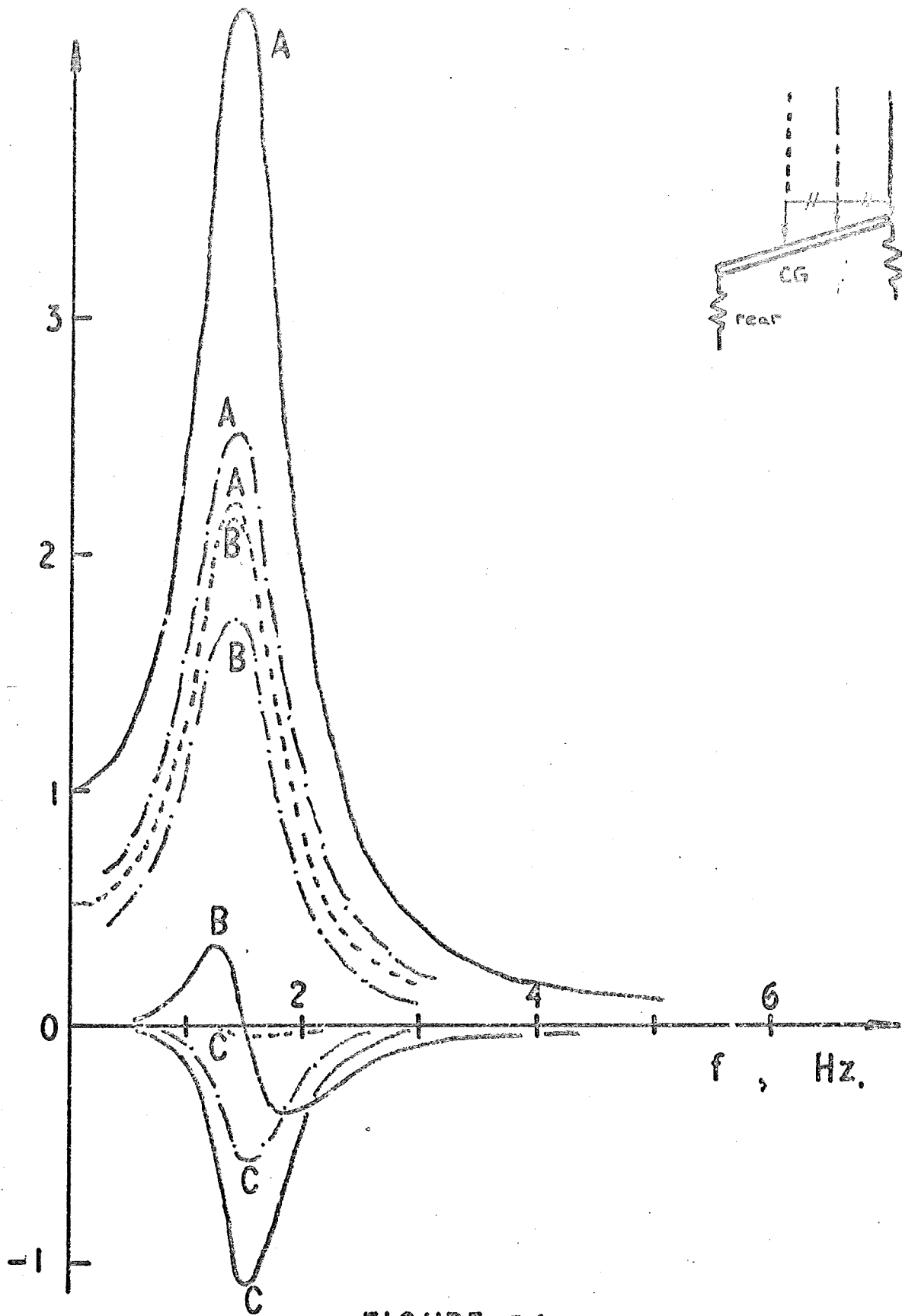


**FIGURE 26**

Functions  $A(f)$ ,  $B(f)$ ,  $C(f)$  against frequency

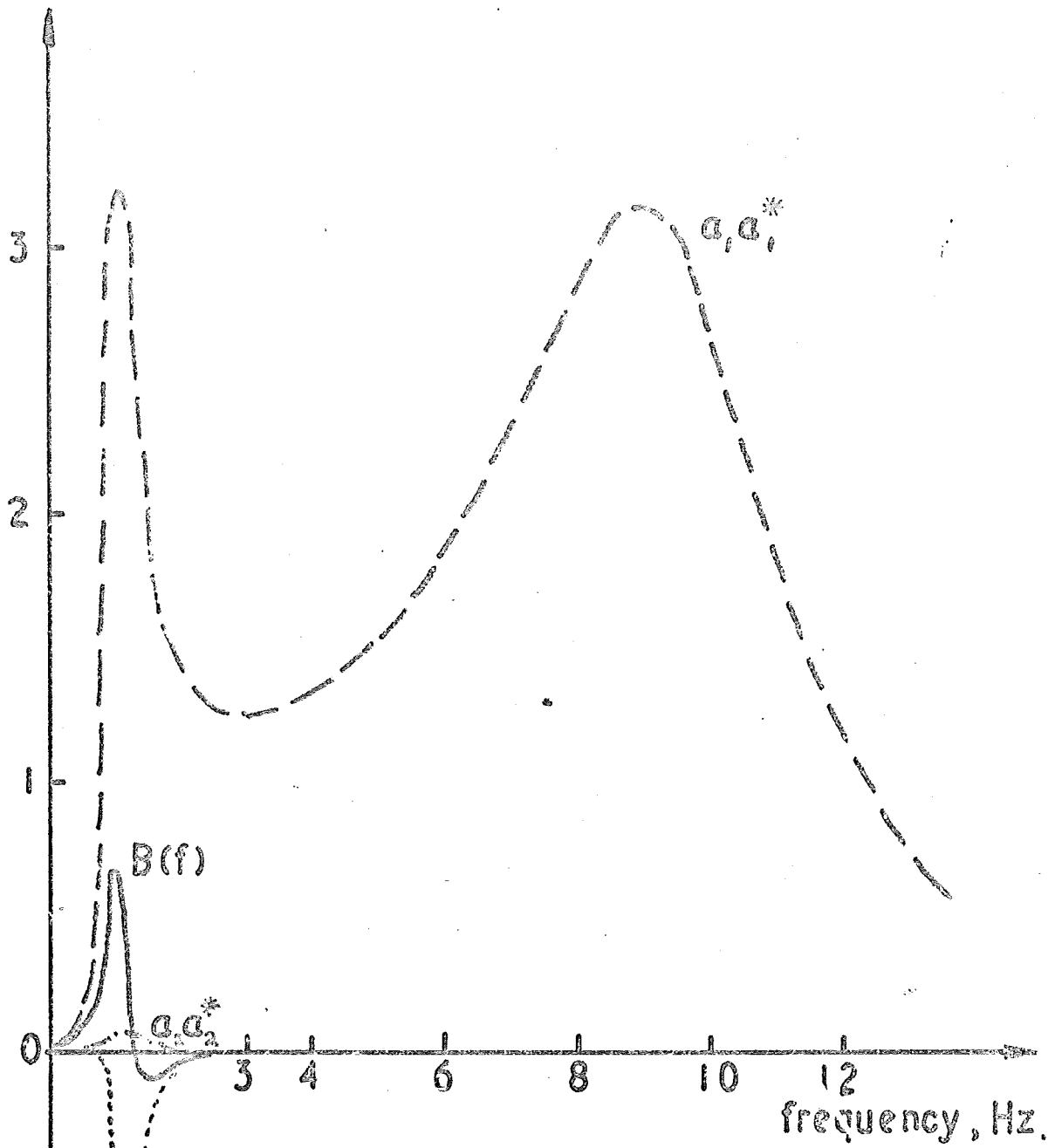


FIGURE 27

Transfer functions, front spring, vehicle A

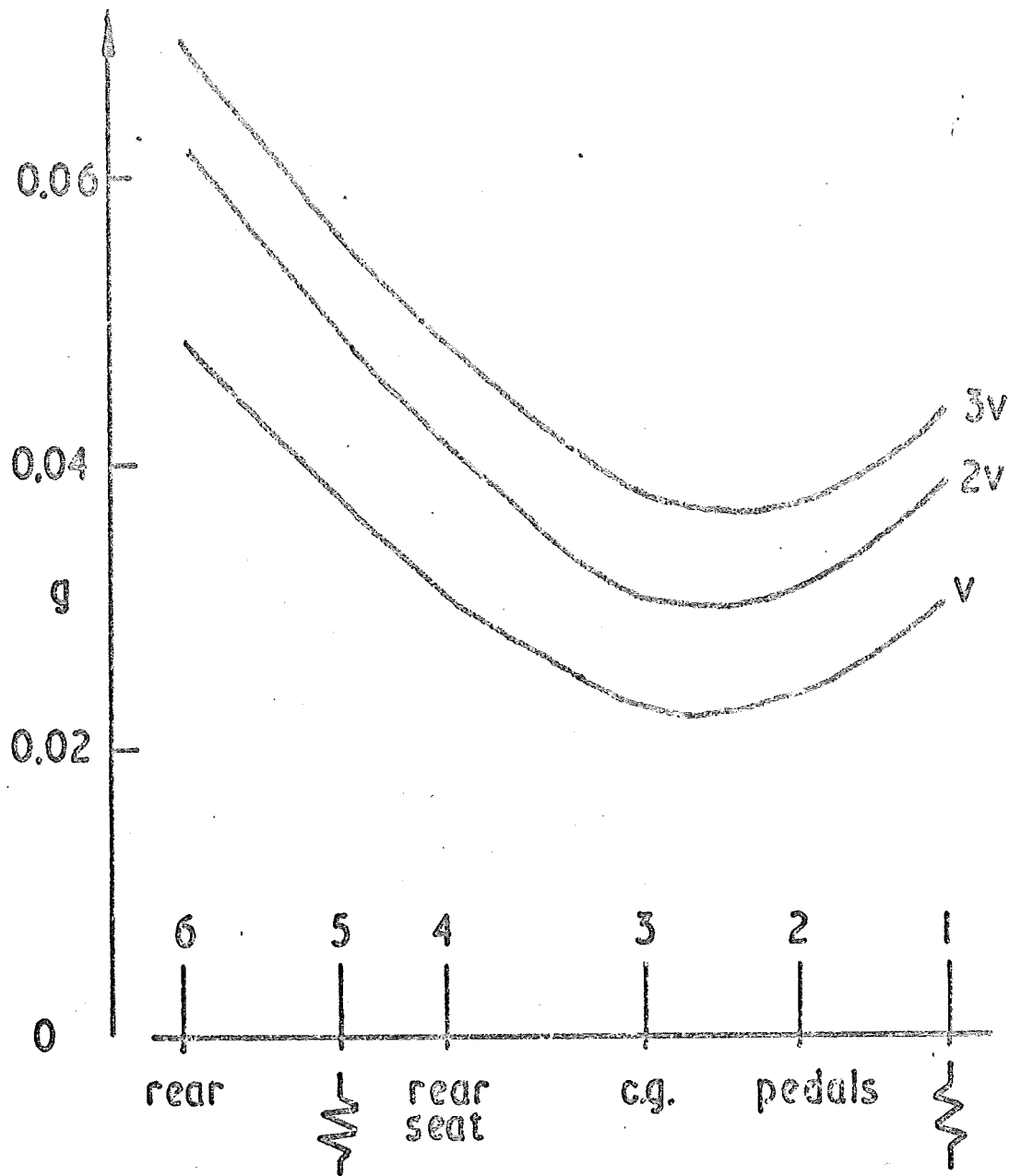


FIGURE 28

RMS vertical accelerations, vehicle A, route A

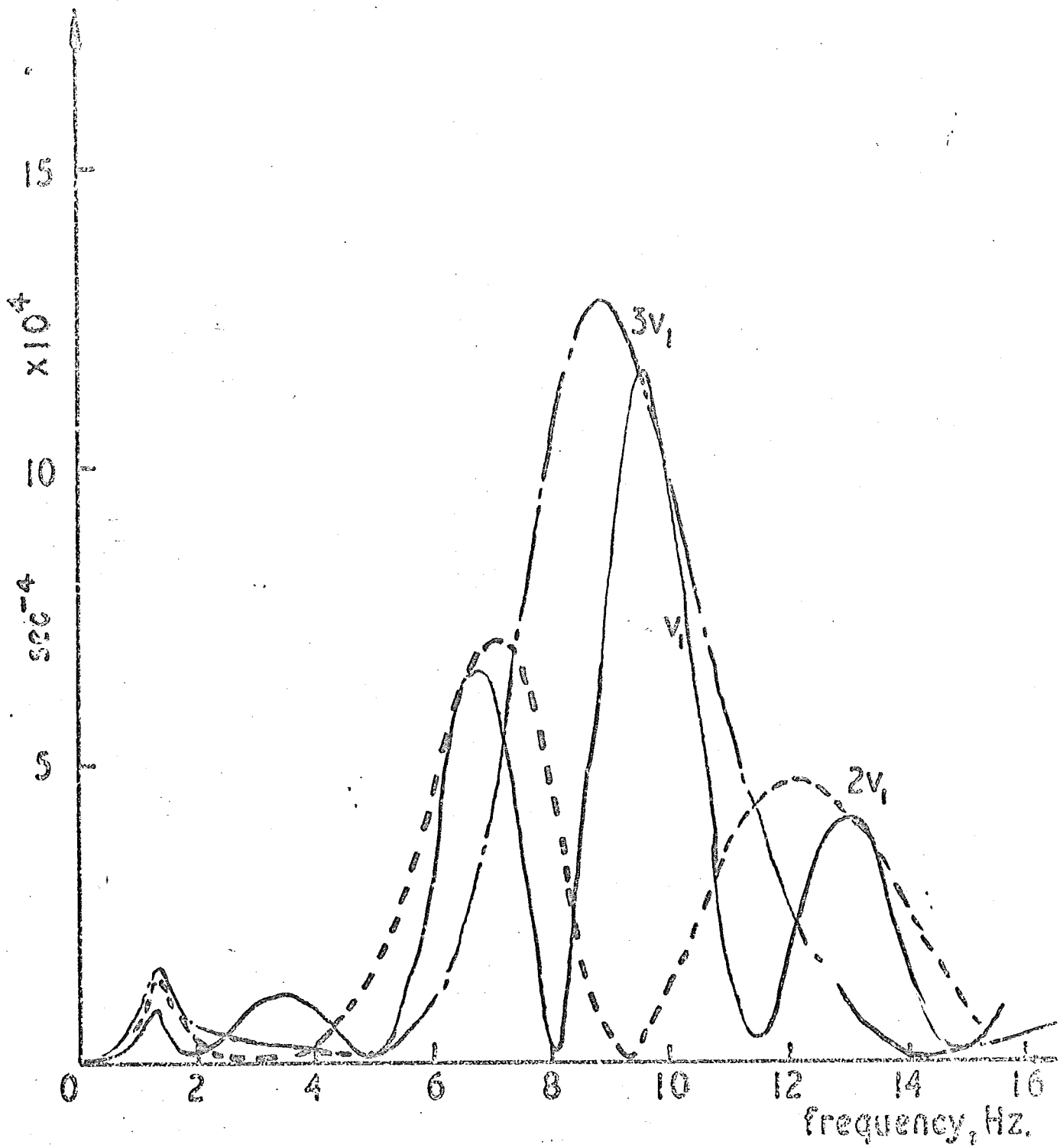


FIGURE 29

Double input transfer function, vehicle A, acceleration response on chassis position 3 (see figure 28)

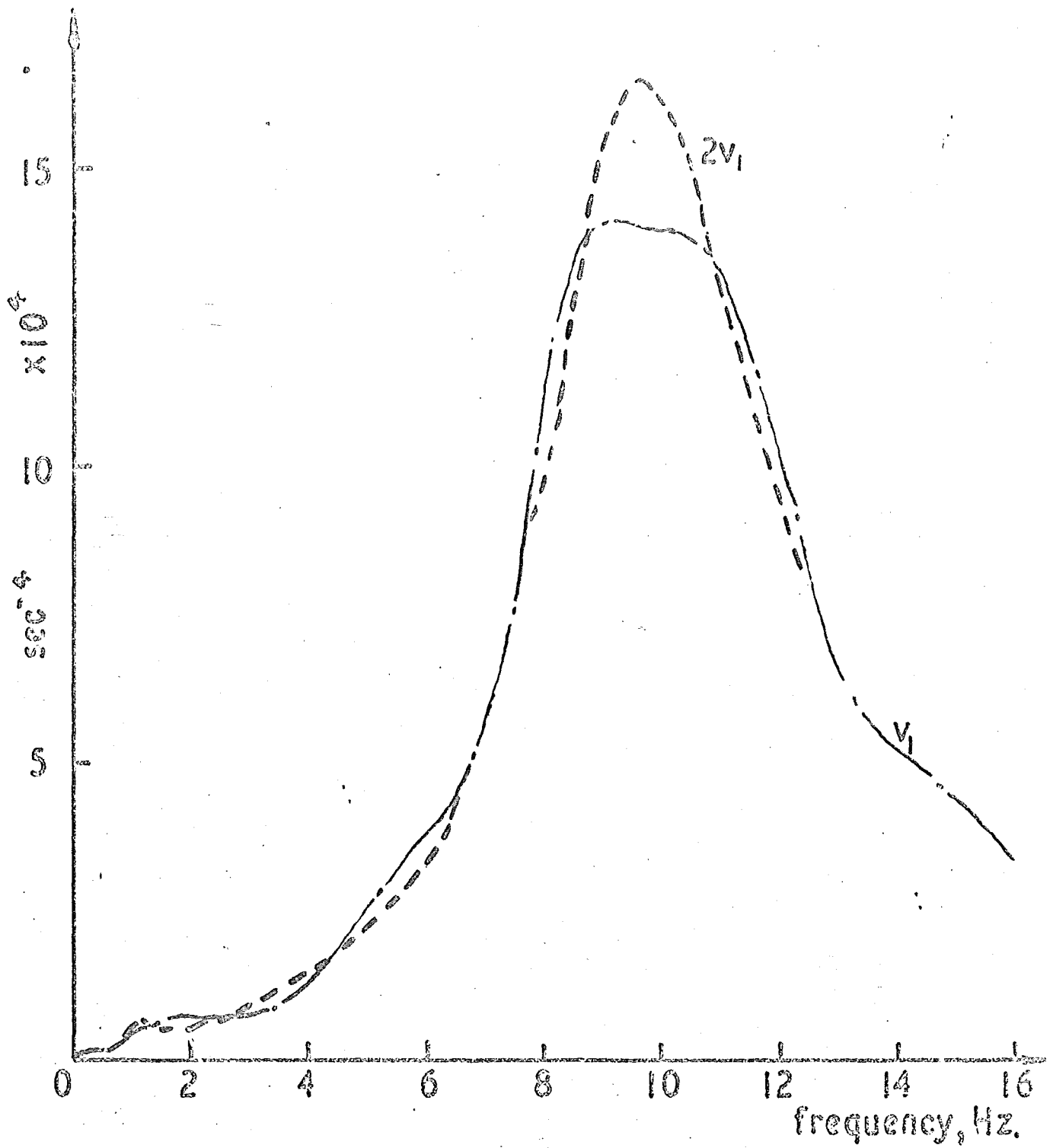


FIGURE 30

Double input transfer function, vehicle A, acceleration response on chassis position 1 (see figure 28)

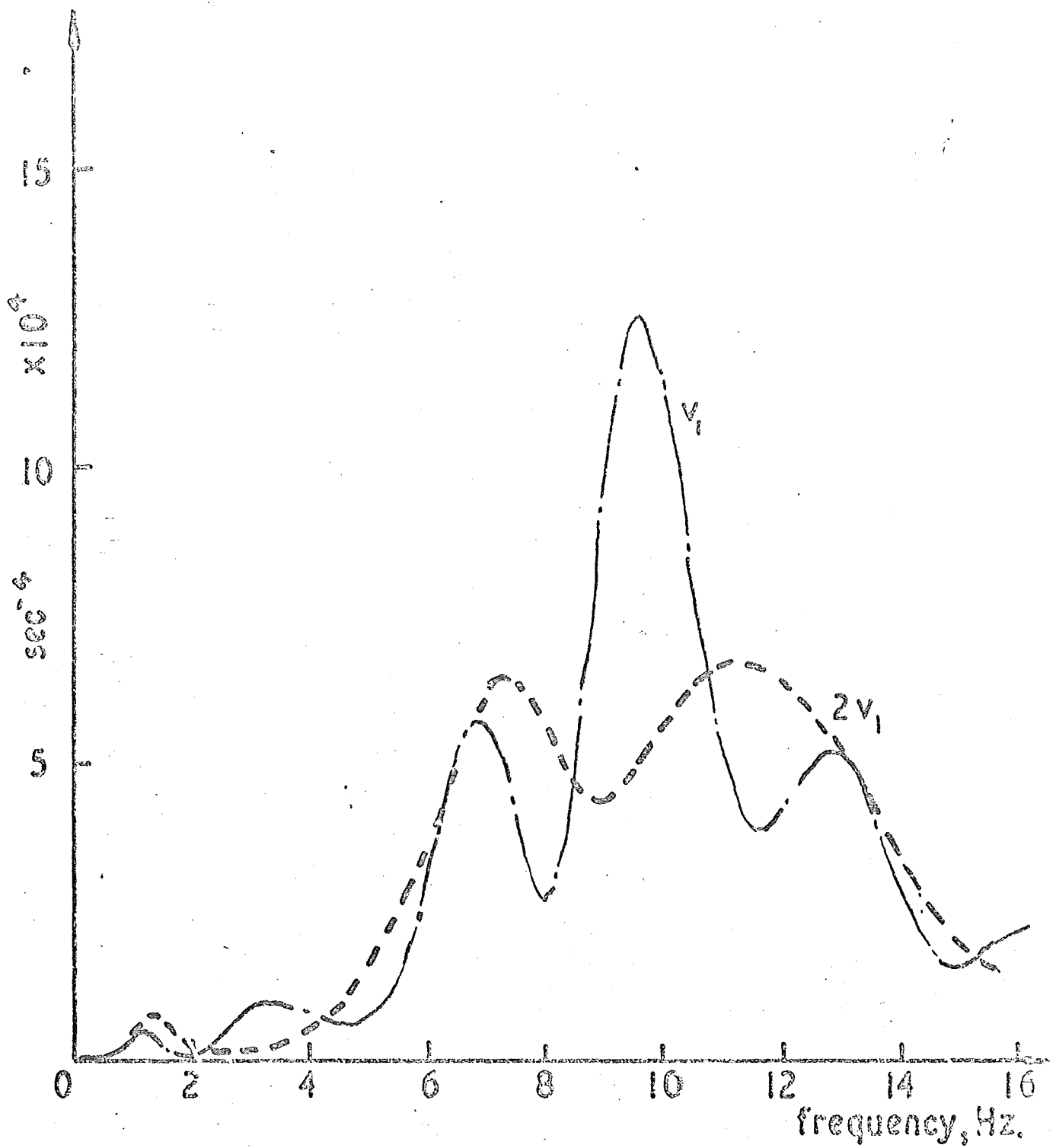


FIGURE 31

Double input transfer function, vehicle A, acceleration response on chassis position 2 (see figure 28)

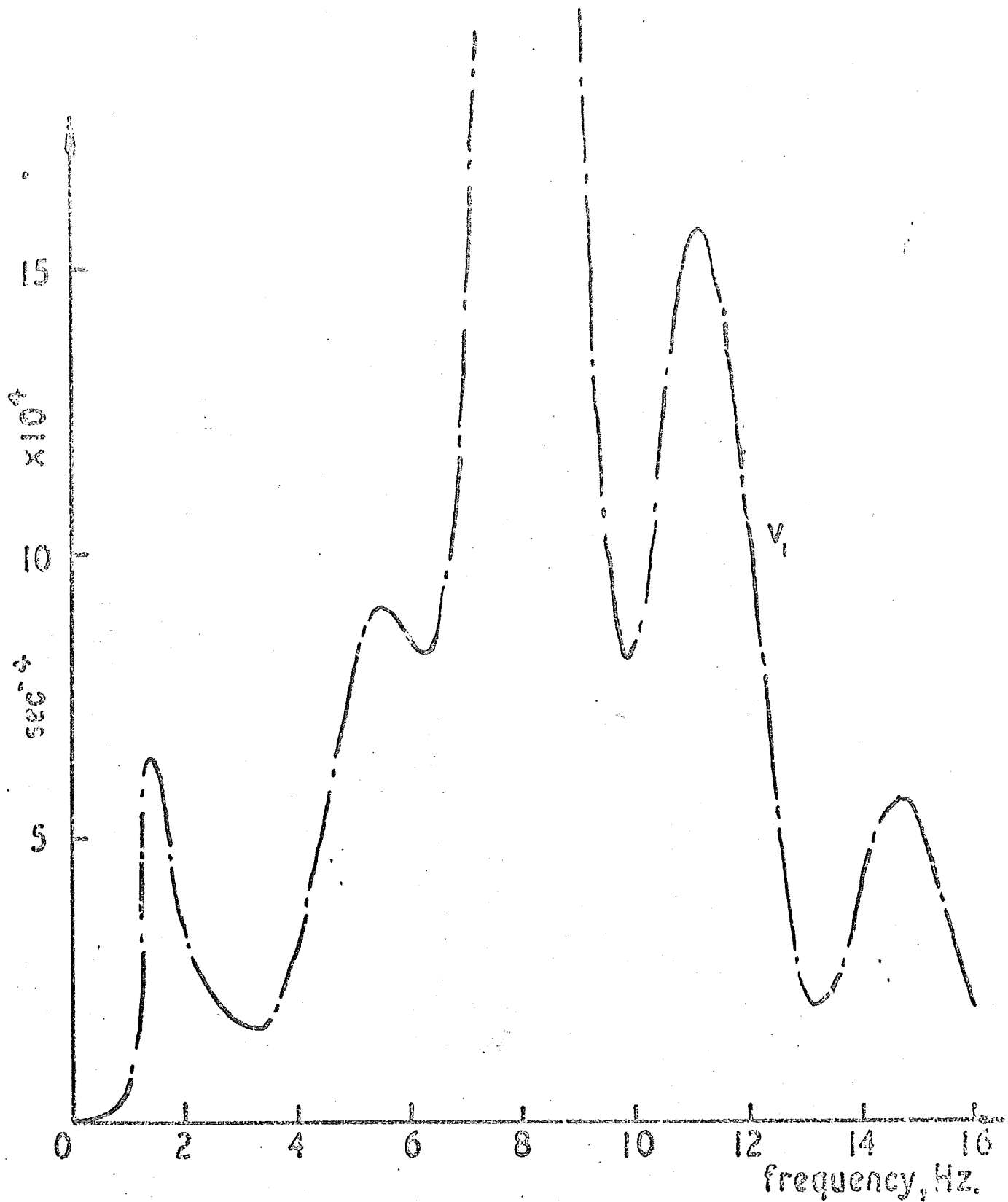


FIGURE 32

Double input transfer function, vehicle A, acceleration response on chassis position 6 (see figure 28)

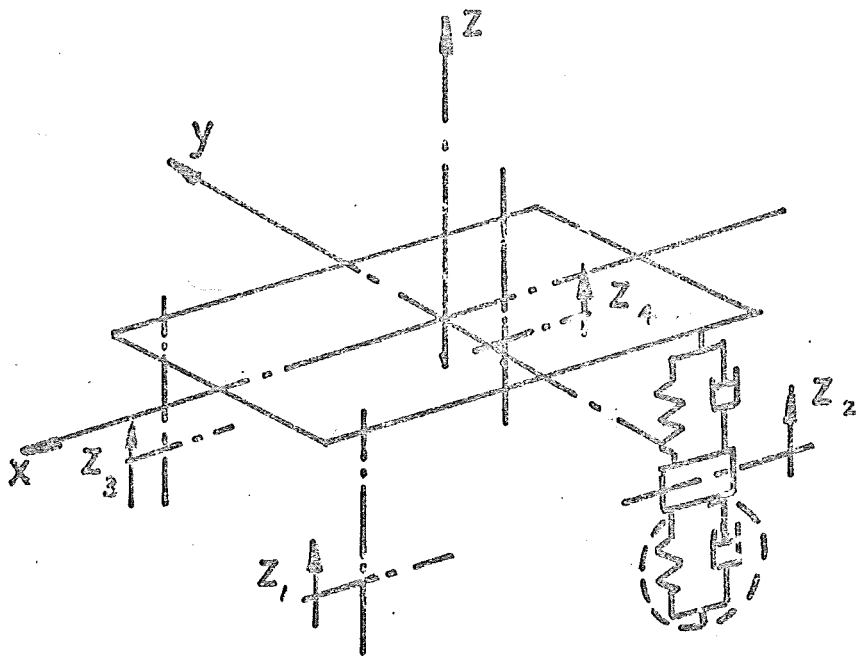


FIGURE 33

4-input, 7-degree of freedom vehicle model

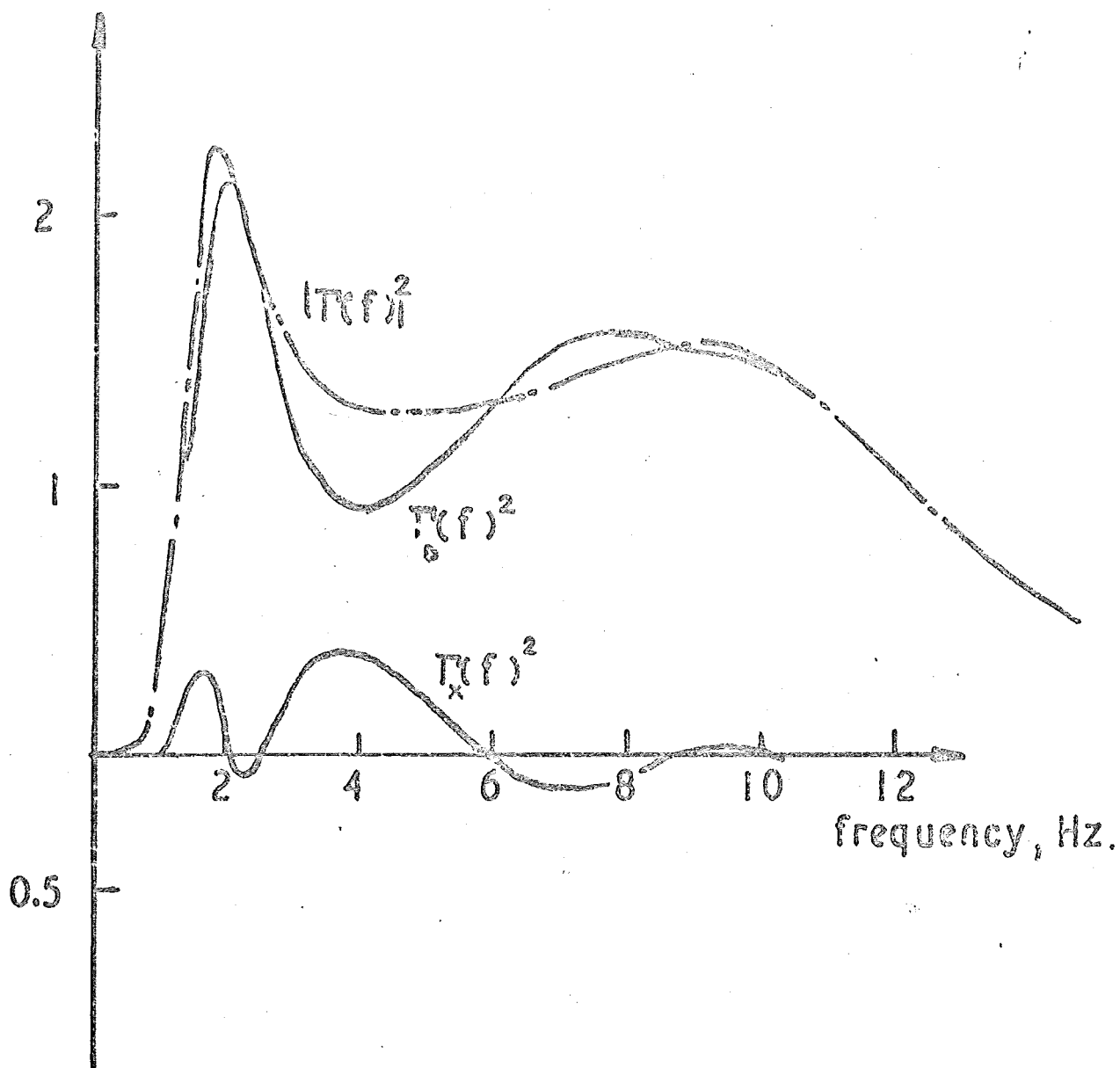


FIGURE 34

Transfer functions, vehicle B, force in spring

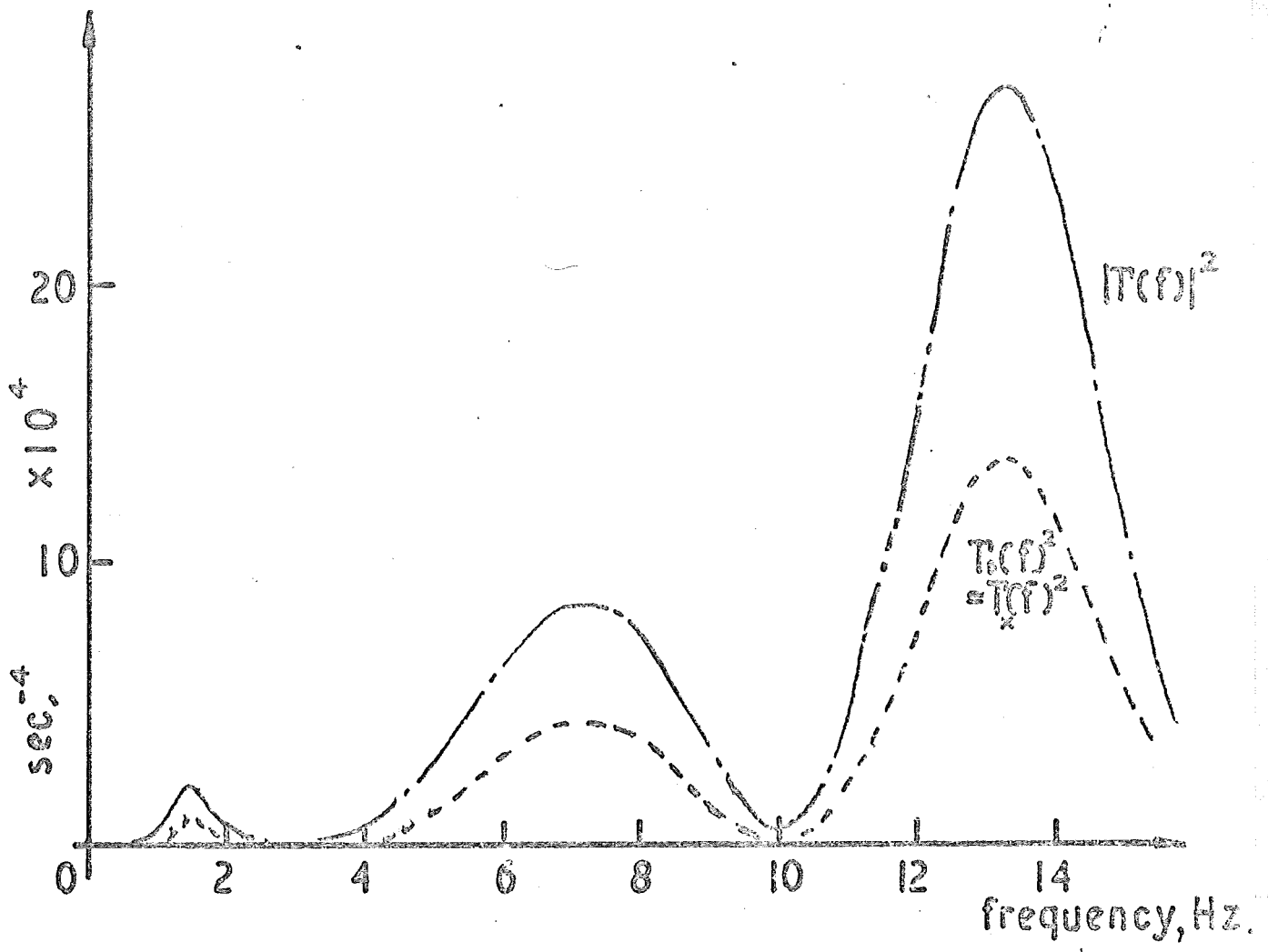
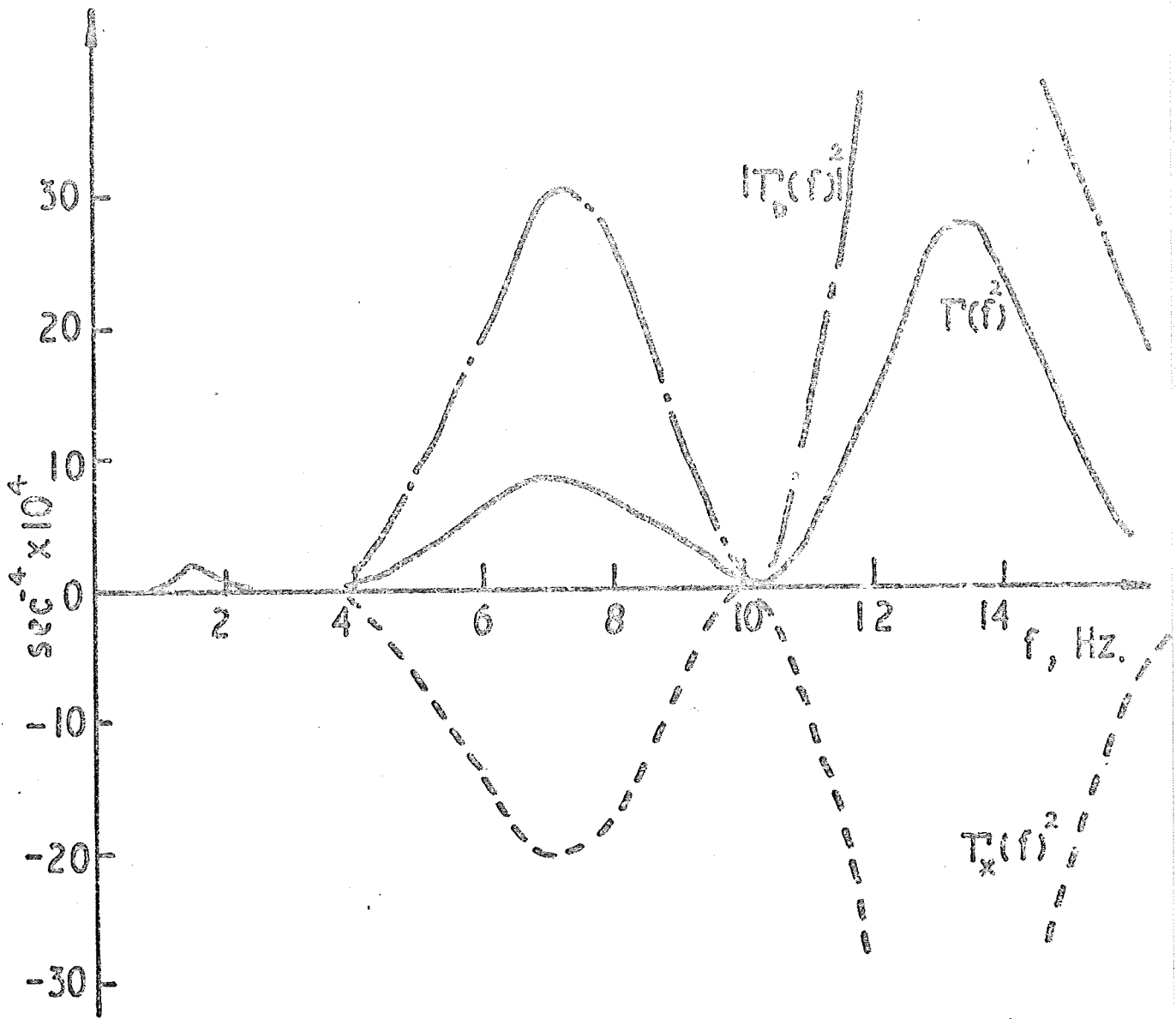


FIGURE 35

Transfer functions, vehicle B, acceleration at c.g.



**FIGURE 36**  
 Transfer functions, vehicle B, sill acceleration

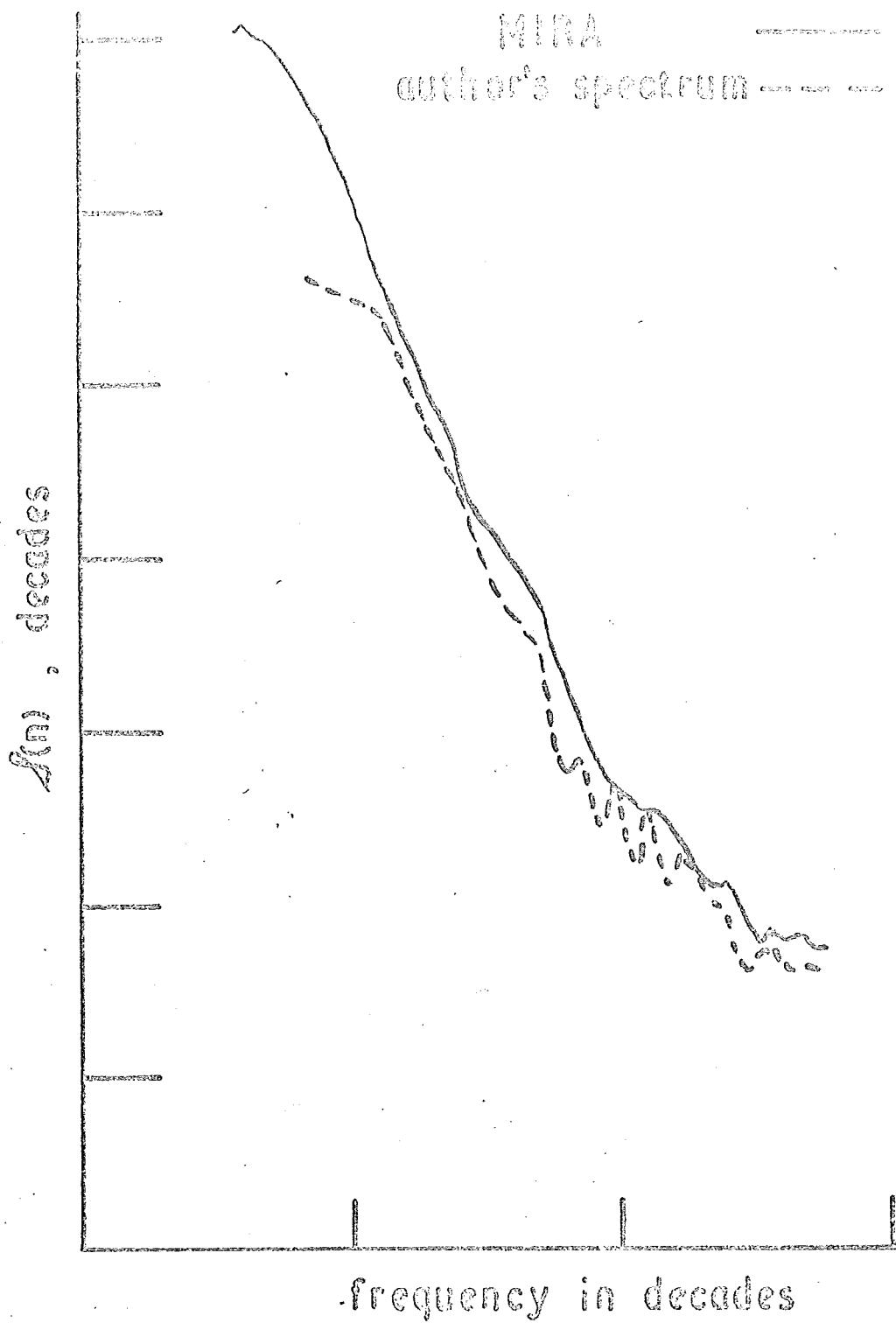


FIGURE 37

Comparison of spectrum produced by MIRA with digitally produced spectrum

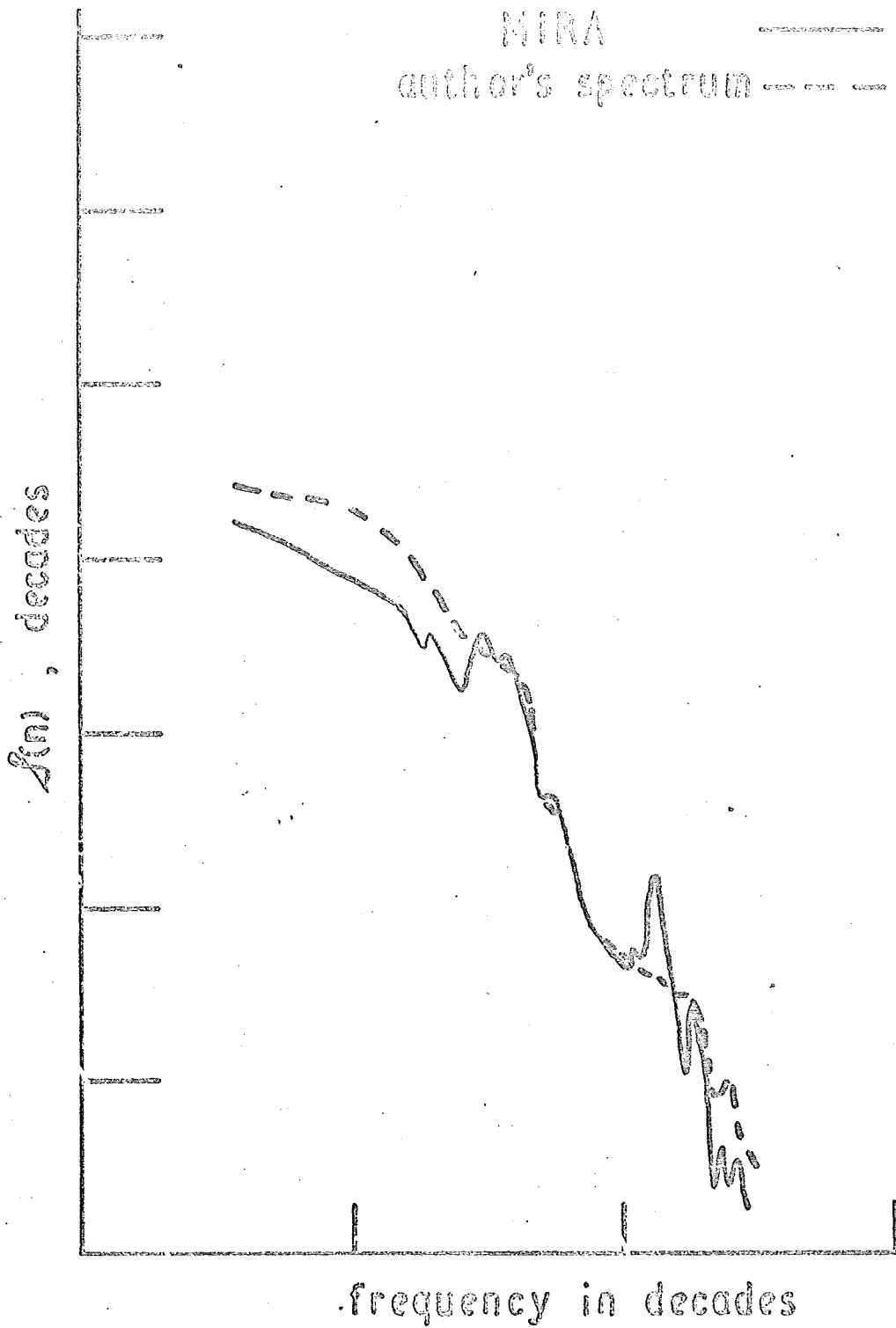
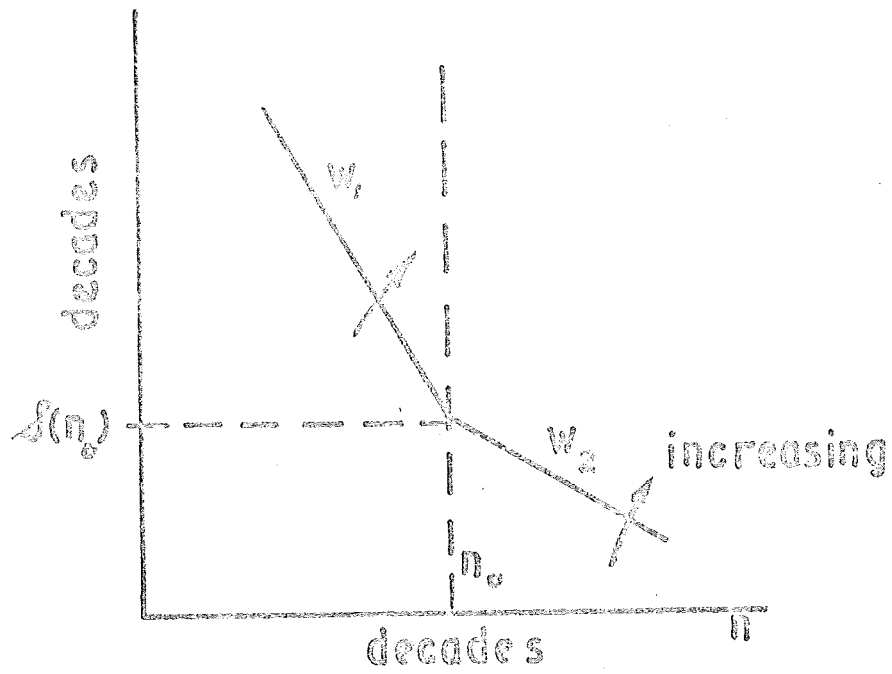


FIGURE 38

Comparison of spectrum produced by MIRA with digitally produced spectrum



A good road  $\Rightarrow$  a low value of  $w_1$   
and a high value of  $w_2$

FIGURE 39

Road classification parameters

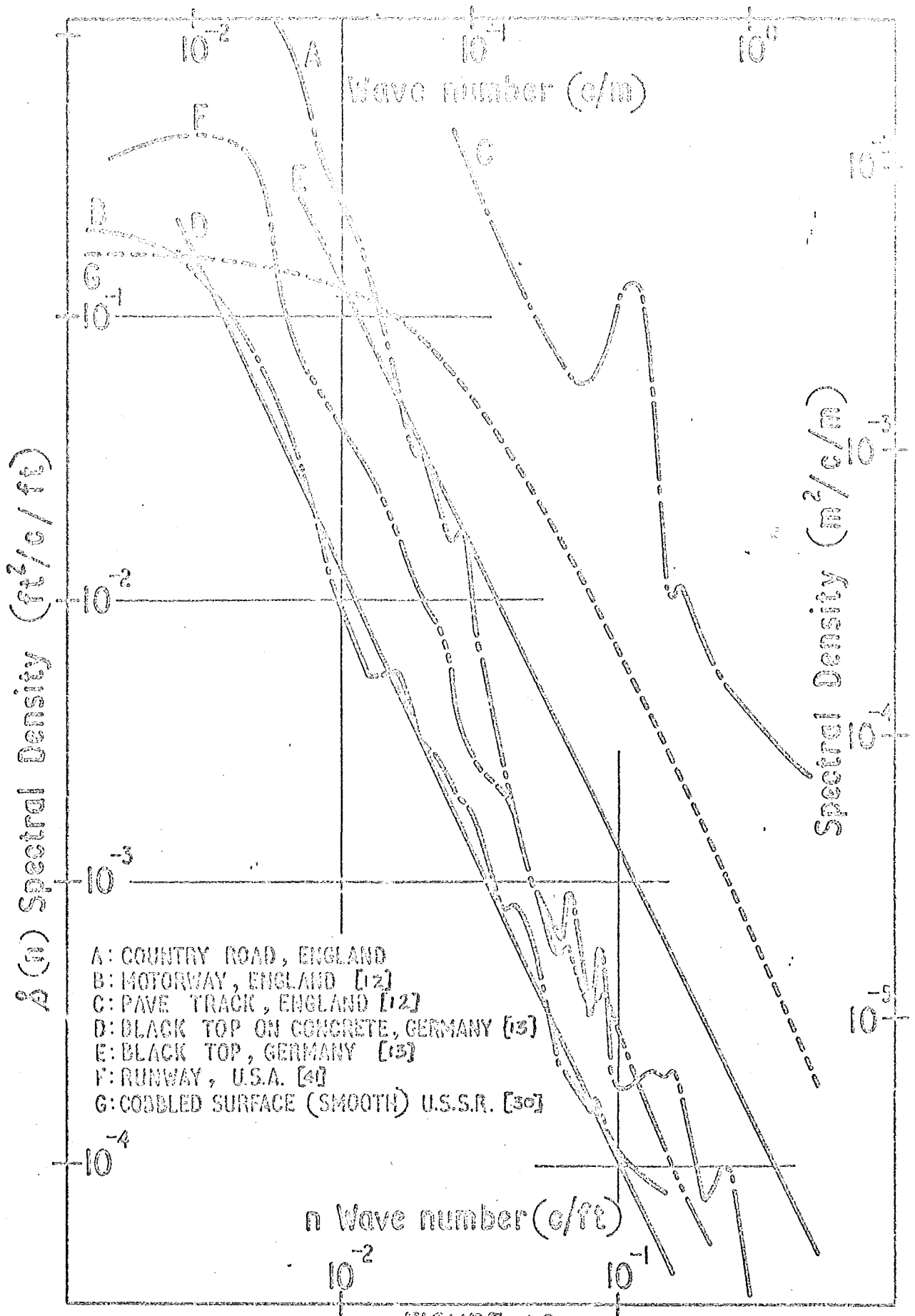


FIGURE 40  
Road Profile Spectra

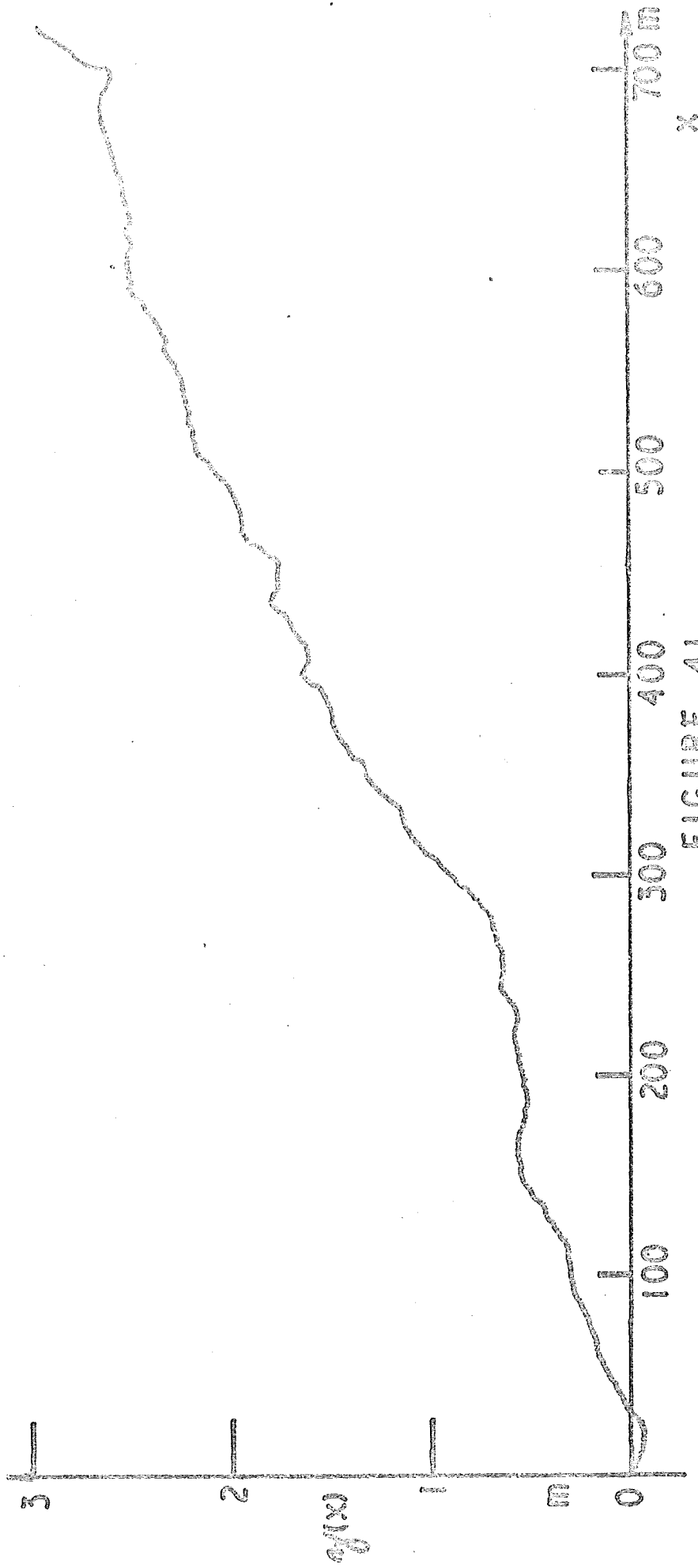


FIGURE 41

Reduced levels, route B, 2/1/20

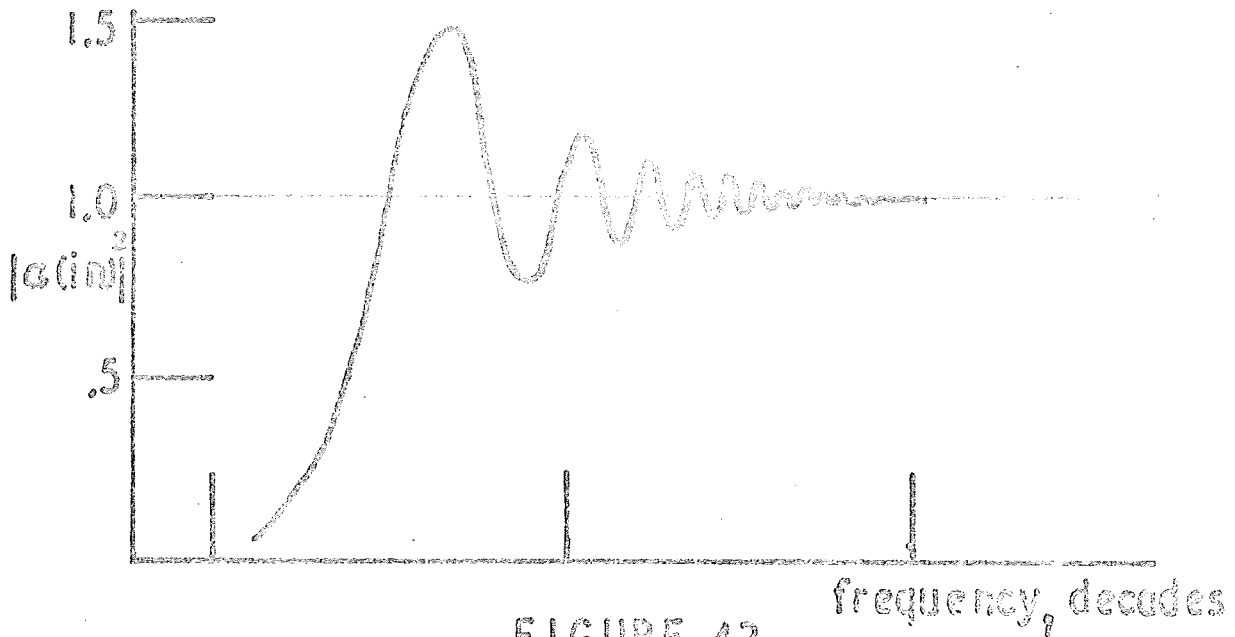


FIGURE 42

Attenuation function of linear moving average filter

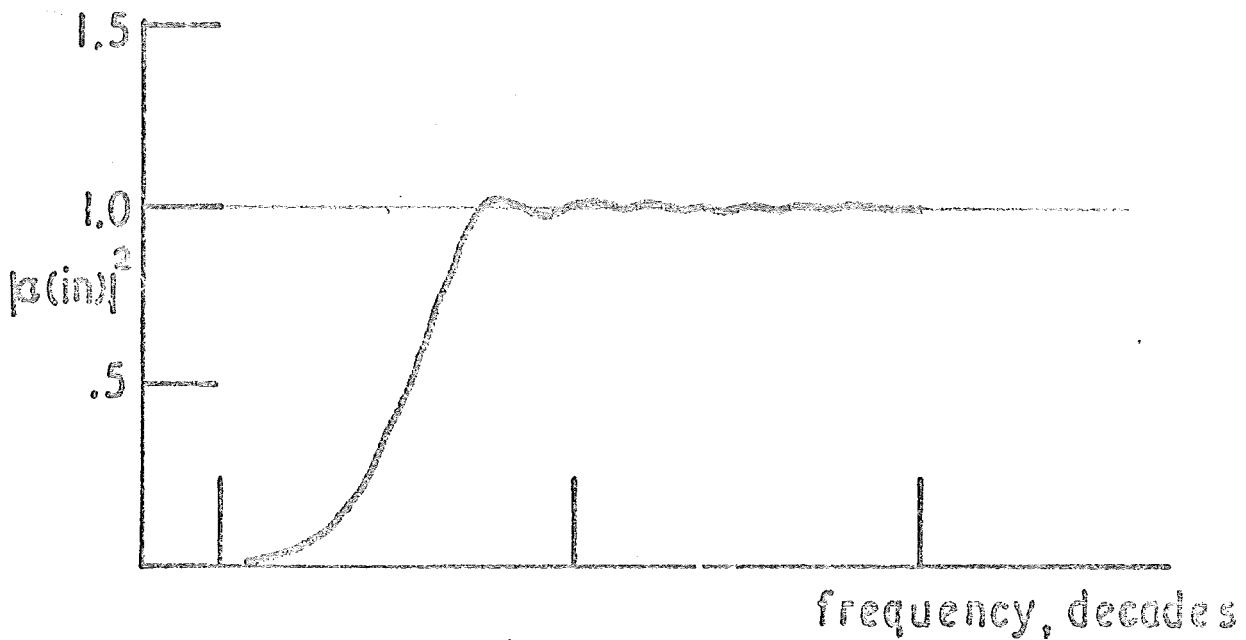


FIGURE 43

Attenuation function of filter after MARTIN

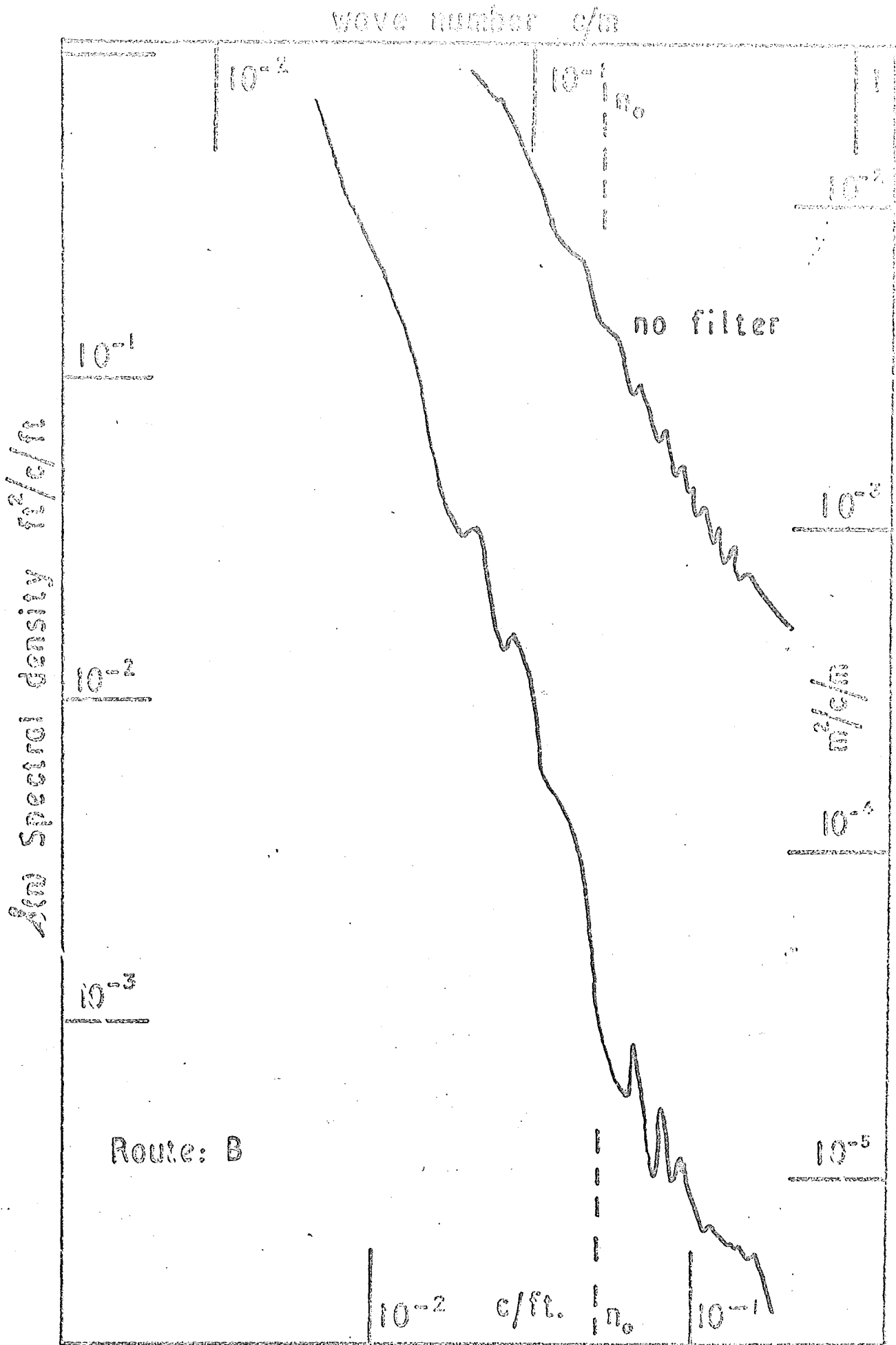


FIGURE 44

Road profile spectra

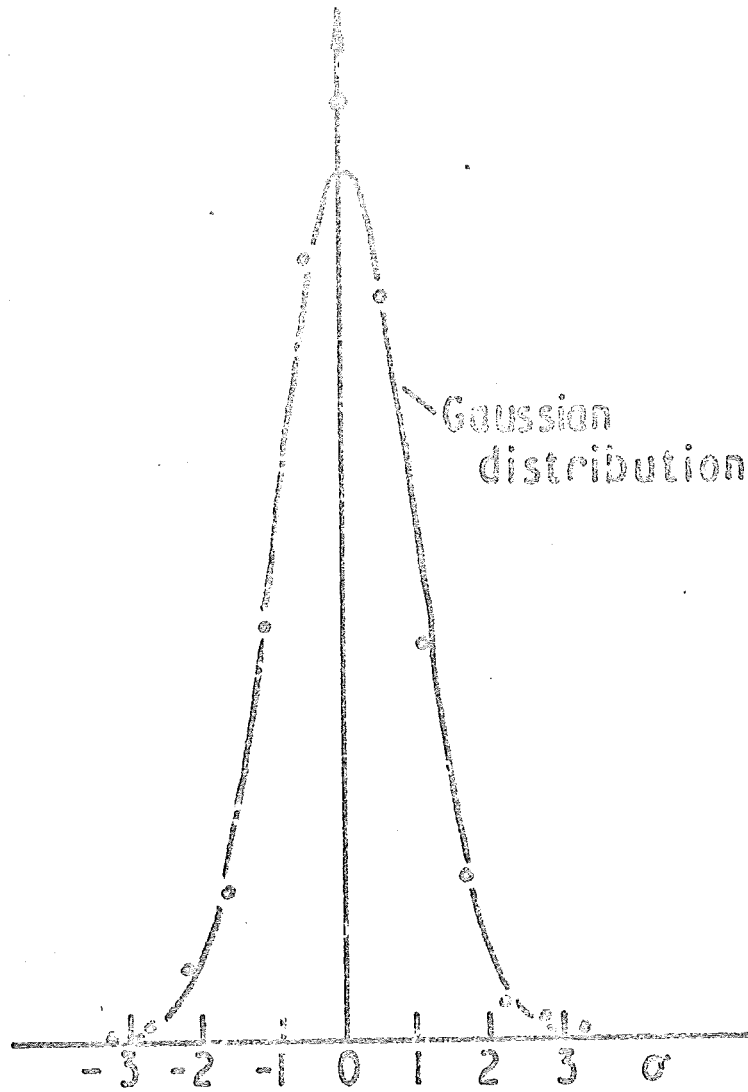


FIGURE 45

Probability density function, route B.

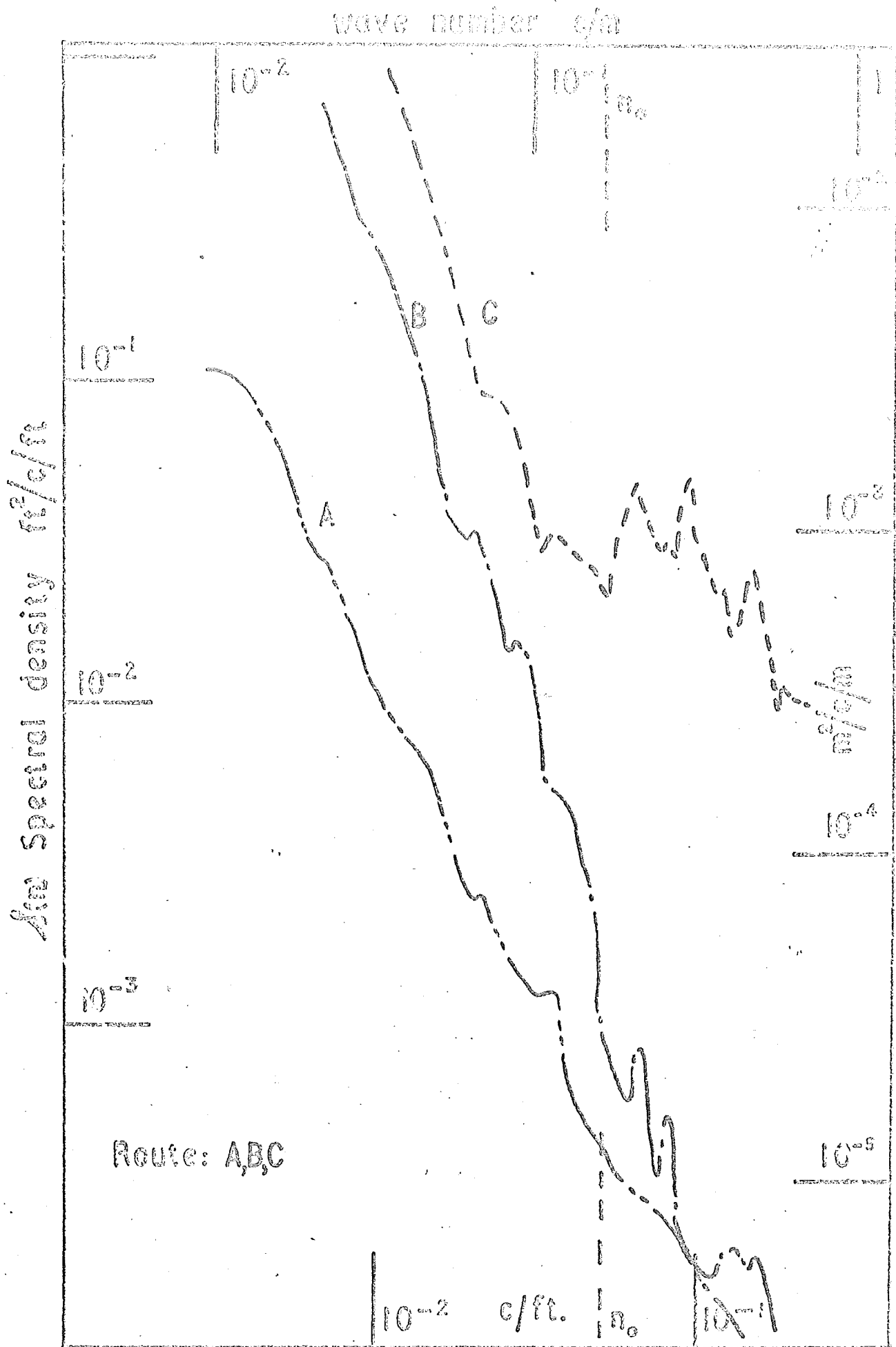


FIGURE 46

Road profile spectra

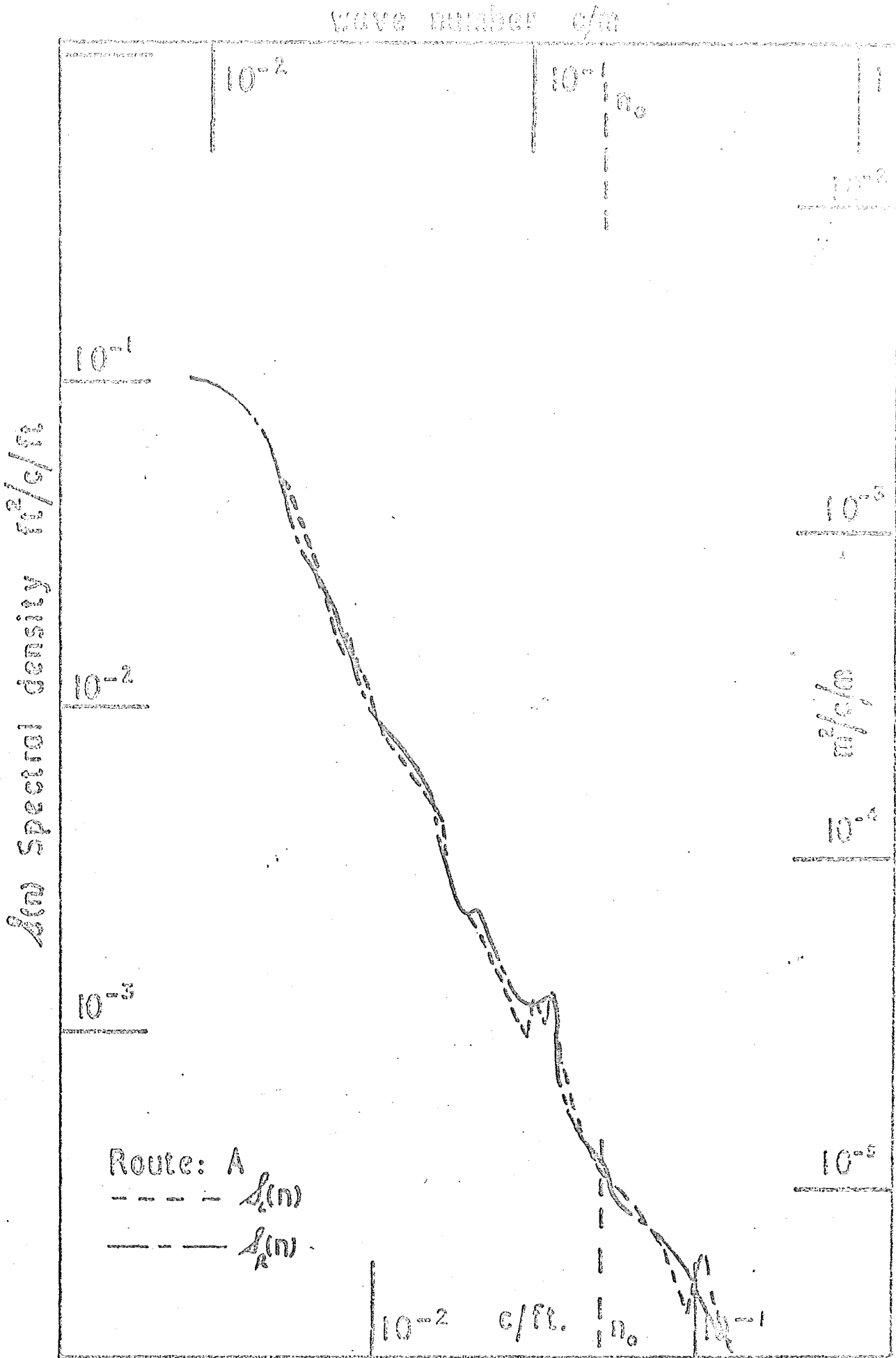


FIGURE 47

Road profile spectra



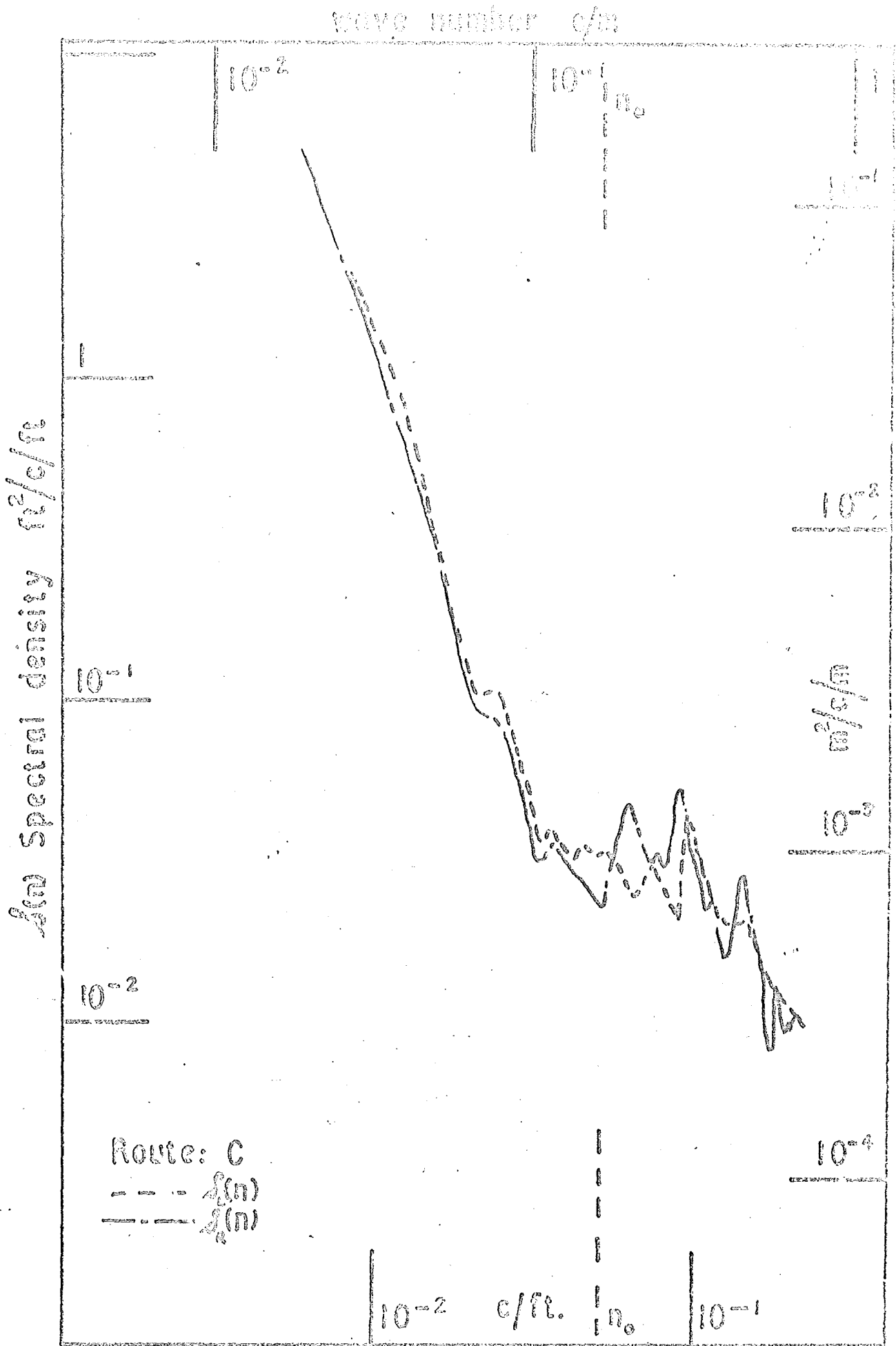


FIGURE 49

Road profile spectra

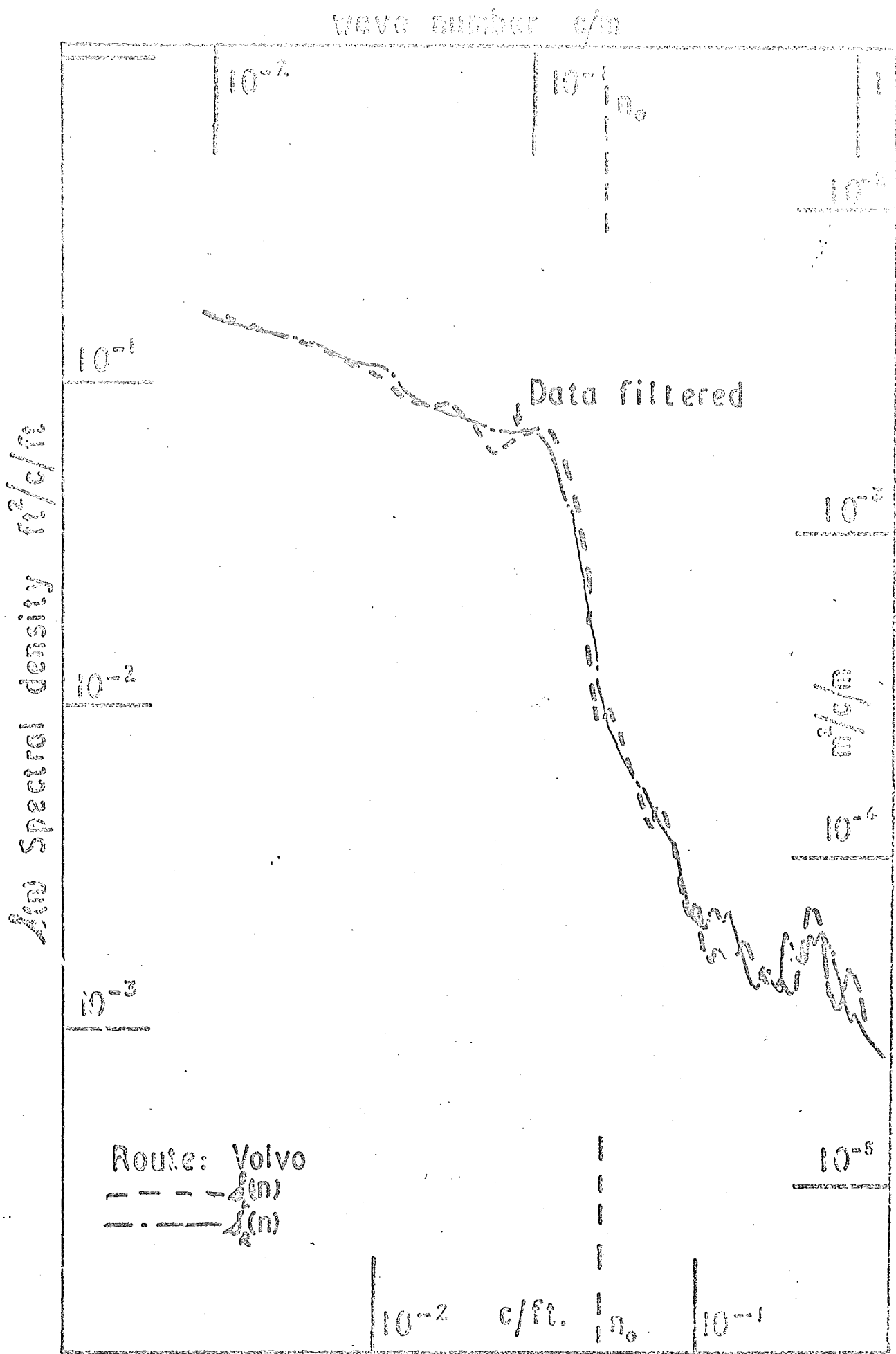


FIGURE 50

Road profile spectra

$$R(-\tau) = R(\tau)$$

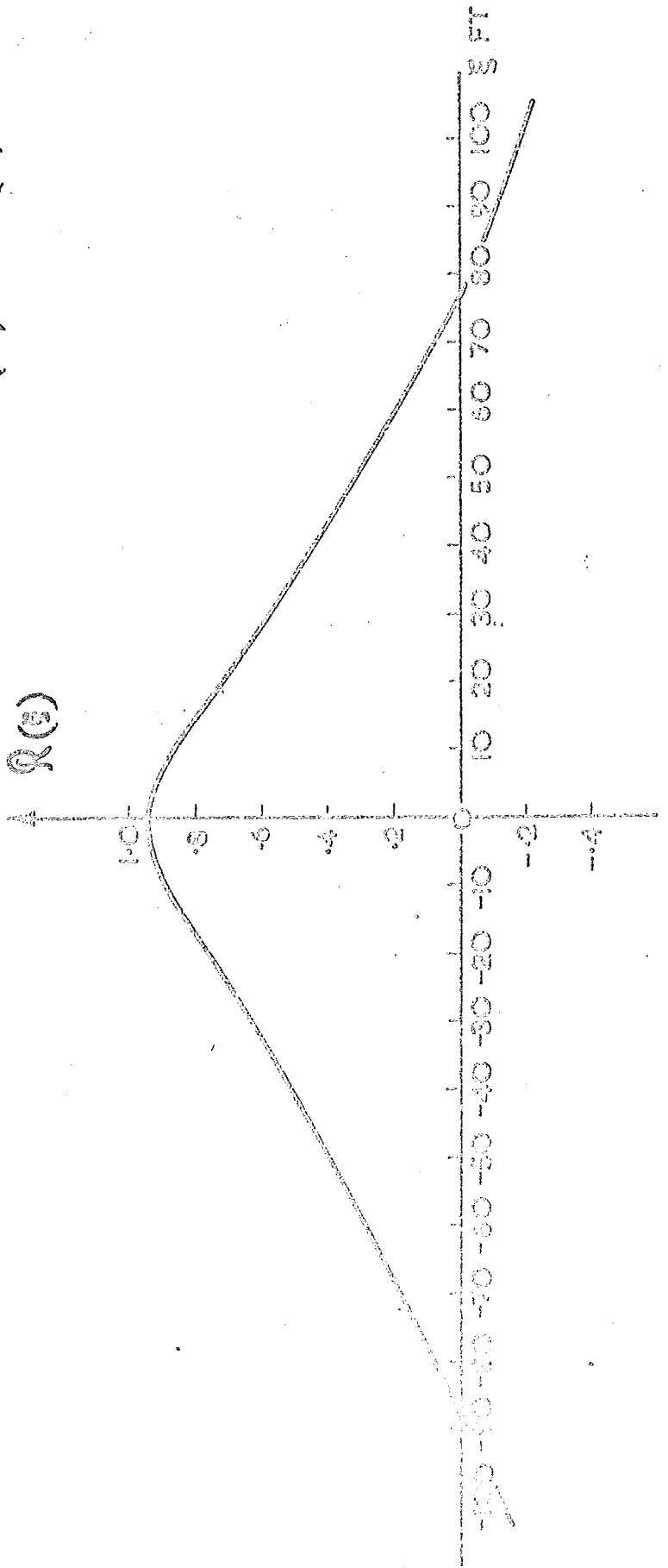
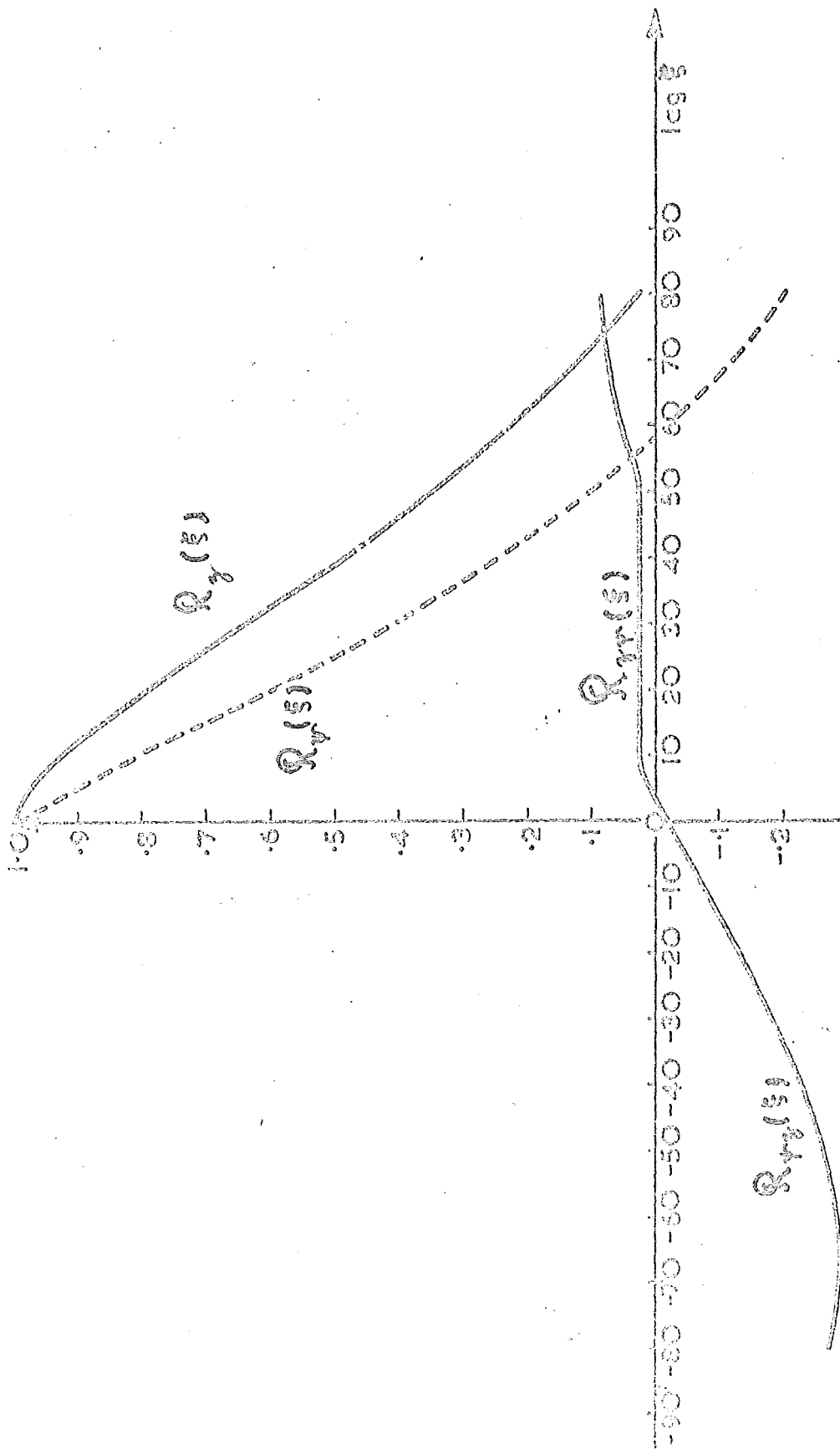


FIGURE 51

Normalised cross correlation function, route B



**FIGURE 52**

Normalised correlation functions, route B

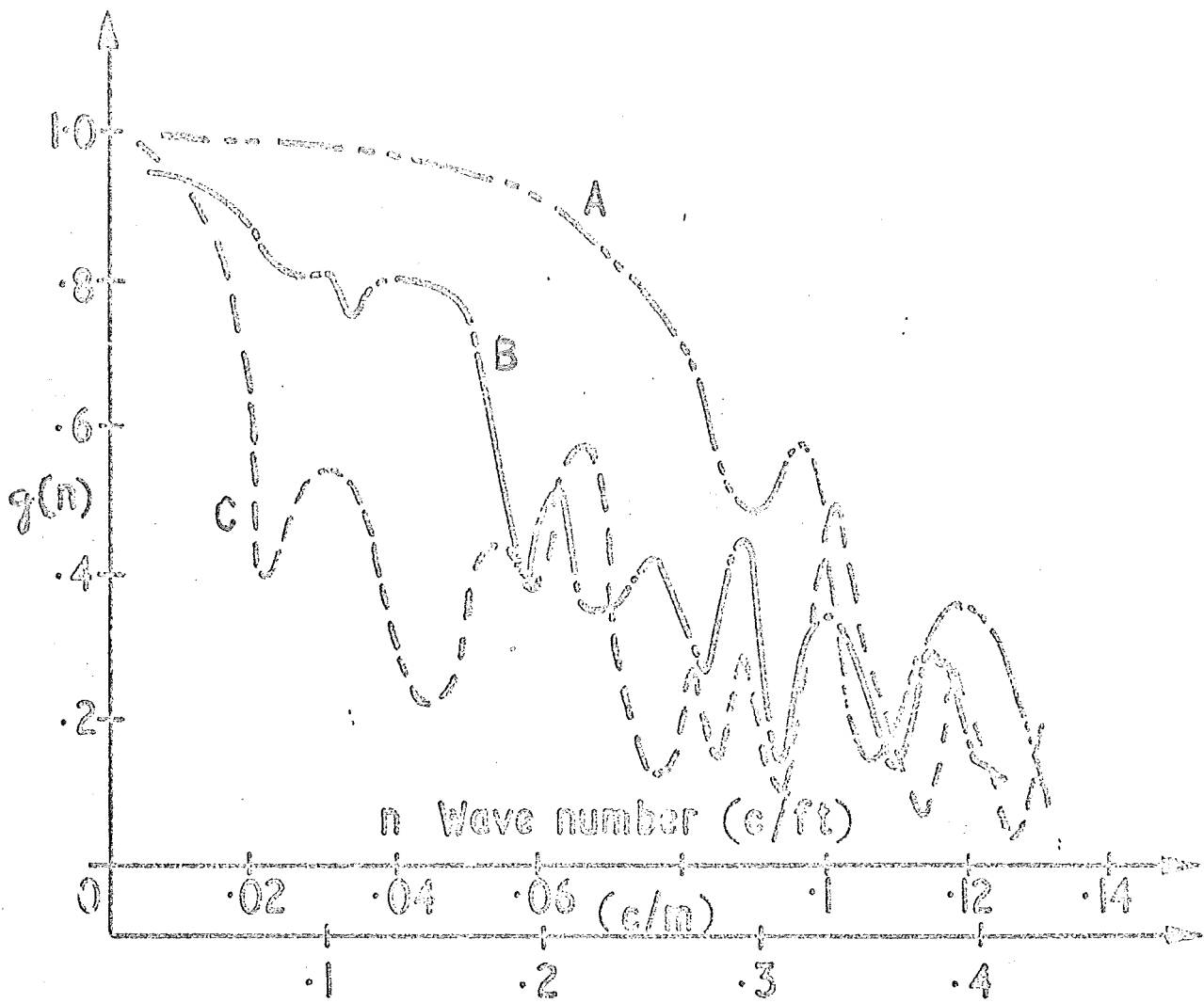


FIGURE 53

Coherency Function for Routes A, B, C

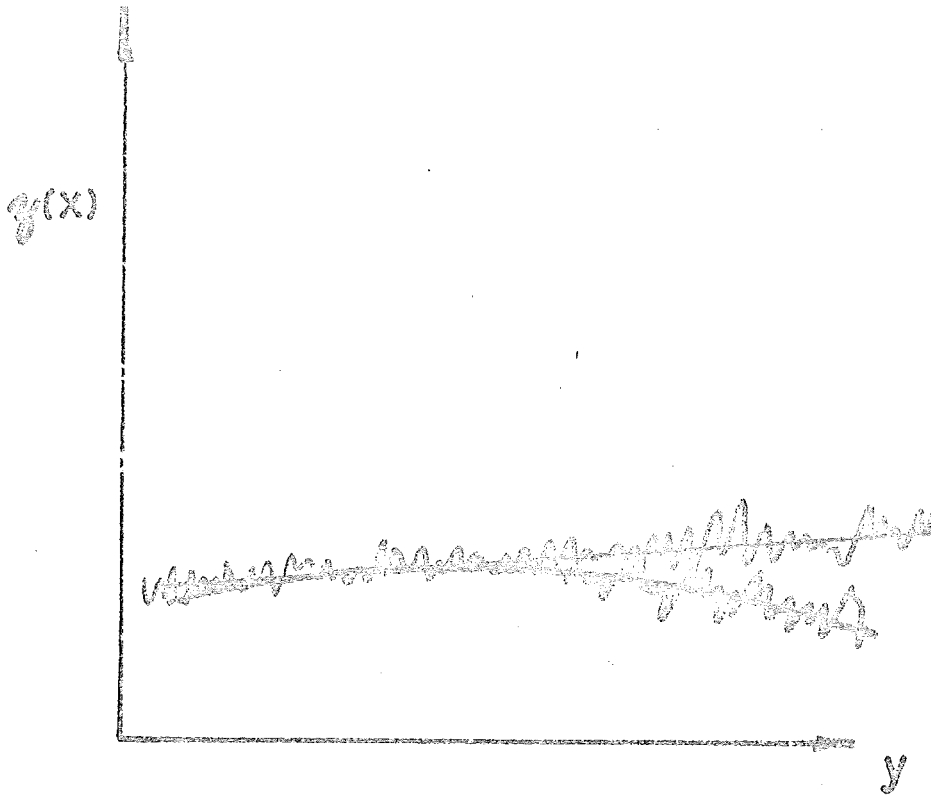


FIGURE 54

Road surface in lateral direction

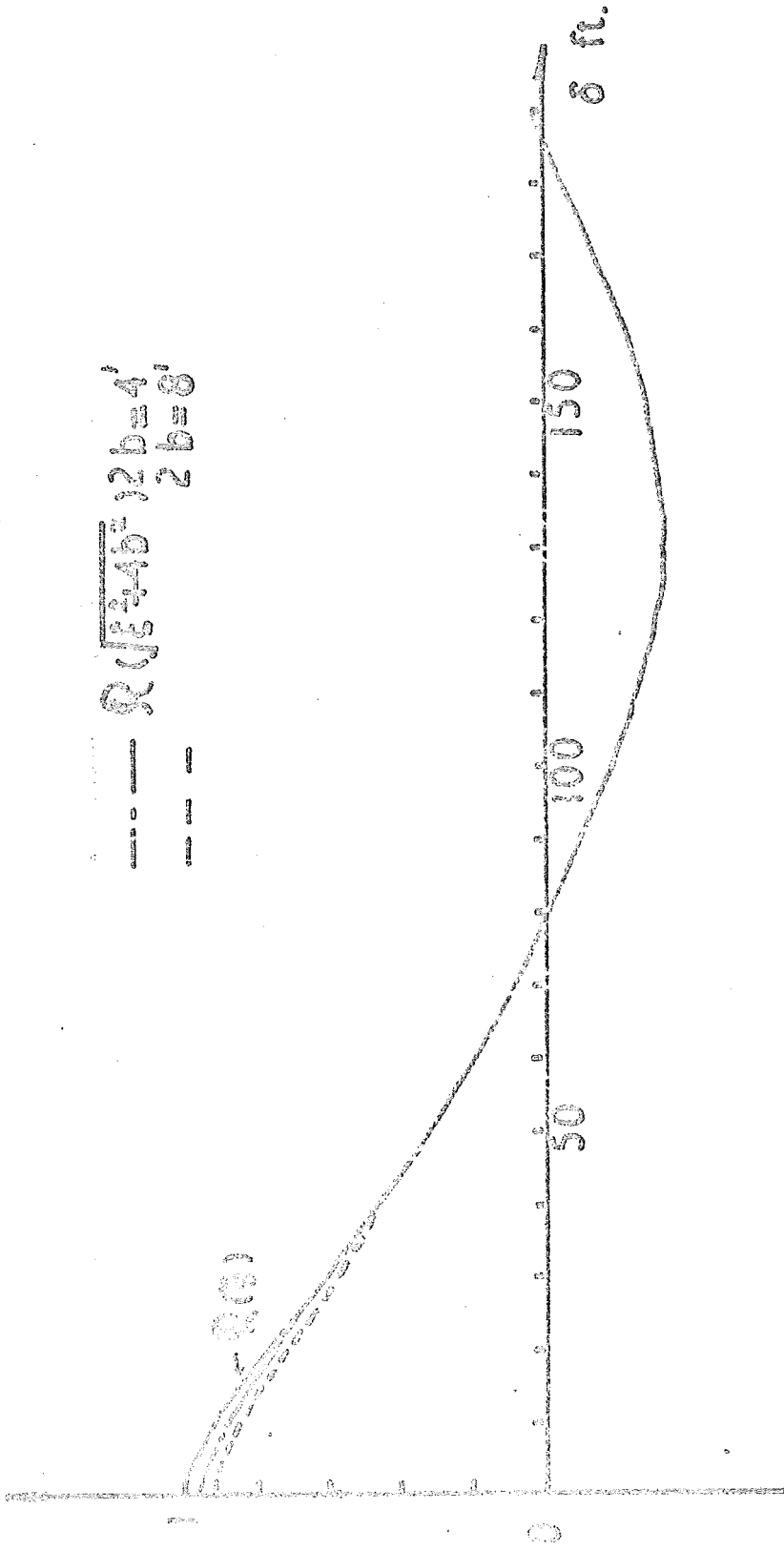


FIGURE 55

Correlation functions, route B considered as a completely homogeneous surface.

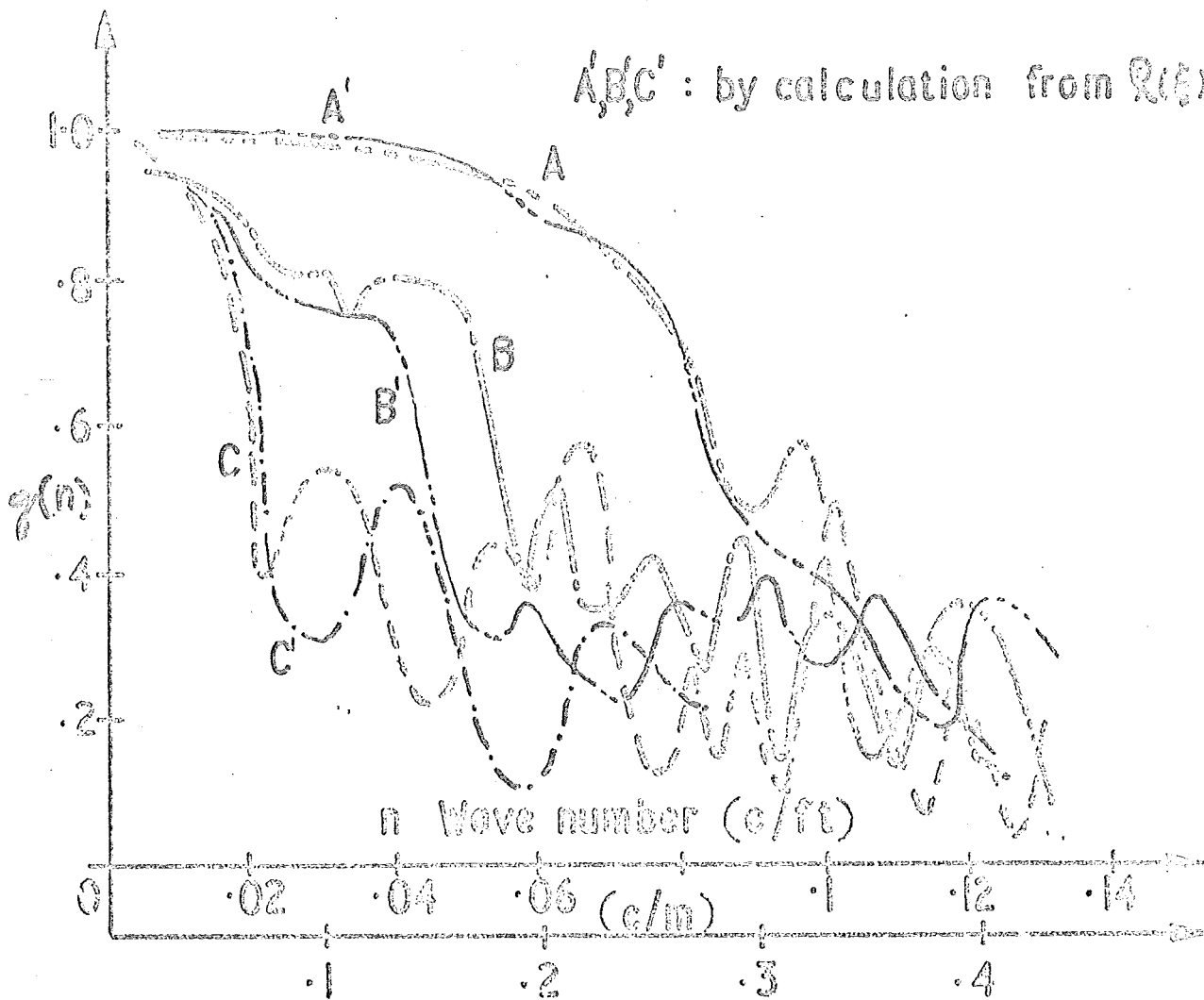


FIGURE 56

Coherency Function for Routes A, B, C

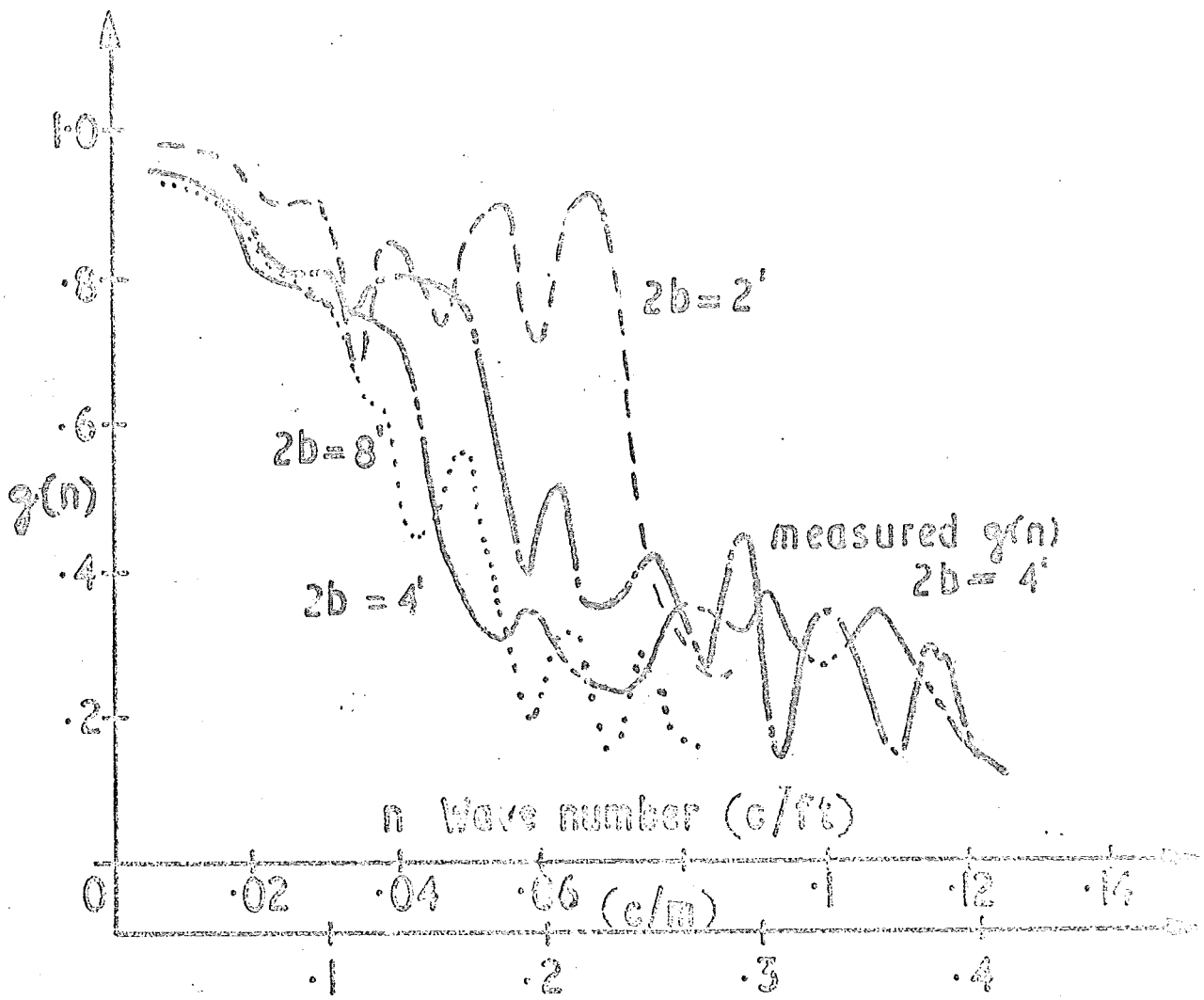
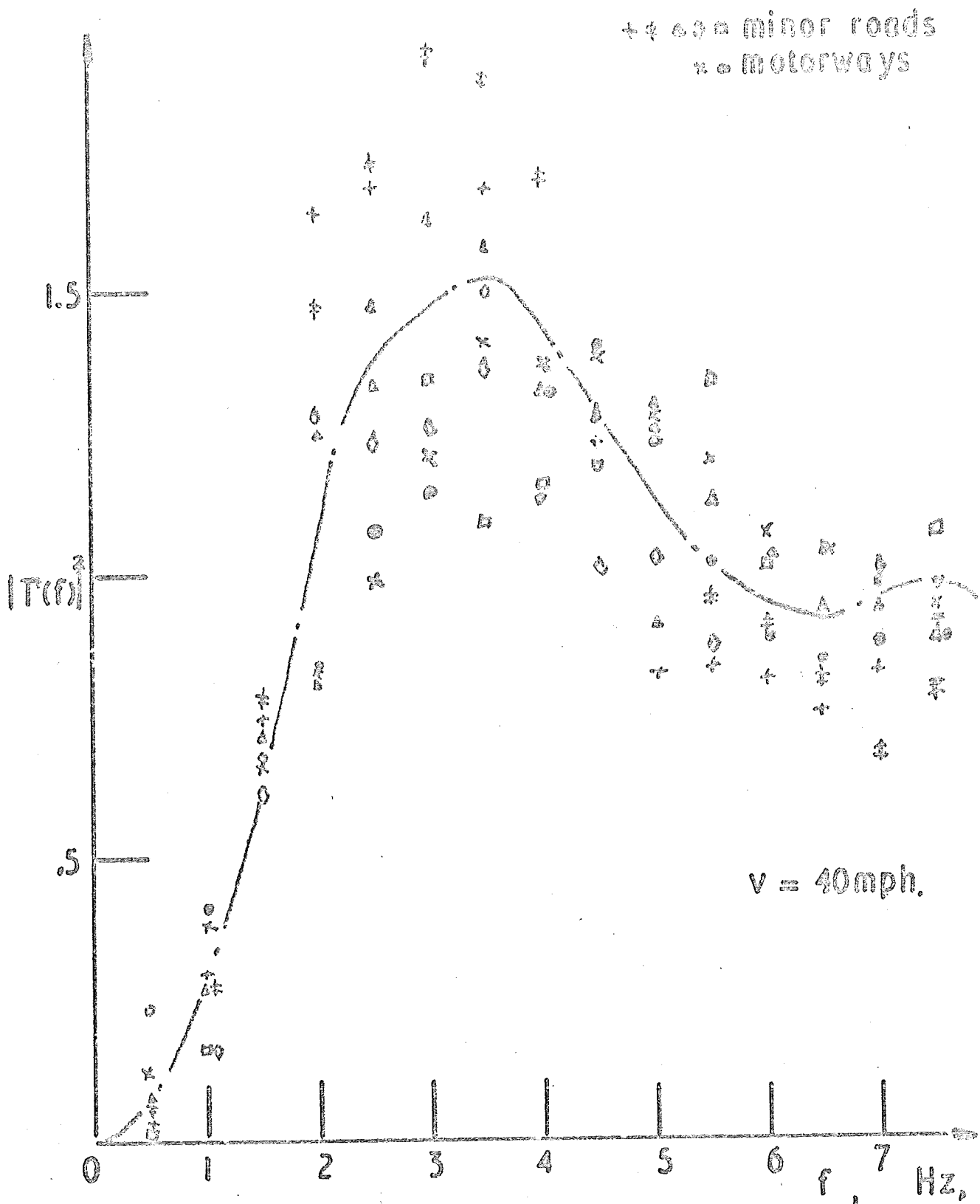


FIGURE 57

Coherency Function for Route B



**FIGURE 58**

Experimental results,  $|T(f)|^2$  against frequency, vehicle B, front spring.

△ = bad roads  
+ = minor roads

$v = 20 \text{ mph}$

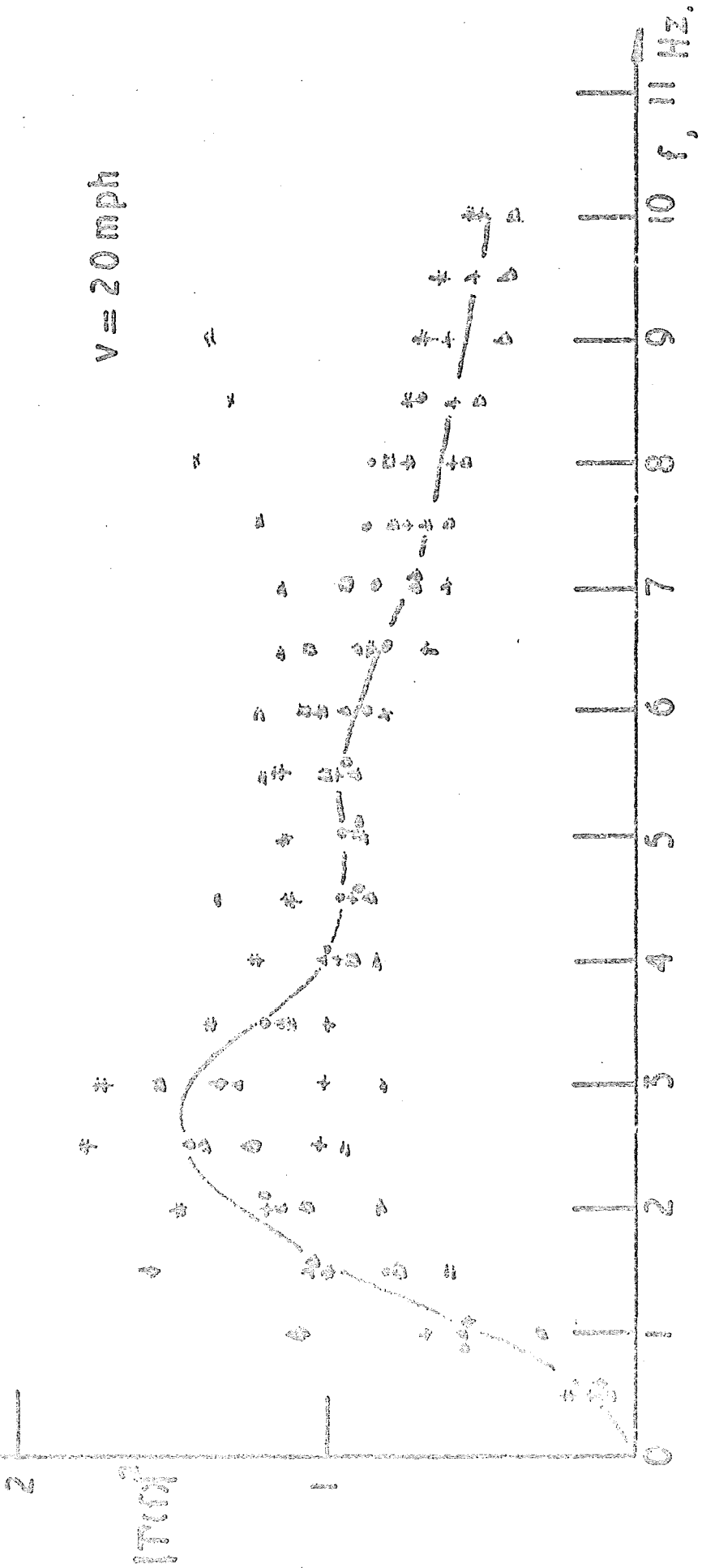


FIGURE 59

Experimental results,  $|T(f)|^2$  against frequency, vehicle B, front spring.

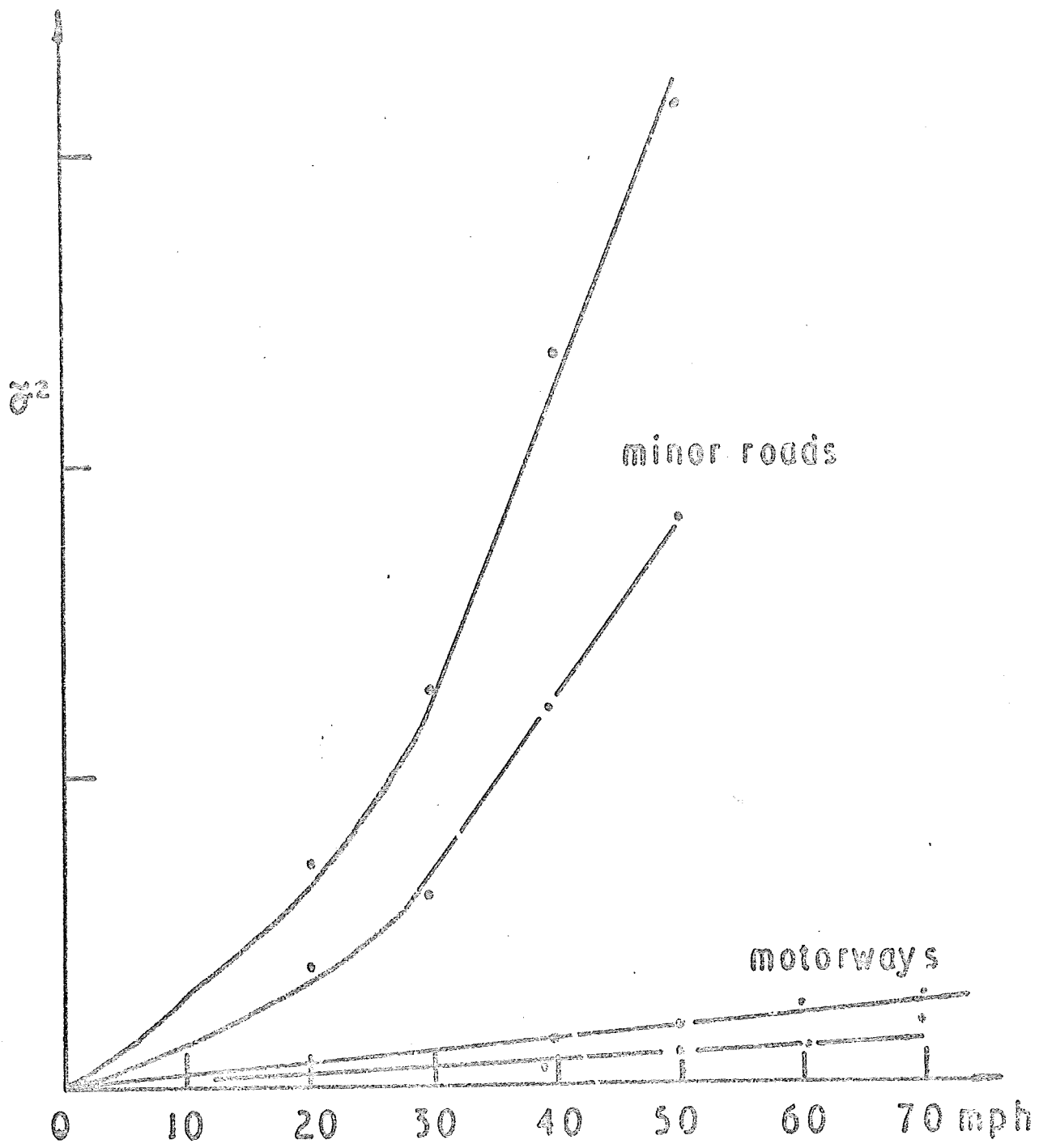


FIGURE 60

Experimental results, vehicle B, mean square response, front spring

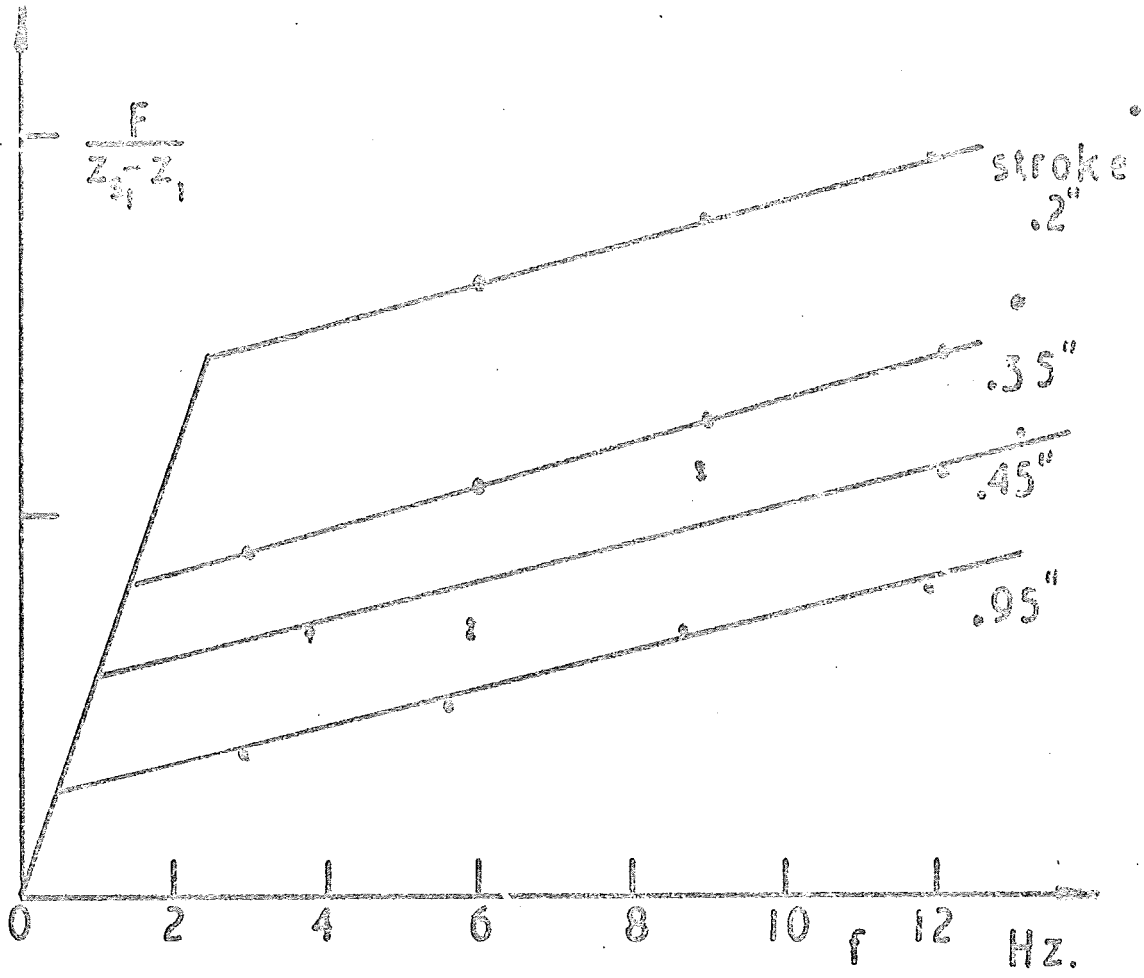


FIGURE 61

Vehicle damper receptance

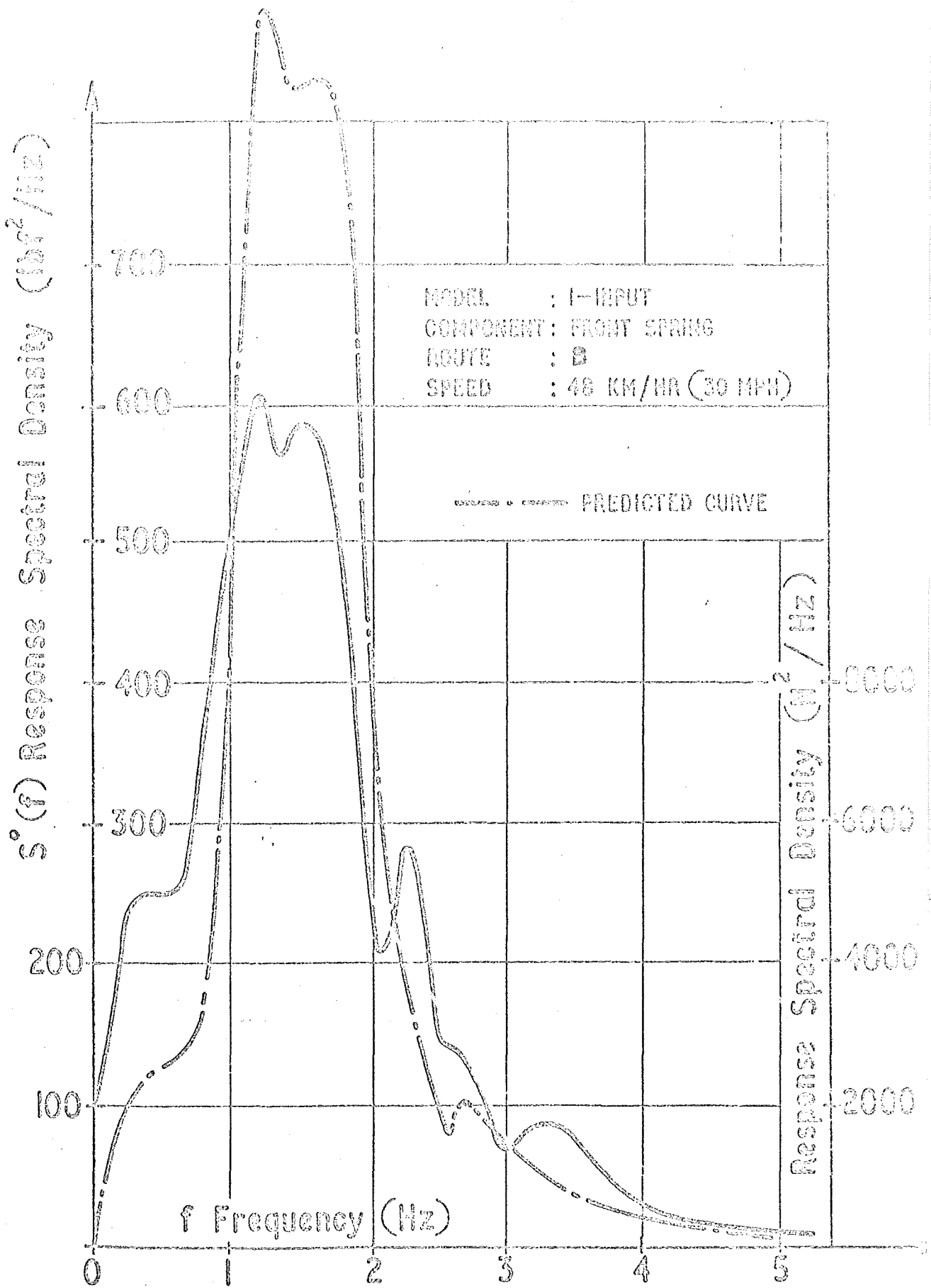


FIGURE 62

Predicted and Experimental Response Spectra.

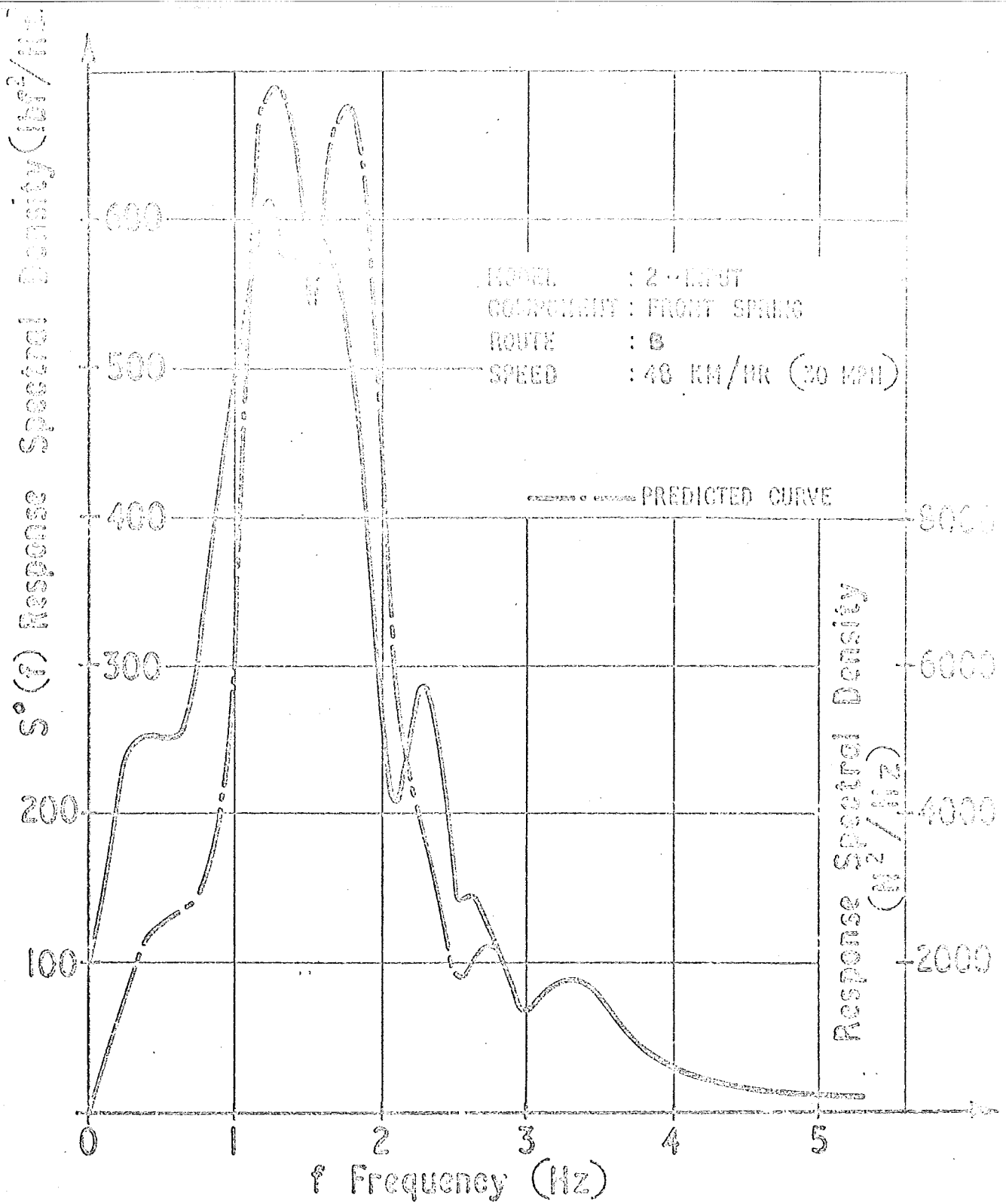
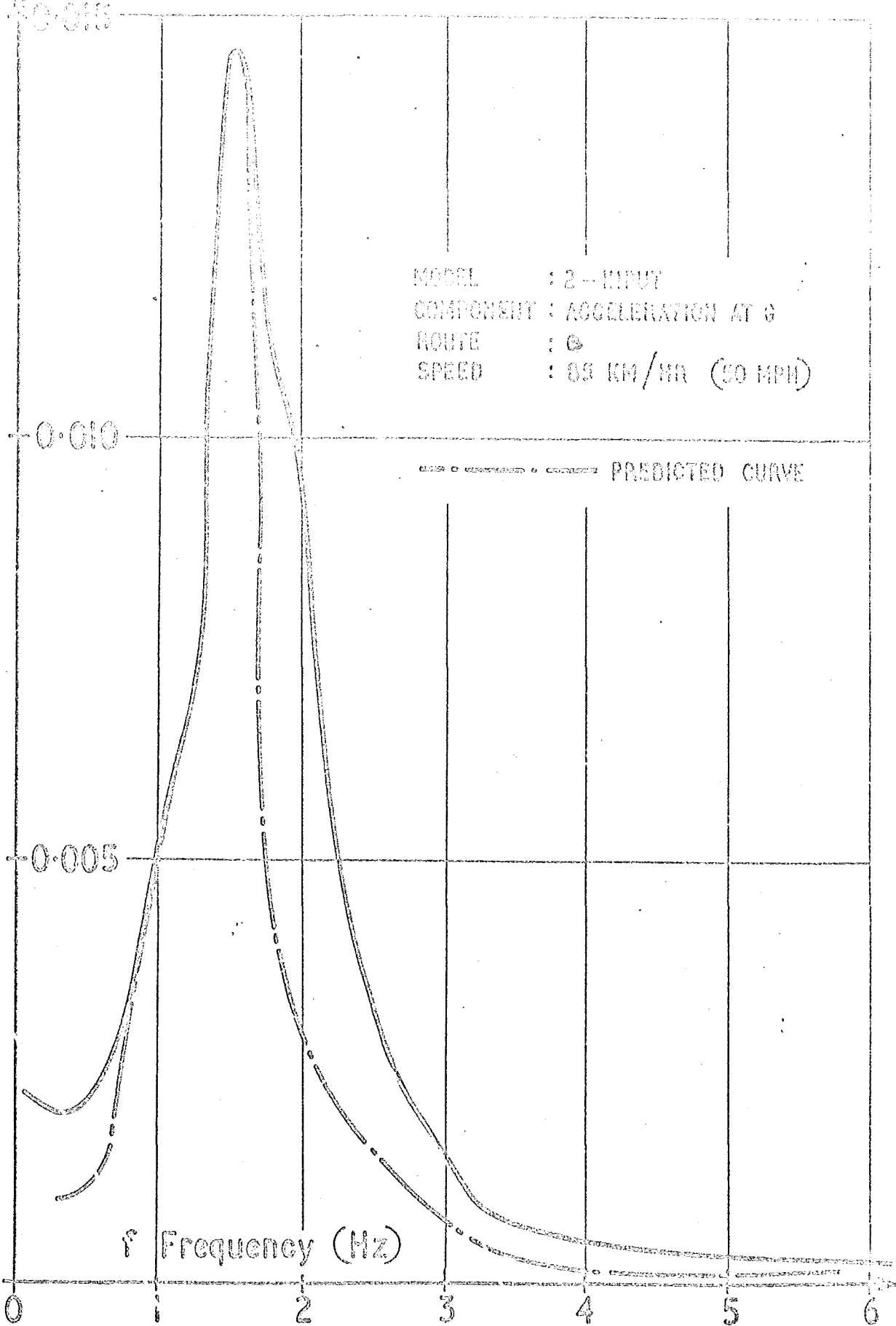


FIGURE 63

Predicted and Experimental Response Spectra.

$S^{\circ}(f)$  Response Spectral Density ( $g^2/Hz$ )



MODEL : 2-INPUT  
COMPONENT : ACCELERATION AT G  
ROUTE : 0  
SPEED : 89 KM/HR (50 MPH)

--- PREDICTED CURVE

f Frequency (Hz)

FIGURE 64

Predicted and Experimental Response Spectra

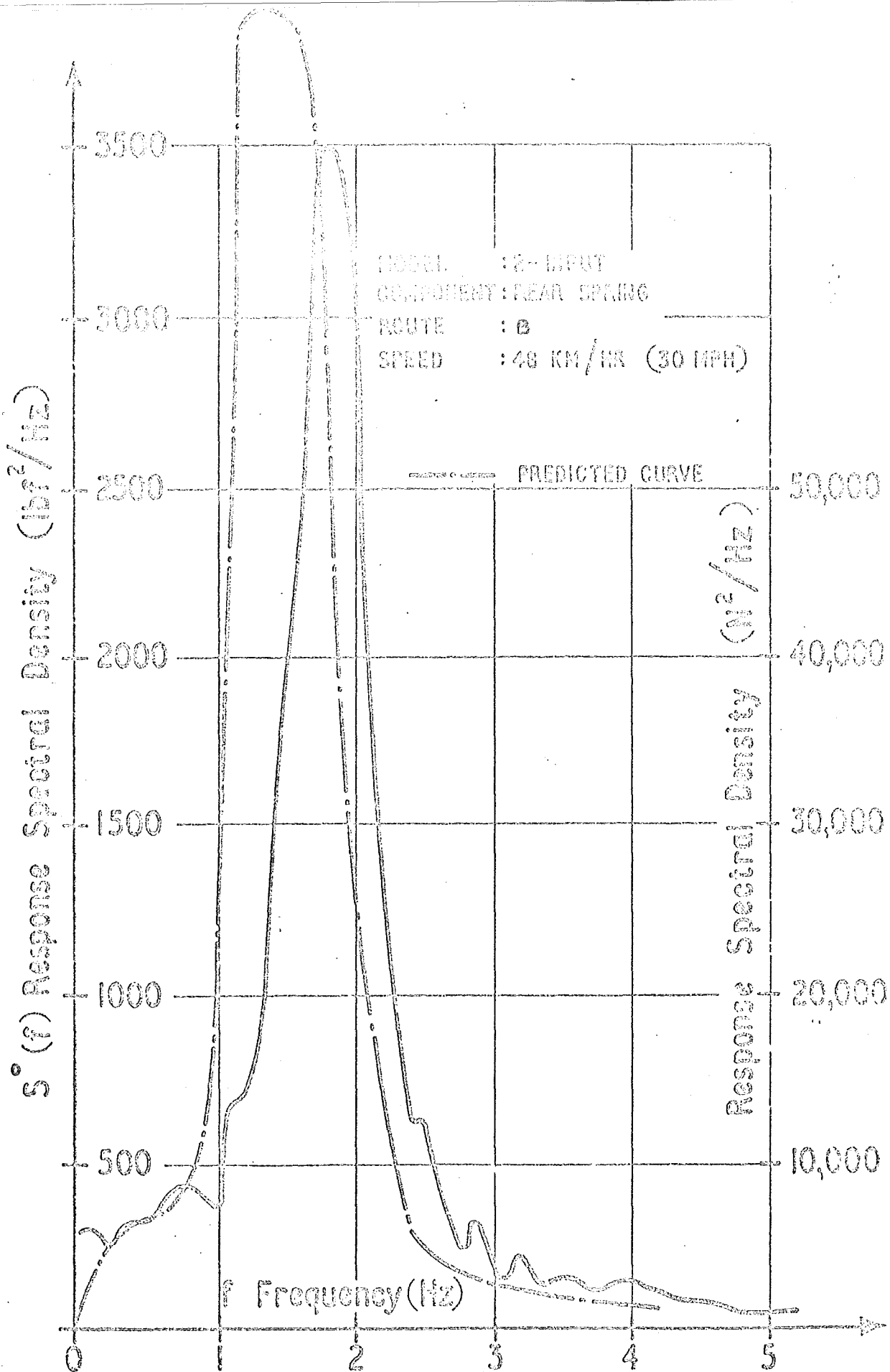


FIGURE 65

Predicted and Experimental Response Spectra



FIGURE 66

Component-vehicle model

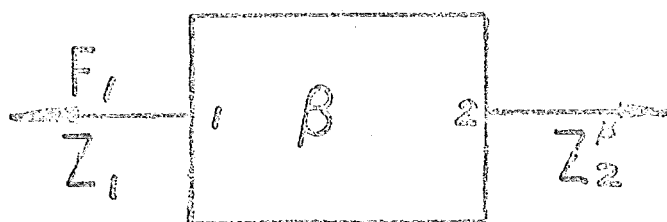
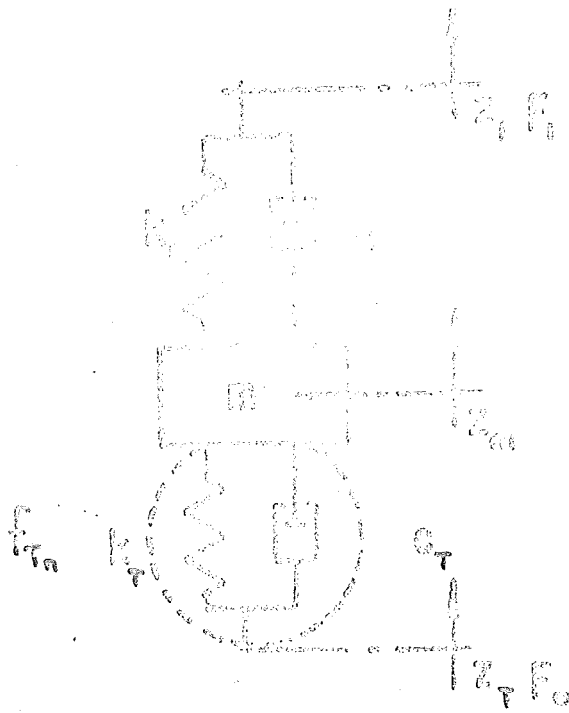
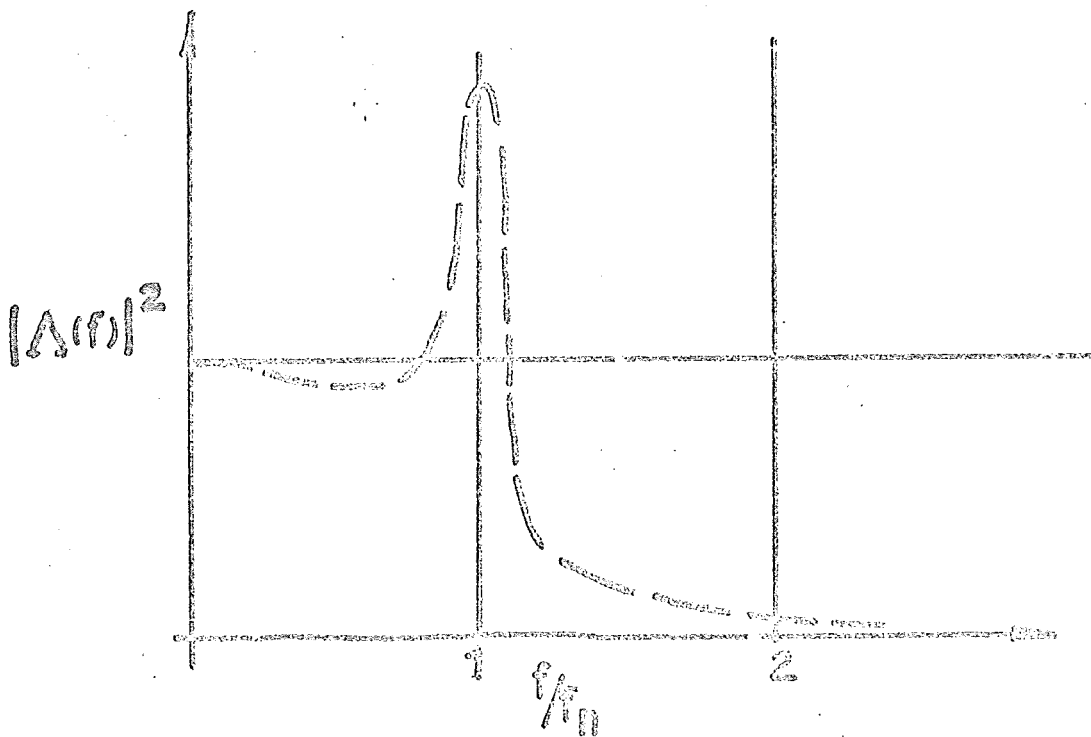


FIGURE 67

Component model modified



**FIGURE 68**  
 Vehicle suspension system  $\chi$



**FIGURE 69**  
 Simulation error function